UNIVERSIDAD COMPLUTENSE DE MADRID

FACULTAD DE CIENCIAS BIOLÓGICAS

Departamento de Microbiología III

TESIS DOCTORAL

El virus del moteado suave del pimiento (PMMoV : estudio de la función de una glutaredoxina de "Capsicum chinense" en la interacción virus-planta
Pepper mild mottle virus (PMMoV) : study of the role of a "Capsicum chinense" glutaredoxin in plant-virus interaction

MEMORIA PARA OPTAR AL GRADO DE DOCTOR

PRESENTADA POR

Saravana Kumar Ramasamy Mariyappan

Directora

María Teresa Serra Yoldi

Madrid, 2014

UNIVERSIDAD COMPLUTENSE DE MADRID
FACULTAD DE CIENCIAS BIOLÓGICAS
DEPARTAMENTO DE MICROBIOLOGÍA III

CONSEJO SUPERIOR DE INVESTIGACIONES CIENTÍFICAS
CENTRO DE INVESTIGACIONES BIOLÓGICAS
LABORATORIO DE PATOGÉNESIS DE VIRUS DE PLANTAS Y
MECANISMOS DE RESISTENCIA EN PLANTAS

EL VIRUS DEL MOTEADO SUAVE DEL PIMIENTO (PMMoV): ESTUDIO DE LA FUNCIÓN DE UNA GLUTAREDOXINA DE *Capsicum chinense* EN LA INTERACCIÓN VIRUS-PLANTA.

TESIS DOCTORAL

SARAVANA KUMAR RAMASAMY MARIYAPPAN

Madrid, 2013

UNIVERSIDAD COMPLUTENSE DE MADRID
FACULTAD DE CIENCIAS BIOLÓGICAS
DEPARTAMENTO DE MICROBIOLOGÍA III

PEPPER MILD MOTTLE VIRUS (PMMoV): STUDY OF THE ROLE OF A *Capsicum chinense* GLUTAREDOXIN IN PLANT-VIRUS INTERACTION

In partial fulfillment of the requirements for the degree of "Doctor of Philosophy (PhD)"
at Universidad Complutense submitted by

SARAVANA KUMAR RAMASAMY MARIYAPPAN

V^{o}B^{o} Directoras de tesis

Dra: María Teresa Serra Yoldi
CIB. CSIC

Dra: Isabel Garcia Luque
CIB. CSIC

Fdo.: Saravana Kumar Ramasamy Mariyappan

Madrid, 2013

CENTRO DE INVESTIGACIONES BIOLÓGICAS
CONSEJO SUPERIOR DE INVESTIGACIONES CIENTÍFICAS

Acknowledgements

Many people I have to thank for completing my thesis and I apologize if I forget to mention them. My first and foremost thanks to my supervisor Dr. M ª Teresa Serra Yoldi, whom I learned about the science ethics and make me to remember the science ethics for all the days. Her patience and support is not only for my professional carrier it is above to that I learned how to independently think for the science and without her full support I can't able to complete my thesis. Thanks a lot Dr. Maite for providing a platform to my science carrier.

I thank to my co-supervisor Dr. Isabel García Luque, for her help and thoughtful suggestions over my experiments. She widens the research and also carefully looking at how the experiments will go. And also I thank Dr.Isabel for her critical comments over my writings and also for her jovial talks.

I thank to the Professors Dr. Juan Carlos Gutierrez and Mª José Valderrama from the Department of Microbiología-III, Universidad Complutense (UCM), Madrid, Spain.

I would like to thank Professor Dr. Enrique Herrero of Universidad de Lleida and their lab group people, such an energetic and self-motivated group and my special thanks to Dr. Gemma Belli with whom I did my yeast experiments and I am very much impressed with her patience throughout my stay at Lleida. She helped me to conduct my experiments at the last day of my stay at Lleida even though the next day was the New Year 2012.

I thank Professor Dr.Victoriano Valpuesta and Dr. Sonia Osorio of Universidad de Malaga where I analyzed Pyridine nucleotide experiments. I express my thanks to Dr. Sonia for helping me to learn the kinetic analysis experiments.

I would like to express my sincere thanks to Dr. Carmen Castresana (CNB, CSIC. Madrid) for providing me the clones of PRs, 9-LOX and GST genes and Dr Mullineaux (University of Essex, UK) for providing me the GR containing clone.

Above to that my special thanks to Irene Culsan my labmate who helped a lot for my experiments and results. Irene I feel very happy and comfortable to work along with you for the last two years. I thank Dr. Fatima Tena for her support in my experiments and probe making. I express my thanks to Paula Doblas and Remedios Pacheco Pino with whom I interact very much.

I thank Dr. María Jesús, Martínez Hernández director of CIB, Madrid for her immense help. I would like to thank Dr.Julio Salinas Muñoz, Dr. Francisco Tenllado and Dr. Tomás Canto from the Environmental Department at the CIB, where I conducted my northern hybridization experiments and they have given the pleasant environment during my stay at CIB.

I thank Dr.Mario Garcia Lacoba for helping me to sort out the structural prediction. I thank Guillermo Padilla for teaching me the statistical analysis. I thank Mónica María Fontenla Lago and Pablo, Jalon Rico of CIB photography service for their help throughout my experiments.

I thank Dr.Laura Isabel,De Eugenio Martinez from Dr. M[a] Jesús Martínez lab who gave better knowledge in enzyme kinetic analysis for my experiments. I thank Dr.Maria Colmenares Brunet for my initial periods of research. My thanks to Dr. Ana María Alonso Ayala, Pedro José Alcolea Alcolea, and Mr. Abel Fernandez from Prof. Vicente Larraga Rodriguez de Vera lab group who gave the moral support at CIB.

I have no words to express my thanks for my parents and their blessings motivated me a lot. I express my special thanks to Mrs. Manju, my life partner who shared my emotional feelings, also gave support during my mood swings and also for her help in my thesis. I would like to thank my family members who morally support for my carrier Dr.Birla (elder brother), Mr.Manikandan (younger brother) my sister-in-laws (Dr.Viji and Ms.Vanita), my in-laws and my brother-in-law satish.

I would like to thank my Indian friends (Ram, senthil, Ravi, G.karthi, P.S.Karthi, Raghunath, Dinesh, Gowtam, Babu and Raja) who gave pleasant environment during my stay and helping for my stays at Madrid. Gowtam I have to say special thanks at many of my crucial issues.

Above all my sincere thanks to Consejo Superior de Investigaciones Científicas (CSIC), a governmental scientific body of Spain which provides me the funding for the four years to carry out my experiments and helped me to widen my knowledge. Thanks to all España people for giving me the sweet memories at my important point of life.

My almighty thanks to my Goddess who gave me the courage to carry out my research and also gave me the chance to learn the research.

ABBREVIATIONS:

aa	: Amino acid
avr	: Avirulence.
bp	: Base pair
$Cacl_2$	: Calcium chloride
cDNA	: Complementary DNA
CP	: Coat protein
dNTP	: deoxyribonucleotide triphosphate
DNA	: Deoxyribo nucleic acid
dpi	: Days post-inoculation
dUTP	: 2´-Deoxyuridine, 5´-Triphosphate
EDTA	: Ethylene diamine tetra acetic acid
ET	: Ethylene
GARPO	: Peroxidase-conjugated goat anti-rabbit antibody.
GFP	: Green fluorescent protein.
g	: Gravity.
Grx	: Glutaredoxin
gRNA	: Genomic RNA
GR	: Glutathione reductase
GSH	: Glutathione
GST	: Glutathione-s-transferase
H_2O_2	: Hydrogen peroxide
HED	: Hydroxyethylene disulfide
HR	: Hypersensitive response
IgG	: Immunoglobin
IPTG	: Isopropyl β- D -thiogalactoside
JA	: Jasmonic acid
KDa	: kiloDalton
kV	: Kilovolt
LAR	: Local acquired resistance
LB	: Luria-Bertani
LOX	: Lipoxygenase
M	: Molar
MOPs	: 3-(N-Morpholino)propanesulfonic acid
MP	: Movement protein
mRNA	: messenger RNA
MS	: Murashige and Skoog.
$NAD(P)^+$	: Oxidized Nicotinamide adenine dinucleotide (phosphate) $^+$
NAD(P)H	: Reduced Nicotinamide adenine dinucleotide (phosphate)
NLL	: Necrotic local lesion
nm	: Nanometer
nt	: Nucleotide
OD	: Optical density
OEC	: Oxygen evolving complex
ORF	: Open reading frame

PBS	: Phosphate buffered saline
PCR	: Polymerase chain reaction
PD	: Plasmodesmata
PME	: Pectin methyl esterase
PNs	: Pyridine nucleotides
PVDF	: Polyvinylidene flouride
R	: Resistance gene
RF	: Replicative form
RNA	: Ribonucleic acid
rRNA	: Ribosomic RNA
rpm	: Revolutions per minute
PR	: Pathogenesis-related protein
ROS	: Reactive oxygen species
SA	: Salicylic acid
SAR	: Systemic acquired resistance
SD	: Synthetic defined
SDS	: Sodium dodecyl sulphate.
SDS-PAGE	: Sodium dodecyl sulphate-polyAcrylamide gel electrophoresis
SEL	: Size exclusion limit
sgRNA	: Subgenomic RNA
siRNA	:Small interfering RNA
SSC	: Saline sodium citrate
TAE	: Tris Acetate EDTA
t-BOOH	: tert-butyl hydroperoxide
Tris	: Tris(hydroxymethyl)aminomethane
Trx	: Thioredoxin
tRNA	: transfer RNA
Tween	: Polysorbate
µF	: Microfarad
µg	: Microgram.
v/v	: Volume to volume
UV	: Ultra Violet
YPD	: Yeast peptone dextrose
YPG	: Yeast peptone glycerol

Cited Virus:

TMV	: Tobacco mosaic virus.
ToMV	: Tomato mosaic virus.
PMMoV-I	: Pepper mild mottle virus-Italian strain.
PMMoV-S	: Pepper mild mottle virus-Spanish strain.
PNRSV	: Prunus necrotic ringspot virus

INDEX

RESUMEN

Las enfermedades virales causan cuantiosas pérdidas económicas en los cultivos en todo el mundo debido principalmente a las alteraciones morfológicas y fisiológicas que producen en las plantas y que se traducen en importantes pérdidas en la producción (rev. Hull, 2002). En el caso de los cultivos de pimiento tienen un especial interés las denominadas cepas pimiento de los tobamovirus que infectan los cultivos de pimiento resistentes a los virus del mosaico del tabaco (TMV) y del tomate (ToMV) y que se han descrito en todo el mundo. En España una de estas cepas, el *Virus del moteado suave del pimiento* (PMMoV) es uno de los mas prevalentes en los cultivos de pimiento de la provincia de Almería, con brotes epidémicos importantes entre 1984 y 2004 (Tenllado *et al.,* 1997; Fraile *et al.,* 2011). Este virus afecta a todas las especies del género *Capsicum*, incluyendo aislados que son capaces de evadir la resistencia mediada por los genes L^1-L^4 (rev Gilardi *et al.,* 1999; Genda *et al.*, 2007; Antignus *et al.*, 2008). En España se han descrito aislados pertenecientes a los patotipos $P_{1,2,}$ y $P_{1,2,3}$. La cepa española (PMMoV-S) es un patotipo $P_{1,2,}$ y fue aislada de cultivos de pimiento de la provincia de Almería (García-Luque *et al*., 1990) y la cepa italiana es un patotipo $P_{1,2,3,}$ y fue aislada en Sicilia (Italia) (Wetter *et al*., 1984).

En trabajos previos de nuestro laboratorio se identificó un gen que codifica una Glutaredoxina (Grx) cloroplastídica de *Capsicum chinense* L^3L^3 PI 159236, cuya expresión se inducía durante las infecciones compatibles e incompatibles de las cepas I y S de PMMoV, respectivamente (Gilardi, 2000). También se había establecido que la expresión constitutiva de la proteína completa fusionada al gen delator GFP en plantas de *Nicotiana benthamiana* se localizaba en el cloroplasto, mientras que una deleción en su region N de 63 aa se localizaba en el núcleo (Montes-Casado *et al.,* 2010).

Las Grxs tienen actividad thiol-disulfuro oxidoreductasa y pueden reducir los grupos disulfuro intramoleculares de las proteínas o los grupos disulfuro formados entre una molécula de glutation (GSH) y una Cis de una proteína (Vlamis-Gardikas y Holmgren, 2002). La Grx fue descubierta en 1976 como un sistema donador de hidrógeno para la enzima ribonucleótido reductasa de *Escherichia coli* (Holmgren, 1976). Son proteínas de bajo peso molecular que están ampliamente distribuidas en todos los organismos. En *Arabidopsis* se han descrito más de 30 Grxs, codificadas por familias multigénicas, a diferencia de lo que ocurre en *E. coli* y *Saccharomyces cerevisiae* (Lillig *et al.,* 2008), que presentan un menor número de Grxs.

Las Grxs están involucradas en la protección de las proteínas frente a la oxidación irreversible de sus grupos thiol (Lemaire, 2004), uno de los mecanismos moleculares sensibles al estado redox de la célula y que pueden ser modificados por la producción de ROS generados durante procesos celulares tales como la fotosíntesis, la respiración o la invasión por patógenos (Foyer and Noctor 2003; Lemaire, 2004).

En los últimos años se ha producido un notable avance en el conocimiento de las Grxs de plantas y se postula que deben desempeñar importantes funciones no sólo en el mantenimiento del potencial redox celular, sino también en la regulación de la funcionalidad de proteínas específicas y en la expresión de ciertos genes (Vlamis-Gardikas *et al.,* 2002; Ndamukong *et al.,* 2007; Zaffagnini *et al.,* 2008).

Consideramos que el estudio de esta Grx de *C. chinense* (*Cch* Grx) nos permitirá desvelar su posible función en la activación de los mecanismos de resistencia vegetal frente a PMMoV-I y nos aportará nuevos conocimientos sobre la respuesta de la planta en las interacciones planta-virus.

En el presente trabajo nos proponemos los siguientes objetivos:

1. Caracterización molecular, celular y bioquímica de la proteína *Cch* Grx.

2. Análisis del efecto de la expresión constitutiva de *Cch* Grx, en plantas de *N. bentamiana,* sobre la acumulación viral de PMMoV-I a lo largo del ciclo de infección.

3. Estudio de la respuesta de defensa de las plantas frente a PMMoV-I mediada por la sobre-expresión de *Cch* Grx.

4. Análisis de la contribución de *Cch* Grx en el mantenimiento del estado redox de los nucleótidos piridínicos en la célula.

5. Análisis de la función de *Cch* Grx en la tolerancia de las plantas frente al estrés abiótico.

6. Estudio en levaduras de la función de *Cch* Grx en el mecanismo de ensamblaje de los grupos Fe-S.

Para ello disponemos de plantas transgénicas de *N. benthamiana* que expresan de forma constitutiva la proteína nativa *Ch* Grx, (*Nb:Grx*) y la proteína nativa fusionada al gen delator de la proteína verde fluorescente (GFP), (*Nb:Grx-GFP*), así como plantas que expresan una forma truncada de la proteína, con una deleción de 63 aminoácidos en el extremo N de la proteína, también fusionada a la GFP (*Nb:ΔGrx-GFP*). *N. benthamiana* es un huésped susceptible al virus PMMoV-I y por ello se ha utilizado para obtener las

plantas transgénicas con el fin de analizar el efecto de la sobreexpresión de la proteína *Cch* Grx de *C. chinense* en el proceso de la infección viral y en la respuesta de la planta frente a la misma.

Hemos expresado también la proteína *Cch* Grx madura en *E. coli* y en *S. cerevisiae* para deteminar su actividad tiol oxidreductasa y su función en la formación y ensamblaje de los grupos Fe-S, respectivamente.

El análisis computacional de la secuencia aminoacídica reveló que la Grx de *C. chinense*, contiene un sitio activo CSYS perteneciendo por tanto a la clase monotiol del grupo I de las Grxs (Couturier *et al.,* 2009a), que han sido descritas en plantas, insectos y hongos pero no en procariotas. Y en este trabajo hemos podido establecer que pertenece al subgrupo C5/S12 al tener el motivo WCSYC/S como sitio activo, que es único para las Grxs de plantas. La proteína ha sido denominada *Cch* GrxS12

El árbol filogenético muestra a la *Cch* GrxS12 en el mismo grupo que la de tomate, y todas las demás de plantas agrupadas, mientras que la *S. cerevisae* está localizada en una rama diferente.

El análisis estructural de la *Cch* GrxS12 efectuado con el servidor I-TASSER sobre la proteína GrxS12 de álamo (Couturier *et al.,* 2009b) muestra que tiene el patrón característico de la familia de proteínas Trx con un centro de cuatro láminas β rodeado de 5 α-hélices. Ambas comparten el sitio activo WCSYS y otros residuos importantes como ^{75}TVP^{77}, ^{87}GG^{88} y la presencia de un segundo residuo de Cys que se ha descrito está involucrado en la unión al GSH por parte de la proteína de álamo (Couturier *et al.,* 2009b), lo que indicaría que ambas proteínas comparten las mismas propiedades bioquímicas y fisiológicas.

Para caracterizar la función tiol-oxidoreductase de la proteína *Cch* GrxS12 la proteína madura se expresó en *E. coli* fusionada a una cola de His en el extremo N que facilitaba su purificación mediante una columna de afinidad. La proteína *Cch* His-Grx soluble purificada tenía un Mr de 12.9 kDa y mostró actividad GSH-disulfuro oxidoreductasa, siendo activa en el ensayo clásico de actividad Grx usando HED (Holmgren and Åslund 1995), a diferencia de otras Grx de tipo monotiol pertenecientes a la clase II, tal como AtGRXcp de *A. thaliana* (Cheng *et al.,* 2006) y de forma similar a la Grx de tipo monotiol de la clase I, como la proteína PtrGrxS12 de *Populus* (Couturier *et al.,* 2009b) si bien su actividad específica, 0.12 U/nM, fue 10 veces inferior a la de esta proteína.

Análisis iniciales en nuestro laboratorio –mediante expresión transitoria en hojas de *N. benthamiana*- mostraron que la proteína completa fusionada en su región C-terminal a la proteína delatora GFP se localizaba en el cloroplasto, mientras que la proteína *Cch* Δ2M-Grx-GFP, en la que se habían eliminado los primeros 63 aa que codifican el péptido señal para su localización en el cloroplasto, se localizaba en el núcleo (Montes-Casado *et al*., 2010), no habiéndose descartado que esta localización fuera debida a la presencia de GFP libre en los experimentos de expresión transitoria. Para analizar esta posibilidad, hemos obtenido protoplastos de plantas de *N. benthamiana* que expresan constitutivamente estas proteínas y hemos corroborado mediante su observación al microscopio confocal que la proteína completa se localiza en el cloroplasto, y que la proteína truncada se localiza en el núcleo y en el citoplasma como la proteína libre GFP. Mediante análisis de immunotransferencia con el inmunosuero anti Grx, obtenido previamente en el laboratorio, ha quedado descartado que sea la proteína libre GFP la que se está detectando en los análisis realizados. Los datos son concordantes con la predicción del programa chloroP que revelaba que los primeros 63 aa eran necesarios para que la proteína se localizara en el cloroplasto.

Las Grxs monotiol participan en diversas funciones celulares como reguladoras del estado redox de las proteínas y en la protección frente al estrés oxidativo celular (Cheng *et al*. 2006; Herrero y de la Torre-Ruiz, 2007). La sobre-expresión de un gen en plantas es la mejor forma de analizar la función del gen redundante (Ito y Meyerowitz, 2000; Nakazawa *et al.,* 2001). En este sentido, utilizamos las plantas de *N. benthamiana* transgénicas obtenidas en el laboratorio y descritas anteriormente para estudiar el efecto de *Cch* GrxS12 sobre la infección de PMMoV-I.

Cuando las plantas transgénicas fueron infectadas, incluyendo como control plantas de *N. benthamiana* transformadas con GFP, no se observaron diferencias en los primeros estadios de la infección, sin embargo, en los últimos estadios si se observó una mayor recuperación de las plantas que expresaban las tres formas de la Grx respecto a las plantas control. El análisis de la acumulación de la proteína de cubierta viral a los 7, 14 y 28 dpi reveló que al principio las tasas de acumulación eran semejantes, si bien a 14 y 28 dpi se detectó una menor acumulación en las plantas que expresan las tres formas de la Grx. El análisis de la acumulación del RNA viral corroboró que a los 7 dpi se acumulaba de igual forma en los cuatro tipos de plantas, pero a 28 dpi se observaba una notable caída en las tres líneas que expresaban las tres construcciones de la Grx, con respecto a las

plantas control, especialmente en las plantas *Nb:GrxGFP*, quizás debido a una mayor acumulación de la proteína. A los 28 dpi es el momento en que la recuperación es clara (Pérez-Bueno, 2003). Estos resultados son concordantes con los anteriores del laboratorio en que se estableció que en los estadios tardíos de la infección existía un menor número de células infectadas en las plantas que expresaban las tres construcciones de la Grx que en las control (Montes-Casado *et al*., 2010)

Estos resultados revelaban que al principio de la infección parecía no estar afectado ni el movimiento viral como ya había sido puesto de manifiesto para la infección de PMMoV-S-YFP (Montes-Casado *et al*., 2010), ni la replicación, que pudimos corroborar mediante la infección de protoplastos de las cuatro líneas de plantas analizadas, y el posterior análisis del contenido y la cinética de acumulación de la CP viral, por cuanto que éste es un indicador de la replicación viral (Hull, 2002).

Si bien, las Grxs monotiol han sido descritas como capaces de conferir resistencia a diferentes estreses abióticos, (Sundaram *et al.,* 2009; Sundaram and Rathinasabapathi, 2010), en este trabajo y en el anterior del laboratorio (Montes-Casado *et al*., 2010) es la primera vez que se describe una Grx de plantas que confiere resistencia frente a la infección viral. Adicionalmente, revelan que la proteína híbrida *Cch* GrxS12-GFP mantiene su actividad como ha sido descrito con anterioridad para otras Grxs híbridas (Rouhier *et al.,* 2006). Por otro lado, es interesante puntualizar que no se requiere una localización cloroplastídica para que tenga el efecto antiviral, por cuanto que la proteína de deleción, localizada en el núcleo y en el citoplasma también tiene el efecto protector.

De forma similar, la sobreexpresión de otro miembro de la familia de las tioredoxinas, NtTRXh3, en plantas de tabaco reduce la patogenicidad de los virus del mosaico del tabaco y del pepino e iba acompañada de la inducción del gen PR-1a (Sun *et al.,* 2010).

Para profundizar en los mecanismos de resistencia mediados por la sobreexpresión de la *Cch* GrxS12 hemos analizado las tasas de expresión/acumulación de los mRNAs de las proteínas PR-1, PR-2a and PR-5 que son marcadores de la señalización mediada por ácido salicílico (SA) (Ryals *et al.,* 1996) y de PR-2b, un marcador de la respuesta mediada por etileno (ET) (van Loon *et al*., 2006), en las cuatro líneas de plantas transgénicas a los 7, 21 y 28 dpi. En los estadios iniciales (7 dpi) no se detectó mRNAs de las proteínas PRs reguladas por el SA en las plantas control inoculadas con tampón, pero sí el mRNA de la PR 2b, indicando que los genes dependientes de ET se activan por el

daño mecánico. En los últimos estadios analizados (21 y 28 dpi), la expresión de los genes de las PRs-regulados por SA se incrementó en las plantas control, mientras que prácticamente no se detecta la expresión del gen de la PR regulada por etileno. La tasa de acumulación de los genes de las PRs regulados por SA fue particularmente alta en las plantas *Nb:Grx:GFP*. Si bien la expresión de genes de PRs mediados por SA ha sido descrito en plantas de tabaco en floración y senescentes (Lotan *et al.,* 1989, Obregón *et al.,* 2001), el incremento observado en las plantas que expresan la *Cch* GrxS12, respecto a los controles, parece estar asociado a su expresión, porque no se observó este incremento en las plantas control que expresan GFP libre.

En las hojas inoculadas con PMMoV-I, a los 7 dpi se induce la expresión de los genes de las PRs regulados por SA, pero a este tiempo post-inoculación no se observan diferencias entre las plantas transgénicas estudiadas. En las hojas superiores no inoculadas, no se observó expresión, o fue muy débil, ni de los genes que codifican las PRs ácidas ni de las básicas, tal y como era de esperar al tratarse de una interacción compatible donde no existe resistencia frente al virus y éste alcanza tasas de acumulación elevadas en estas hojas. En estadios tardíos de la infección (21 y 28 dpi), se observó un incremento en la acumulación de los mRNAs de los genes PRs regulados por SA, mientras que la acumulación de los regulados por ET fue insignificante. La acumulación de los mRNAs de los genes de las PRs regulados por SA había sido ya descrito por Tena (2012) en este mismo sistema huésped-virus, quien también describió la activación de un mecanismo de defensa antiviral en las hojas recuperadas de las plantas de *N. benthamiana* infectadas con PMMoV-I a los 28 dpi. Pero es interesante resaltar que nuestros resultados mostraron que la sobre-expresión de la proteína *Cch* GrxS12 y de las proteínas derivadas de ella, en las plantas de *N. benthamiana,* provoca una fuerte inducción de estos genes en las plantas control y una inducción más temprana en las plantas inoculadas con PMMoV-I. Lo que sugiere que la expresión constitutiva de estas proteínas favorece el establecimiento más temprano del mecanismos de defensa de la planta frente a PMMoV-I descrito anteriormente (Tena, 2012).

Nuestros resultados están en concordancia con los descritos para la proteína GRX480 de *A. thaliana,* que cuando se expresa ectópicamente en plantas de *Arabidopsis* permite la expresión del gen PR-1, regulado por SA, mientras que inhibe la expresión de los genes regulados por ácido jasmónico (JA) (Nadmukong *et al.,* 2007).

Además del incremento en la expresión de los genes de las PRs reguladas por SA, la expresión constitutiva de *Cch* GrxS12 en plantas de *N. benthamiana* también incrementoó la expresión del gen que codifica 9-LOX, que está implicada en una respuesta de defensa independiente de la ruta de señalización de JA (Vellosillo *et al.,* 2007). Aunque a 7 dpi se observó una débil acumulación de su mRNA en las hojas inoculadas con tampón de las plantas transgénicas que expresan *Cch* GrxS12 y las proteínas derivadas, este incremento fue más patente en las hojas inoculadas con PMMoV-I cuando se comparaban con las hojas inoculadas de las plantas que expresan GFP. Pero este incremento fue mucho mayor en las hojas recuperadas de las plantas infectadas a 28 dpi, coincidiendo con la mayor reducción de la acumulación viral. En trabajos anteriores se ha descrito que la expresión del gen 9-LOX se reduce en interacciones huésped-patógeno compatibles (Hwang and Hwang, 2010), mientras que su expresión y actividad incrementa en la respuesta de defensa HR (Rancé *et al.,* 1998; Montillet *et al.,* 2002; Göbel *et al.,* 2002; Gullner et al., 2010; Hwang and Hwang, 2010).

En su conjunto, estos resultados sugieren que *Cch* GrxS12 y las proteínas derivadas de ella activan más de un mecanismo de defensa de la planta en estadios tardíos del desarrollo de las plantas y durante la infección de PMMoV-I.

Para determinar si la expresión constitutiva de *Cch* GrxS12 alteraba las enzimas relacionadas con el glutation, hemos analizado la acumulación de los mRNAs de las proteínas glutation reductasa (GR) y glutation-S- transferasa (GST).

La enzima GR es una enzima clave en los ciclos Grx-GSH y ascorbato-GSH y tiene una función importante en el mantenimiento de los mecanismos antioxidantes de la célula y del estado redox celular mediante la utilización del poder reductor del GSH (Ansel *et al.,* 2006; Lillig *et al.,* 2008). Los resultados obtenidos en el análisis comparativo de la acumulación de su mRNA en las diferentes plantas transgénicas ensayadas, indican que la expresión constitutiva de la proteína *Cch* GrxS12 y de las proteínas de fusión *Cch* GrxS12-GFP y *Cch* Δ2M-GrxS12-GFP en plantas de *N. benthamiana* no afecta a la expresión del gen *gr* a los tiempos analizados, 7, 21 y 28 dpi. Los resultados son variables en las plantas infectadas con PMMoV-I, y parecen indicar que la expresión del gen *gr* en las plantas infectadas con PMMoV-I no depende de la expresión constitutiva de *Cch* GrxS12 sino más bien del tiempo post-inoculación analizado. Estos datos concuerdan con los descritos previamente por Hakmaoui *et al.,* (2012), que encuentran que la actividad GR disminuye en plantas de *N. benthamiana*

infectadas con el virus PMMoV-I en fases tempranas de la infección, 7-21 dpi, mientras que se detecta un incremento a los 28 dpi (Hakmaoui *et al.,* 2012).

Por otro lado, hemos analizado la expresión del gen que codifica la proteína Glutation-S-transferasa (GST), que es un buen marcador de la respuesta de la planta frente al daño celular producido por el estrés oxidativo (Fodor *et al.,* 1997; Sun *et al.,* 2010). También en este caso, la expresión constitutiva de *Cch* GrxS12 no cambia el patrón de acumulación del mRNA GST ni en las plantas control ni en las infectadas con PMMoV-I en fases tempranas de la infección hasta los 21dpi, indicando que su expresión no altera la respuesta de la planta frente al estrés oxidativo ocasionado por la infección viral en este periodo de tiempo (Hakmaoui *et al.,* 2012). Sin embargo, sí que se observan cambios en las plantas infectadas con PMMoV-I a los 28 dpi., apreciándose una disminución en los niveles de acumulación del mRNA GST principalmente en las hojas infectadas y en las recuperadas de las plantas transgénicas *Nb:Grx* y *Nb:Grx-GFP* infectadas con PMMoV-I, que llegan a alcanzar niveles similares a los de las plantas control, mientras que se encontraron niveles altos del mRNA GST en las plantas transgénicas *Nb:GFP* infectadas con PMMoV-I. Teniendo en cuenta que a este tiempo post-inoculación las plantas de *N. benthamiana* infectadas con PMMoV-I presentan un mecanismo de recuperación de los síntomas de la infección y que éste está asociado a una disminución en la acumulación de los niveles de H_2O_2 (Hakmaoui *et al.,* 2012), los resultados observados podrían ser atribuidos a un mejor control de las especies reactivas de oxígeno (ROS) en las plantas transgénicas que expresan *Cch* GrxS12, lo que limitaría el estrés oxidativo producido por el virus a este tiempo post-inoculación en dichas plantas.

Para analizar si la expresión constitutiva de *Cch* GrxS12 provoca algún cambio en la homeostasis redox de las plantas, analizamos la acumulación de las formas reducidas (NADH y NADPH) y oxidadas (NAD^+ y $NADP^+$) de los nucleótidos piridínicos (PN) NAD y NADP en las plantas transgénicas analizadas, tanto en las plantas inoculadas con tampón de inoculación como en las inoculadas con PMMoV-I.

El análisis mostró que la expresión constitutiva de *Cch* GrxS12 y de las construcciones derivadas de la misma en *N. benthamiana* no afecta a los niveles de acumulación de estos nucleótidos ni a su estado de oxidación en las plantas control, indicando que su acumulación es bastante estable, tal y como se ha descrito para cloroplastos de hojas de cebada (Wigge *et al.,* 1993). Los cambios observados parecen

depender más del estado de desarrollo de la planta que de la expresión de la *Cch* GrxS12 localizada en el núcleo y el citoplasma o en los cloroplastos, tal y como se ha descrito previamente (Yamamoto, 1963; Bonzon *et al.,* 1983; Queval and Noctor, 2007).

De los ensayos en plantas infectadas se deduce que la infección con PMMoV-I incrementa significativamente las tasas de acumulación de las formas reducidas NADH y NADPH. De forma similar, se ha descrito un incremento en la acumulación de NADH y NADPH en plantas de *Arabidopsis* infectadas con la bacteria *Pst-AvrRpm1* (Pétriacq *et al.,* 2012). En este sentido, se ha descrito que el incremento en PNs en los mutantes *CMSII* de *N. sylvestris* favorece una mayor tolerancia al estrés oxidativo inducido por ozono y por TMV (Dutilleul *et al.,* 2005). Además, en las plantas *Nb:Grx-GFP*, que acumulan una mayor cantidad de la proteína de fusión *Cch* GrxS12-GFP, a 28 dpi, se observan valores significativamente más altos que los observados en las otras plantas, y que va acompañado de una mayor resistencia frente a PMMoV-I.

De los cuatro PN, los niveles de NADH incrementaron entre 4 y 8 veces los valores de las plantas control, lo que indica que NADH es un buen indicador de la infección de PMMoV-I. El incremento en el contenido de NADH en las hojas infectadas y recuperadas de las plantas infectadas con PMMoV-I, produce un desequilibrio en la relación NADH/NAD^+ que podría inducir la producción de ROS (Millar *et al.,* 2001) o la regulación de los mecanismos antioxidantes de la célula (Dutilleul *et al.,* 2003). Aunque no conocemos la función de NADH en estas plantas transgénicas, sí que en trabajos previos se ha establecido una correlación entre el incremento en el contenido de NADH y/o NADH y NADPH y la resistencia frente a bacterias virulentas (Jambunathan and Mahalingan, 2006; Pétriacq *et al.,* 2012).

Además, los elevados niveles de NADH y de NADPH en las plantas infectadas con PMMoV-I podría desencadenar la expresión de genes de defensa. En plantas de *Arabidopsis* se ha descrito una correlación entre la acumulación de PNs y la inducción tanto de la expresión de genes de defensa de la planta como la resistencia frente a bacterias (Ge *et al.,* 2007; Zhang and Mou, 2009; Pétriacq *et al.,* 2012). Sin embargo, el patrón de acumulación de los mRNAs de las proteínas relacionados con la patogénesis (PR) parece indicar que no existe una correlación entre los niveles de PNs y la inducción de la expresión de los genes que codifican las PRs en las plantas que expresan la proteína *Cch* GrxS12 y las proteínas derivadas, tal y como se deduce del incremento en la acumulación de los mRNAs de las PRs en las plantas control a 21 y 28 dpi sin que se

observen cambios significativos ni en la acumulación ni en el grado de oxidación de los diferentes PNs analizados con respecto a los observados en las plantas que expresan la GFP libre. Esto indicaría que la expresión de los genes de las PRs mediada por la expresión de *Cch* GrxS12 es independiente de los niveles de PNs al menos en las plantas control.

Ha sido descrito que algunas proteínas Grx favorecen la tolerancia frente al estrés oxidativo (Cheng *et al.,* 2006; Cheng, 2008). Para determinar si la expresión constitutiva de *Cch* GrxS12 en *N. benthamina* incrementa la tolerancia a este tipo de estrés, cultivamos las plantas *in vitro* sobre un medio que contiene H_2O_2 o el herbicida paraquat. Los resultados obtenidos indicaron que la expresión constitutiva de *Cch* GrxS12 en plantas de *N. benthamiana* incrementa la tolerancia frente al estrés oxidativo incluyendo el estrés fotooxidativo provocado por paraquat. Teniendo en cuenta que *Cch* GrxS12 es una proteína cloroplastídica, estos resultados sugieren que esta proteína podría tener una función importante en la protección frente al estrés fotooxidativo, tal y como ha sido descrito para la GRXS13 citosólica de *A. thaliana* (Laporte *et al.,* 2012). Este efecto fue independiente de la localización subcelular de la proteína, bien en los cloroplastos o en el citoplasma y el núcleo. Por lo tanto la sobre-expresión de la proteína *Cch* GrxS12 confiere tolerancia a las plantas tanto frente al estrés biótico como abiótico.

Algunas proteínas que contienen grupos Fe-S son abundantes en los cloroplastos, las mitocondrias y en el medio celular (Balk y Lobreaux, 2005). La implicación de las Grx en el ensamblaje de los grupos Fe-S fue primero estudiada en levaduras, en las que se demostró que la deleción del gen que codifica Grx5 causaba una deficiencia en la síntesis de proteínas que contienen grupos Fe-S y que conduce a la acumulación de hierro que incrementa la sensibilidad de las células al estrés oxidativo (Rodríguez-Manzaneque *et al.*, 1999, 2002). La expresión de la proteína *Ch* GrxS12 en el mutante *Δgrx5* de levaduras permitió determinar que esta proteína no era capaz de rescatar las funciones de la proteína nativa Grx5 de levaduras, ni en la actividad de las enzimas con grupos Fe-S ni en la supresión de la acumulación de hierro en el mutante *Δgrx5*. Por lo tanto los estudios de transformación de *Cch* GrxS12 en el mutante *Δgrx5* parecen indicar que esta proteína no participa en la biogénesis y ensamblaje de los grupos Fe-S ni tampoco en la regulación de la homeostasis del hierro en cloroplastos.

Conclusiones

1. El análisis de la secuencia nucleotídica y aminoacídica de *Cch* Grx reveló que es una Grx de tipo monotiol perteneciente al grupo I, subgrupo C5/S12, con un sitio activo WCSYS y una conformación estructural característica de la familia de las Tioredoxinas. La proteína fue denominada *Cch* GrxS12

2. Las observaciones al microscopio confocal de protoplastos de plantas de *N. benthamiana* transgénicas confirmaron que la proteína *Cch* GrxS12 fusionada a la GFP se localiza en los cloroplastos, mientras que la proteína truncada *Cch* Δ2MGrxS12, con una deleción de 63 aa en el extremo N, fusionada a la GFP, se localiza en el citoplasma y en el núcleo.

3. La proteína *Cch* GrxS12 purificada posee actividad tiol oxidoreductasa *in vitro* ya que reduce el enlace disulfuro formado entre el glutation y el sustrato en el ensayo HED.

4. En estadios tempranos de la infección, la expresión de la proteína *Cch* GrxS12 en plantas de *N. benthamiana* no inhibe la acumulación viral, lo que indica que no afecta a la replicación de PMMoV-I, tal y como se confirmó en el análisis de la cinética de acumulación de la CP del virus en protoplastos, ni al movimiento célula a célula viral.

5. La expresión constitutiva de las diferentes formas de la proteína *Cch* GrxS12 en plantas de *N. benthamiana* resulta en una disminución de la acumulación viral en estadios tardíos de la infección. La expresión de las proteínas de fusión con la GFP también produce un descenso en la acumulación de PMMoV-I, indicando que ambas formas de la proteína fusionadas a la GFP conservan esta actividad.

6. A tiempos tardíos del desarrollo de las plantas tramsgénicas, la expresión de *Cch* GrxS12 incrementa la acumulación de los mRNAs de las proteínas PRs reguladas por SA pero no las mediadas por etileno, tanto en las plantas control como en las infectadas con PMMoV-I.

7. La expresión de *Cch* GrxS12 en plantas de *N. benthamiana* incrementa la tolerancia frente al estrés oxidativo causado tanto por H_2O_2 como por el herbicida paraquat, lo que indica que la proteína es también capaz de proteger frente al estrés abiótico en condiciones *in vitro*.

8. La proteína truncada *Cch* Δ2MGrxS12-GFP, localizada en el citoplasma y en el núcleo es también capaz de reducir la acumulación de PMMoV-I y proteger frente al estrés oxidativo, indicando que la localización en los cloroplastos no es requerida para el efecto de inhibición viral ni para la protección frente al estrés abiótico.

9. La expresión de *Cch* GrxS12 no altera el contenido de los nucleótidos piridínicos NAD y NADP en las plantas control, indicando que el incremento en la expresión de los genes de las PRs, inducida por *Cch* GrxS12 en las plantas control en estadios tardíos del desarrollo de la planta, es independiente de la acumulación de estos nucleótidos.

10. La infección de PMMoV-I en las plantas transgénicas provoca un incremento en la acumulación de los niveles de NADH y NADPH. El incremento de los niveles de NADH es un buen marcador de la infección de PMMoV-I.

11. El incremento en la resistencia frente a PMMoV-I, la elevada acumulación de PRs y el incremento en los niveles de NADH y NADPH en plantas de la línea *Nb:Grx-GFP* estaba asociada a una mayor acumulación de la proteína *Cch* GrxS12-GFP en estas plantas.

12. La expresión de *Cch* GrxS12 no altera la acumulación del mRNA de la enzima antioxidante GR, pero reduce la acumulación del mRNA de la enzima GST a tiempos tardíos de la infección viral.

13. *Cch* GrxS12 no participa en el mecanismo de ensamblaje de los grupos Fe-S porque no rescata el fenotipo de supresión de acumulación de hierro o la actividad de enzimas que contienen grupos Fe-S en el mutante de levaduras Δ*grx5*.

SUMMARY

Diseases caused by plant viruses are one of the major problems for agriculture production all over the world. In pepper crops (*Capsicum spp), Pepper mild mottle virus* (PMMoV) is one of the most destructive virus. This virus belongs to the *Tobamovirus* genus. In *Capsicum spp,* resistance against tobamovirus is governed by an allelic serie of genes: the *L* genes and *Hk* gene. Based upon the pathogen aggressiveness against *L*-gene mediated resistance, *Tobamoviruses* has been classified as pathotypes P_0, P_1, $P_{1,2,}$ $P_{1,2,3}$ and $P_{1,2,3,4}$. PMMoV is the most pathogenic tobamovirus towards the *L* resistance gene. The Italian strain of PMMoV (PMMoV-I) was used in this work. It belongs to the pathotype $P_{1,2,3}$ which is able to infect systemically the L^1- L^3 *Capsicum* plants, and it is localized in the L^4 plants.

In our laboratory, it has been previously isolated a Glutaredoxin (Grx) from *C. chinense* plants whose mRNA is induced in both the compatible and the incompatible interactions after the infection with PMMoV-I and PMMoV-S, respectively.

Grx are small thiol disulfide oxidoreductases that catalyze the reduction of disulfide bonds either in the target proteins or in the substrates in the presence of glutathione (GSH). Grxs are well conserved in all organisms and their function in *Escherichia coli*, yeast and mammal are well characterized. Since very little information was available for the function of these Grx proteins in plants and also against plant pathogens, the main aim of this work was to carry out the molecular and biochemical characterization of the *C. chinense* Grx (*Cch* Grx) protein and to analyze its function in PMMoV-I infection and/or plant response.

To address these objectives the previous work from our group constructed *Nicotiana benthamiana* Domin transgenic plants constitutively expressing the native choroplastic Grx protein *Cch* Grx (Grx Exp), *Cch* Grx fused to GFP (Grx:GFP) and a derivative with a deletion of 63 aa at its N terminus fused to GFP (*Cch* Δ2M:Grx:GFP) that does not located to the chloroplasts but to the nuclei. *N. benthamiana* Domin plants are susceptible to all of the tobamoviruses and it is appropriate to study the role of *Cch* Grx in a plant-virus compatible interaction. The Italian strain of *Pepper mild mottle virus* (PMMoV-I) was chosen to carry out this study, because preliminary experiments from our laboratory had shown that at latest stages of the infection their constitutive expression in this host lead to a reduced viral accumulation that it was due to a reduced number of infected cells, but not to a reduced cell-to-cell movement. By

transient expression in *N. benthamiana* plants it was also established that the protein was located to the chloroplast, and that the 63 aa N- deleted protein was located to the nuclei.

Cch Grx protein sequence analysis shows that it belongs to Group I monothiol Grx and it is positioned in the S12 subgroup with a WCSYS active site, them we referred to it as *Cch* GrxS12. The BLAST analysis shows that the protein belongs to single domain Grxs and further the phylogenetic tree shows that the protein is showing maximum identity with the Grxs reported from plants and much divergence with the Grx reported from yeast. CSYS active site Grxs and Grx-like proteins were found to be conserved among the plants and yeast but not reported from prokaryotes. The 3-D structural predictions for the protein show that it belongs to the Trx-fold family proteins which are characterized by having centrally located β-strands surrounded by α-helices. The structure predicted in this work for *Cch* GrxS12 was found to be identical to the structure reported for PtrGrxS12 from *Populus*. The comparison of the two Grxs structures revealed that most of the regions including the GSH binding regions were conserved between these two proteins.

To characterize the oxidoreductase activity of the *Cch* GrxS12 protein, it was expressed and purified from *E. coli* and the *in vitro* activity of the protein was measured by HED assay, in which the oxidization of NADPH was measured. The protein was found to be positive in the HED assay and thus possesses the oxidoreductase activity.

To confirm the subcellular localization of *Cch* GrxS12, protoplasts were obtained from the *N. benthamiana* transgenic lines and the GFP-fused proteins were observed by confocal microscopy, confirming that *Cch* GrxS12 fused to GFP was targeted to the chloroplast whereas the 63aa truncated Grx fused to GFP was located in both the cytoplasm and the nucleus, as free GFP.

The *Cch* GrxS12 accumulation level was analyzed in the different *Cch* GrxS12-expressing transgenic lines by means of Western blot using *Cch* GrxS12 specific immunoserum available from our laboratory. The analysis showed that *Cch* GrxS12 accumulation was ten times higher in the *N .benthamiana* line expressing native *Cch* GrxS12 fused to GFP than in the other plant lines.

The effect of the constitutive expression in *N. benthamiana* plants of *Cch* GrxS12 targeted to either the chloroplast or to the nucleus and cytoplasm on PMMoV-I viral infection

was analyzed during early (7 dpi) up to late (28 dpi) stages. At 21 dpi the plants start to recover from the PMMoV-I infection.

The inhibitory role of *Cch* GrxS12 against PMMoV-I accumulation was studied by analyzing the viral CP and RNA accumulation. Expression of *Cch* GrxS12 in *N. benthamiana* plants was found to inhibit the viral accumulation at the later stages of infection but none effect was found at the early stage of infection. The data show that *Cch* GrxS12 is not inhibiting the viral replication, as it was confirmed by the analysis of viral PMMoV-I infection in plant protoplasts from the different transgenic lines. It was found that viral CP accumulation was uniform at the different time points analyzed and it was also found that the percentage of infected protoplasts was the same among the GFP-expressing plant line and *Cch* GrxS12-expressing ones.

To study the underlying resistance mechanism mediated by *Cch* GrxS12 against PMMoV-I, the accumulation level of SA-regulated acidic PR protein mRNAs (PR-1, PR-2a and PR-5) and ethylene (ET)-regulated basic PR protein mRNA (PR-2b) were analyzed in the GFP expressing and *Cch* GrxS12 over expressing lines during early and late stage of infection. At early stages of infection, the accumulation level of SA-regulated PR mRNAs got increased in the PMMoV-I inoculated leaves when compared to the mock inoculated control leaves while the ET-regulated basic PR mRNA accumulation was found to be the same between the mock-inoculated control plants and PMMoV-I inoculated ones. This shows that SA-regulated PR protein genes were induced by PMMoV-I infection whereas the ET-mediated PR protein gene was induced by mechanical injury. Further in the inoculated and in the systemic leaves, no difference in PR mRNAs accumulation exists between *Cch* GrxS12 over expressing lines and GFP expressing line. At late stage of PMMoV-I infection (21 and 28 dpi), the accumulation level of SA-regulated PR mRNAs was found to be higher than the ethylene-regulated PR mRNA. In addition, in the mock-inoculated control plants, over-expression of *Cch* GrxS12 leads to the accumulation of a high level of SA-regulated PR mRNAs and it was found to be higher than that of the ET-regulated PR one. Further, in the PMMoV-I infected plants, the over-expression of *Cch* GrxS12 enhanced the accumulation level of SA-regulated PR mRNAs when compared to the GFP expressing line. *Cch* GrxS12 was found to have little effect in ET-regulated PR mRNA. At 28 dpi, analysis of the recovered plant leaves shows a high level of PR mRNA accumulation in all of the infected plants, being higher in the Grx expressing plant lines.

To analyze whether *Cch* GrxS12 was able to induce one or more defence pathway, the mRNA expression level of 9-LOX, which is independent of JA and SA pathways, was analyzed. At 7 dpi, in the PMMoV-I inoculated plants an increase in 9-LOX mRNA accumulation was found in the *Cch* GrxS12 expressing lines while at 28 dpi the increase was found in the recovered leaves which shows that *Cch* GrxS12 over-expression could be able to activate more than one plant defence response pathway during the plant development and also during PMMoV-I infection.

Analysis of the antioxidant enzyme machinery of the cell system such as GR and GST were also found to get vary along the PMMoV-I infection. GR mRNA accumulation got decreased in the PMMoV-I infected plants and the expression of *Cch* GrxS12 was not found to alter the expression of GR mRNA. The accumulation level of GST mRNA was found to get increased during the PMMoV-I infection at 7 and 21 dpi but at 28 dpi, the accumulation level got reduced in the *Cch* GrxS12 expressing lines what suggests that *Cch* GrxS12 could be able to reduce the oxidative stress conditions caused by the PMMoV-I infection at that time.

To analyze the role of *Cch* GrxS12 in maintaining the redox status of the cell, and also to have better insight in the Grx-mediated PR mRNA accumulation, the oxidized and reduced forms of the pyridine nucleotides (PN) [NAD^+, NADH, $NADP^+$ and NADPH] were analyzed at the late stage of plant growth (21 and 28 dpi) in the control and *Cch* GrxS12 over-expressing lines. Overall the level of NAD^+, NADH, $NADP^+$ contents got increased at 28 dpi when compared with 21 dpi whereas the level of NADPH was found to be lowered.

Analysis of the PNs in the mock-inoculated control plants shows that expression of *Cch* GrxS12 does not seemingly alter the redox status of these metabolites as their level were found to be the same between the control and *Cch* GrxS12-over expressing lines. On the other hand, infection with PMMoV-I altered the PNs levels, where the accumulation level of the reduced form of the PNs such as NADH and NADPH got increased when compared with the mock-inoculated control plants. The accumulation level of NADH and NADPH was particularly higher in the *Nb:Grx-GFP* line where the Grx accumulation was also found to be higher. Among the reduced PNs, the level of NADH content was found to be 4-8 times higher in the PMMoV-I infected plants and thus revealed that NADH content is a good marker for PMMoV-I infection. Comparative analysis of the PNs between the mock-inoculated controls, PMMoV-I infected and recovered plant samples shows that alteration in the PNs level is not influencing the PR mRNAs

accumulation and thus suggesting that *Cch* GrxS12-mediated PR mRNAs accumulation is independent of PN alteration.

Cch GrxS12 gene contribution against abiotic stress tolerance was studied by the *in vitro* root growth of the different transgenic lines in H_2O_2- and paraquat-containing media. The *Cch* GrxS12 over-expressing lines were found to have better growth than the GFP expressing line in the media containing either H_2O_2 or paraquat and this confirms that *Cch* GrxS12 increases the abiotic stress tolerance of the plants. Further, the *Cch* Δ2M-Grx-GFP transgenic line was also found to have better growth than GFP control line, thus suggesting that *Cch* GrxS12 contribution against abiotic stress tolerance was independent of chloroplast or cytoplasm/nuclei localization.

Besides pathogen resistance and oxidoreductase functions, novel function of *Cch* GrxS12 protein in Fe-S cluster assembly was also studied by transforming into the yeast *Δgrx5* mutants in which the function of Grx in Fe-S cluster assembly is well documented (Rodríguez-Manzaneque *et al.*, 2002). Fe-S cluster containing proteins are playing important roles in plants chloroplast and mitochondria. Many plant Grxs and the Grxs reported from other organisms are able to perform this Fe-S cluster assembly function. In order to study the involvement of *Cch* GrxS12 in the Fe-S cluster assembly or Fe-S biogenesis mechanism *Cch* GrxS12 was expressed into the yeast Δ*grx5* mutant. For transforming into yeast Δ*grx5* mutant the sequence coding for the mature *Cch* GrxS12 protein was cloned into the yeast integrated plasmid and yeast strains expressing the *Cch* GrxS12 protein were selected. The selected yeast strains containing the *Cch* GrxS12 were analyzed for their ability to restore the activity of Fe-S containing enzymes and the suppression of free Fe accumulation in Δ*grx5* mutant. The *Cch* GrxS12 protein transformed in Δ*grx5* yeast strain could not be able to suppress the iron accumulation or to restore the activity of Fe-S cluster containing enzymes. Thus suggesting that *Cch* GrxS12 is not able to participate either in the biogenesis of Fe-S cluster assembly or in the regulation of iron homeostasis in the chloroplasts.

1.INTRODUCTION

1.1. General characteristics of *Pepper mild mottle virus*

Spain is the second largest country from the European Union in terms of agricultural production with about 24 million hectares of utilized agricultural land as it is shown in the census of 2009, so that plant health is a big concern for Spain. Among the diseases that occurred in plants, those caused by viruses affect the morphology and physiology of the plants and thus cause enormous economic losses worldwide (rev. Hull, 2002). In the case of pepper crops, a special interest is focused towards the so-called pepper strains of the tobamovirus. These strains are destructive for pepper crops mainly in the fruits, where they induce reduction in size, malformation, blistering and necrosis (Fig.1.1). One of these pepper strains, *Pepper mild mottle virus* (PMMoV) (Wetter *et al.,* 1984), was found to be one of the most prevalent tobamoviruses in pepper crops in the province of Almería, SE Spain, in epidemic outbreaks between 1984 and 2004 (Tenllado *et al.,* 1997; Fraile *et al.,* 2011). This virus affects all the species of the *Capsicum* genus, having isolates that are able to evade the L^1-L^4-gene-mediated resistance (rev Gilardi *et al.,* 1999; Genda *et al.*, 2007; Antignus *et al.*, 2008). Disease symptoms are very mild and hardly discernibles in the vegetative stage of the crop and are essentially visualised during fruit formation (Gilardi *et al.,* 1999). The virus can cause 100% economic loss by spreading to the entire field due to the easiness of mechanical transmission from plant to plant or from contaminated cell debris or during cultivation.

Fig.1.1. Symptoms caused by PMMoV in *C. annuum* fruits.

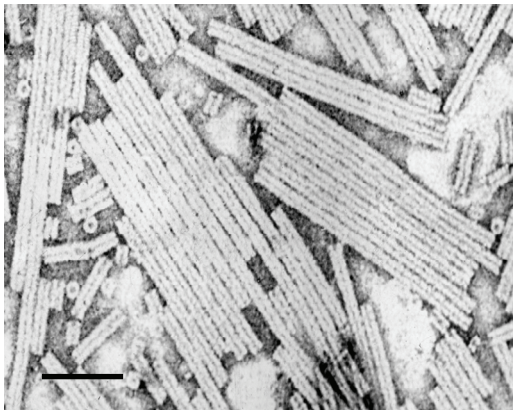

Fig.1.2. Electron microscope view of negatively stained PMMoV particles. Bar represents 0.1 μm.

The virus is transmitted through infected seeds and they can survive in the soil for months (Ikegashira *et al.,* 2004; Tena *et al.,* 2012). Earlier, fumigation of soil with methyl bromide was done to prevent the disease but the product was banned by the Montreal Protocol in developed countries since 2005. Consequently, an alternative strategy is required for disease control (Goldbach *et al.,* 2003). The strategy should take into account the prevention of the devastating effects of diseases caused by pathogens. There is also a need to have a deep knowledge of the plant-virus infection cycle and the plant genes involved in control of virus spread in order to find new approaches for the control of plant viral diseases.

Resistance against tobamovirus in *Capsicum* spp. is manifested through the induction of necrotic local lesions (NLL) and virus confinement to the primary infection sites as the result of the activation of a hypersensitive reaction (HR). This resistance is governed by a serie of four genes known as L^1-L^4, located at the locus *L* (Boukema *et al.,* 1980). Tobamoviruses infecting pepper plants are classified into five subgroups as pathotypes P_0, P_1, $P_{1,2,}$ $P_{1,2,3}$ and $P_{1,2,3,4}$ on the basis of their increased pathogenicity against the *L* gene-mediated resistance. Viruses belonging to the P_0 pathotype induce HR in the four L^1-L^4 resistance genotypes. Viruses that belong to the P_1 one evade the L^1 mediated resistance and induce the HR in L^2- L^4 plants. Viruses from the $P_{1,2}$ pathotype infect L^1 and L^2 plants systemically, but are localized in L^3 and L^4 plants and viruses from the $P_{1,2,3}$ pathotype infect the L^1- L^3 plants systemically, eliciting the HR only in the L^4 plants (Boukema,1982). Viruses from the $P_{1,2,3,4}$ pathotype infect systemically the four *L* plants.

PMMoV is the most pathogenic tobamovirus towards the *L* gene-mediated resistance. Viral isolates belonging to the pathotypes $P_{1,2}$, $P_{1,2,3}$ and $P_{1,2,3,4}$ have been described. The Spanish strain (PMMoV-S) corresponds to a $P_{1,2,}$ pathotype and it was isolated from pepper plants infected in Spain (García-Luque *et al*., 1990). The Italian strain (PMMoV-I) corresponds to a $P_{1,2,3}$ pathotype and it was isolated from pepper plants infected in Sicily (Italy) (Wetter *et al*., 1984). Recently a new PMMoV isolate was described in Japan (PMMoV-L4BV $P_{1,2,3,4}$) that was able to overcome L^1 to L^4 gene mediated resistance (Genda *et al*., 2007). PMMoV has been identified as the major RNA viruses found in human faeces (Zhang *et al.,* 2006) and the virions recovered from feces were able to infect the plants (Zhang *et al.,* 2006; Colson *et al.,* 2010). This

finding has led to the proposal that PMMoV can be used as an effective indicator of fecal pollution in surface waters (Rosario *et al.,* 2009; Hamza *et al.,* 2011).

PMMoV belongs to the *Tobamovirus* genus. Virus particles are rigid helical rods of about 300 nm in length and 18 nm in diameter. Each particle consists of about 2130 copies of 17-18 kDa coat protein (CP) subunits which are arranged as a helix surrounding the viral RNA (Fig. 1.2). The genome of PMMoV-S consists of a plus single-stranded RNA molecule of 6357 nt (Alonso *et al*., 1991) with a CAP (^{7}mGpppG) structure at the 5 'end of the RNA bound to a leader sequence fragment of 69 nt called "Ω fragment". It has been shown that this structure acts as a translation activator for both prokaryotes and eukaryotes (Gallie and Walbot, 1992). At the 3'-end, the genome has 199 nt non-coding sequence (3'UTR) which adopts a structure of truncated tRNA (Avila-Rincón *et al*., 1989). Both ends increase the translation of viral RNA (Gallie and Walbot, 1992; Gallie, 1996). The viral RNA contains four open reading frames (ORFs) which encode four different proteins (Fig. 1.3). The first ORF (nt 70-3423) encodes a 1117 aa protein called 126K protein. The suppression of the amber stop codon (UAG) in the 126K protein enables the read-through of nt 4908, so that an 1612 aa protein is translated that has been designated as 183K protein. The third ORF (nt 4909-5682) encodes a protein of 257 aa, named as 30K protein. Finally, the fourth ORF (nt 5685-6158) encodes the 156 aa viral CP (Alonso *et al.,* 1991).

The 126 and 183K proteins are translated from the viral genomic RNA (gRNA), while the 30K and CP are translated from 3'-coterminal subgenomic RNAs (sgRNAs), that are synthesized by using the negative strand as template, where are located the subgenomic promoters (rev. in Hull, 2002). The 126K protein has two domains, the methyltransferase domain (aa 1 to 494), necessary for the formation of the CAP structure in the gRNAs and sgRNAs (Dunigan and Zaitlin, 1990), and the helicase domain in the C- terminus of the protein (aa 833 to 1086) necessary to unwind double-stranded RNAs formed during viral replication and it has been implicated in the recognition of the 3'-end of RNA to initiate the synthesis of minus strand RNA (Goregaoker and Culver, 2003; Tena *et al*., 2012). An inter-domain region without any known specific function in virus replication is located between those two domains (Koonin and Dolja, 1993).

Fig.1.3. Genome organization of tobamoviruses. The boxes show the coding region of the genome. A CAP structure is found at the 5´-end and the 3´end possesses the non-coding region with a truncated tRNA structure. The genomic RNA is the template for the 126 and 183 kDa replicase proteins. The two other ORFs coding for the 30kDa protein and the CP are translated from subgenomic RNAs.

The other functions of the 126K protein are the ability to elicit the resistance mediated by the *Hk* gene in pepper plants, assigned to the methyltransferase domain (Matsumoto *et al.*, 2009) and its capability to trigger the HR in tobacco plants containing the *N* resistance gene after tobamovirus infection, assigned to the helicase domain (Padgett et al., 1997; Erickson *et al.,* 1999), as well as the thermoactivation of PMMoV-S at higher temperatures (Tena et al., 2012).

The 183K protein contains the RNA-dependent RNA polymerase (RdRp) motif, at the carboxy end of the protein, in addition to the methyltransferase and helicase domains, common to the 126K protein. Its involvement in several viral processes, such as the interaction between 126 and 183K proteins, needed for viral replication, has been well established (Goregaoker *et al.*, 2001).

Both, 126 and 183K proteins, are required for viral replication (Ishikawa *et al.*, 1986; Lewandowski and Dawson, 2000). The 126K protein is also needed for short distance viral movement (Hirashima and Watanabe, 2001). Furthermore, the 126K of both TMV and ToMV have been identified as suppressors of gene silencing (Kubota *et al.,* 2003; Ding *et al.,* 2004, Wang *et al.,* 2010).

The 30K protein or viral movement protein (MP) is necessary for the cell-to-cell movement of tobamoviruses (Deom *et al.,* 1987; Meshi *et al.,* 1987) through plasmodesmata,

increasing their size exclusion limit (Wolf *et al.,* 1989). The movement of viral RNA through plasmodesmata takes place by interaction with the MP through a nucleic acid binding domain which helps for its unfolding (Wolf *et al.,* 1989; Oparka *et al.,* 1997).

The CP protein is the only structural protein of tobamoviruses. It is required for the viral long distance movement (Holt and Beachy, 1991**;** Simon-Buela and García-Arenal 1999; Tena *et al.,* 2012), since a funtional CP for encapsidation is required for long distance movement of the virus (Nelson and van Bel, 1998). Tobamovirus CP is also involved in the development of symptoms in certain plant species (Culver, 2002) and it has been identified as the inducer of the resistance conferred by the *N*' gene in *N. sylvestris* (Culver and Dawson, 1989) and L^1-L^4 genes in *Capsicum spp*. (Berzal-Herranz *et al.,* 1995; Gilardi *et al.,* 1998; Dardick *et al.,* 1999; Gilardi *et al.,* 2004; Genda *et al.,* 2007).

1.2. Viral infection cycle

PMMoV infection cycle has not been studied specifically but it is assumed to be the same as that of other members of *Tobamovirus*. Tobamoviruses get its entry into the plant cells through the mechanical damage of cuticle, into partially damage cells, and several processes have to occur before virus cause a successful infection in the host plant: RNA uncoating, viral replication and translation, viral cell-to cell and long-distance movement. In these processes, viral and plant factors are involved and the success of progress depends upon the interaction between plant and virus factors (Hull, 2002).

1.2.1. Uncoating of TMV

To initiate TMV infection, RNA must be uncoated. Shortly after the entry of virus inside the cell, the process of particle disassembly starts and it is a bidirectional process (Wu and Shaw, 1996). The 5'-3' uncoating is a co-translational mechanism. When translation is initiated, the ribosomes start to proceed along TMV RNA and translate the 5' ORF and thus produce 126/183K replicase proteins by displacing the coat protein subunits. The process continues until the ribosomes reach the stop codon of the 126/183-K ORFs. Wilson (1985), suggested that the replicase protein released during the process might be helpful for the disassembly of the particles in 3'-5' direction associated to viral replication (Hull, 2002).

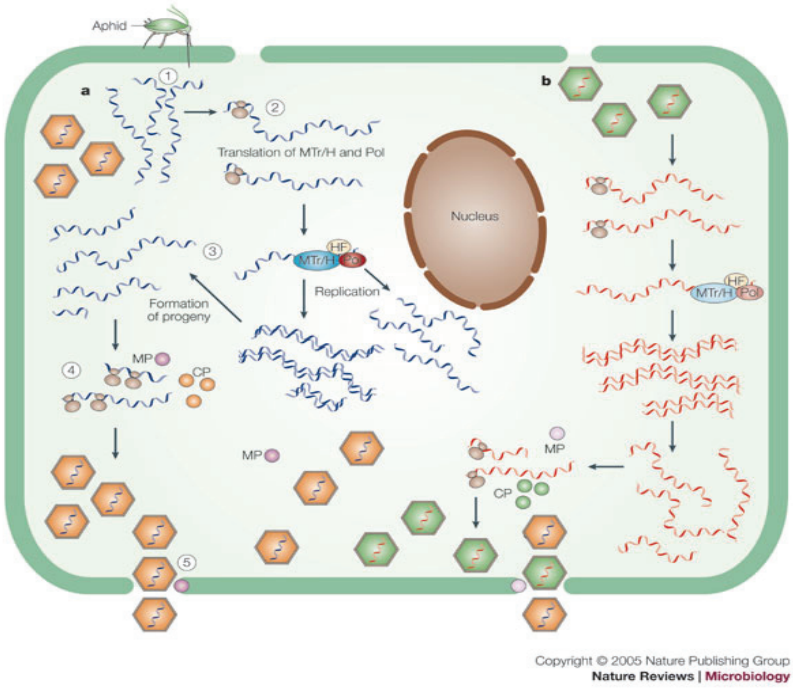

Fig.1.4. Infection life cycle of positive strand RNA virus infection. (rev Roossinck, 2005).

1.2.2. Replication of viral RNA

Once the viral RNA is uncoated, it is ready for viral replication and translation. The mechanism of TMV replication is the same as like other single-stranded RNA virus of positive polarity. The replication of the positive strand RNA begins with the recruitment of the RNA to the cytoplasmic side of membranes to form a replication complex in which the negative-strand RNA is synthesised from the positive viral RNA template. In TMV-infected plants, two kinds of RNA structures have been observed: the replicative form (RF) that is a base-pared structure with full-length double stranded RNA chain, and the replicative intermediate (RI) that is only partially double-stranded RNA and contains single-stranded nascent (+) RNA (Hull, 2002). Mas and Beachy (1999) showed that TMV RNA, the viral replicase and the MP protein co-localized at the endoplasmic reticulum (ER) and that were associated with ER-related vesicles. During the replication process, the 30K and viral CP subgenomic RNAs are also produced (rev. in Hull, 2002). The replication process is thought to involve multiple types of host factors, many of which have not yet been identified (Buck, 1996; Ahlquist *et al*., 2003; Ishibashi *et al.,* 2010; Pallas and García, 2011).

1.2.3. Translation

TMV translation is performed by the host translational machinery from both genomic and subgenomic viral RNAs (Hull, 2002). The studies showed that circularization of viral RNAs increased the efficiency of translation (Thivierge *et al.,* 2005). The M^7GpppG CAP structure and untranslated leader Ω sequence are also helpful for the efficient translation. The tRNA-like structure located at the 3' end of the genome is helpful for the translation. The tRNA region is preceded by several pseudoknots (PKs) of hairpin and loops and it was shown that this domain interacts with the host initiation translation factor (eIF1A). This interaction is important for replication because mutations in this region reduced the synthesis of RNA and viral accumulation. The exact mechanism of action is still unclear, although eIF1A has been suggested to stimulate replication in association with other host factors (Zeenko *et al.,* 2002). It was further proved that eIF1A was also found to be abundant in the infected cell replicative bodies, along with ribosomes, a fact supporting the hypothesis that it is a necessary factor for translation and efficient replication of TMV (Thivierge *et al.,* 2005). However, previous analysis upon the translational activity of PMMoV and TMV ruled out its role in translation since both viruses translated with the same efficiency their encoded 126K proteins (Ávila-Rincón *et al.,* 1989).

1.2.4. Viral movement

Following the initial round of replication in the cells, the virus has to move through the plasmodesmata to nearby cells, a process termed either short distance movement or cell-to-cell movement, until it reaches the vasculature. From the vascular system, viruses spread to the rest of the plant, in a process known as long distance movement. This virus movement is thought to be a passive process along with the flux of photosynthate (Lartey *et al*., 1998); in contrast, cell-to-cell movement is an active function, requiring a specific interaction between the virus and plasmodesmata (PD).

1.2.4.1. Cell-to-cell movement

Cell-to cell movement of tobamoviruses takes place through PD and requires the viral MP. Much experimental work has been done in the interaction between the virus factors and plasmodesmata for cell-cell movement. The interaction is mediated by the MP of TMV which

acts by increasing the exclusion limit (SEL) of plasmodesmata to facilitate virus movement (rev. in Lucas and Gilbertson, 1994; Carrington *et al.,* 1996). The increase in PD SEL during TMV spread is transient, returning to a restricted size after passage of the infection front (Oparka *et al.,* 1997). The MP itself also can move between cells when ectopically expressed (rev. in Niehl and Heinlein, 2011). MP binds cooperatively to viral RNA giving an unfolded protein-RNA complex that translocates through the PD enlarged channels (Citovsky *et al.,* 1990; 1992). MP protein also interacts with several plant proteins (Harries *et al.,* 2010). The first one described was pectin methylesterase (PME) from the cell wall, and a function in increasing the permeability of PD was postulated (Dorokhov *et al.,* 1999; Chen *et al.,* 2000). Interaction with proteins located at plasmodesmata, such as calreticulin is necessary for efficient viral dissemination through plasmodesmata (Chen *et al.,* 2005), and a receptor of the plant host, an ankirin repeat-containing protein (ANKs), that promotes reduction of callose deposits in PD and an increase in PD SEL (Ueki *et al.*, 2010) have also been described. The MP also interacts with cytoskeletal elements such as F-actin (McLean *et al.,* 1995) and microtubules (rev. in Niehl *et al.,* 2013) as well as with ER (Heinlein *et al.*, 1998; Mas and Beachy, 1999; Asurmendi *et al.*, 2004). The mechanism by which MP modifies PD to enable intercellular traffic is not known yet, but recent findings suggested that the SEL increase was due to the microfilament severing activity of MP (Su *et al.,* 2010).

In addition to the MP, the 126K is also involved in TMV cell-to-cell movement (Hirashima and Watanabe 2001; 2003). Although the mechanism remains unknown, recent findings suggested that replicase and MP associate to viral RNA, cytoskeleton elements and host factors to promote TMV viral complex intracellular and intercellular movement (Peña and Heinlein 2012; Liu and Nelson 2013).

1.2.4.2. Long distance movement

The virus moves long distance through phloem in a passive process, following the flow of photosynthate from source to sink tissues (Leisner and Turgeon, 1993; Roberts *et al*., 1997; Nelson and van Bel, 1998). By means of antisense approach, the role of PME was found to support not only the cell-cell movement but also the long distance movement of TMV (Chen, 2003). On the virus side, many experiments have been done in support for the crucial role of viral CP and MP in long distance movement. The CP of TMV is essential for rapid systemic

movement of virus (Dawson *et al*., 1988). Although the role of MP in the systemic movement of virus has not been directly shown, it has been suggested that the MP can work along with CP for long-distance movement of TMV (Lucas and Gilbertson, 1994). However, the results obtained by Gera *et al*., (1995) and Sareila *et al*., (2004) suggested that a functional MP is not required for tobamovirus movement within the phloem. In addition, unloading from the phloem does not seem to require either a MP or a functional CP (Sareila *et al*., 2004).

1.3. Plant-virus interaction

Viruses use various strategies to utilize cellular resources for their infection. The interaction between virus and plant determines the outcome of the defence mechanism. Based on their interaction with the host factors, the plant-virus interactions are classified as compatible and incompatible ones. In compatible host-virus interactions, the infection spreads all over the plant and results usually in the onset of disease symptoms. In this case the plant is susceptible to the viral infection. By contrast, incompatible interactions result in cessation of virus replication and/or movement at or near the sites of inoculation (Maule *et al.,* 2002), and the plants are immune or resistant to the infection.

When plants encounter a pathogen attack, they quickly activate the defence mechanisms to arrest the pathogen attack. The mechanisms developed by the plant to prevent pathogen attack were termed as innate and induced resistance. Innate defence is due to the absence of essential host susceptibility factors (passive resistance) or to the existence of pre-existing physical and chemical barriers that the virus is not able to overcome or to the induction of basal defense mechanisms, at present unknown in plant-virus interactions. One kind of response is an induced basal defence mechanism, where a non-specific defence response is induced by pathogen associated molecular patterns (PAMPs), resulting in PAMP-triggered immunity (PTI). Some viruses can evolve to acquire virulence factors (effectors) that contribute to pathogen virulence, so that viruses succed to produce viral infection, resulting in effector-triggered susceptibility (ETS) (Jones and Dangl, 2006). However, in some cases these virulence factors can be specifically recognized by plant host resistance genes. They behave as avirulence factors (Avr) and a specific defence response is induced, called effector-triggered immunity (ETI). This response is a fast and amplified PTI response, resulting in disease resistance (Jones and Dangl, 2006; Chrisholm *et al.,* 2006). The interaction triggers an HR which involves programmed cell

death, which show similarity with the process of apoptosis described in animal cells (rev. Greenberg and Yao, 2004), production of reactive oxygen species (ROS) (rev. Torres, 2010), accumulation of defense phytohormones, salicylic (SA), jasmonic (JA), abscisic acid (ABA) and ethylene (ET), (rev. en Robert-Seilaniantz *et al.*, 2011), synthesis of antimicrobial compounds and accumulation of metabolites (Dangl and Jones, 2001).

Associated to the HR a defence mechanism is induced that was further structured as local acquired resistance (LAR) and systemic acquired resistance (SAR). Ross showed that when tobacco plants were infected with TMV, the plants developed resistance against a further TMV infection. The resistance developed at the infected leaves was termed LAR, whereas that developed at the distal parts of the plants was termed SAR (Ross, 1961). Both LAR and SAR induced by one pathogen are effective against a large variety of microbes and viruses (Hammerschmidt, 2009).

Several studies have proven that when the plant is infected by a virus many changes occurred at the gene expression level both during the compatible and incompatible interaction (Whitham *et al.,* 2003; Marathe *et al.,* 2004; Postnikova and Nemchinov, 2012). Microarray-based studies of compatible virus-plant interactions have shown that virus infection triggers important changes in plant gene expression, including genes associated with the host defense response to the pathogen. Stress and defence-related genes, such as pathogenesis-related (*PR*) genes, genes involved in mantaining the redox homeostasis, transcription factors, etc., typical for the incompatible interaction response, were up-regulated (rev. Whitham *et al.,* 2006). However, in compatible interactions that defense response is weaker and delayed (rev. Desender *et al.,* 2007; Elvira *et al.,* 2008).

1.4. Identification of a Glutaredoxin in *C. chinense*

Previous work from our group established that during the incompatible interaction between PMMoV-S and *C. chínense* PI 159236 plants, harbouring the L^3L^3 gene, the HR is induced and it activates the synthesis of ROS at early stages of plant-virus interaction (Gilardi, 2000). By using the "mRNA Differential Display PCR" technique (Liang and Pardee, 1992) and RACE-PCR (Chenchik *et al.,* 1998), a cDNA band was isolated whose expression was induced during *C.chinense* compatible (PMMoV-I) and incompatible (PMMoV-S) interactions. The nucleotide sequence analysis reavealed that it corresponded to a mono-thiol glutaredoxin (Grx)

from the chloroplast. Grx may contribute to plant defence against oxidative stress caused by viral infection and also it may contribute to maintain the redox poise of the plant required for proper activation of host defence mechanisms (Gilardi, 2000; Gilardi *et al.,* 2000)

Redox status of the cell plays an important role in the regulation of plant growth, development and signaling pathways (Mahalingam *et al.,* 2003; rev. Torres, 2010). In order to maintain the proper redox status of cell, plants use many redox systems. One of the major system is the Glutathione (GSH)/Grx system, that consists of Grx, GSH, Glutathione Reductase (GR) and NADPH. Grxs reduces the mixed disulfides formed between the protein and GSH by means of N-terminal Cys residue of the CXXC or CXXS active site motif through monothiol mechanism. GSSG and reduced Grx are produced in that reaction. GSSG is again reduced to GSH through GR by the consumption of electrons from NADPH. Monothiol mechanism is performed only by Grxs whereas the dithiol mechanism is also done by Trxs (Juang and Thomas, 1996; Nulton-Persson *et al.,* 2003).

Fig.1.5. Redox cycle of Glutaredoxin system. Oxidized glutathione (GSSG); reduced Glutathione (GSH), Reduced Grx (GRX_{red}), Oxidized Grx (GRX_{ox}).

Grxs comprises a family of low molecular weight proteins possessing oxidoreductase activity. The discovery of Grx dates back to 1976, in which Holmgren identified an unknown protein that could be able to substitute the function of thioredoxin (Trx) in *E.coli*. He named it as Grx, because this protein was found to be dependent on GSG for its redox reactions (Holmgren, 1976). Grxs belong to Trx fold family proteins. Structure of this family proteins is characterized by having four β-strands surrounded by at least three α-helices from bacteriophage T4 Grx to five helices in human Grx2 (Holmgren, 1995). They have a Cys-based active site. Grxs have been reported from different organisms ranging from viruses (Jhonson *et al.,* 1991), prokaryotes (Holmgren, 1976), plants (Minakuchi *et al.,* 1994), yeasts and human (Padilla *et al.,* 1995) in different isoforms. The other major proteins included in this family are Trx, glutathione

S-transferase, DsbA (a protein involved in the disulfide formation *in vivo*), glutathione peroxidase and protein disulfide isomerase (PDI). (rev. Martin, 1995). These structure-conserved active site proteins have been reported from prokaryotes to eukaryotes. Many other proteins also share the characteristics of these family proteins but they are described as a general name of Trx-like structure (Rev.Lemaire, 2004).

1.4.1. Classification of Grxs

Initial classification of Grxs was based on their Cys residues active site as classical dithiol and monothiol Grxs (Rodriguez-Manzaneque *et al.,* 1999). Genome availability of *Populus trichocarpa*, *Arabidopsis thaliana* and *Oryza sativa* have given better insight of Grxs in plants and the number of Grxs reported from these plants were found to be 36, 31 and 48 respectively. As Grxs numbers reported from the plants got increased, the Grxs were further classified into six classes.

Class I Grxs comprises Grxs with CxxC/S active site whereas class II Grxs consists of CGFS active site and both classes have been reported from cyanobacteria to land plants. During evolution, higher plants have undergone gene duplication and gene fusion, so class I Grxs are further subdivided into five subclasses (GrxC1, C2, C3, C4 and C5⁄ S12) and class II into four subclasses (GrxS14, S15, S16 and S17). The naming was based on the presence of Cys or Ser at the fourth position of the active site motif (CxxC or CxxS) of Grx (Couturier *et al.,* 2009a). The other four classes of Grxs are restricted to specific organisms. Class III Grxs are the most abundant Grxs and specific to land plants with a peculiar active site of CCxC or CCxS. 21 Grxs out of the 31 reported in *Arabidopsis* belong to class III Grx (Rouhier *et al.,* 2008).

Class IV, V and VI Grxs possess extra domains in addition to the Grx domain. Class IV Grxs are restricted to terrestrial plants whereas members of Class V are present in bacteria and class VI are restricted to cyanobacteria. The functions of these specific Grxs are at present unknown (Couturier *et al.,* 2009a).

Grxs are expressed under both biotic and abiotic stress conditions. GRX480 from *Arabidopsis* was induced after the infection of plants with *Pseudomonas syringae* and also with SA treatment (Ndamukong *et al.,* 2007). AtGrx17 expression was induced at elevated temperature (Cheng *et al.,* 2011).

1.4.2. Main functions of Grxs

The primary function of Grx is to donate electrons and to reduce a broad range of proteins involved in metabolic and signaling pathways. In addition to the reduction of ribonucleotide reductase in *E.coli* (Aslund *et al.,* 1994), Grxs have also been shown to reduce peroxiredoxin II in poplar (Rouhier *et al.,* 2002), dehydroascorbate reductase in *Chlamydomonas* (Zaffagnini *et al.,* 2008) GR (Collinson *et al.,* 2002) and glutathione-S-transferase (Collinson and Grant 2003). CC type Grx reported from *Arabidopsis* regenerated the peroxiredoxin (Finkemeier *et al.,* 2005). They also participate in the regulation of several transcription factors related to oxidative stress signaling in mammals (rev. Rouhier *et al.,* 2002). In *Arabidopsis*, GRX480 protein regulates the redox state of TGA protein and it is helpful in the formation of TGA/NPR1 complex which in turn leads to the activation of SAR mechanism (Ndamukong *et al.,* 2007).

In addition, Grxs are able to reduce the intra- and inter-disulfide bonds formed in or between proteins and also the mixed disulfides between a protein and GSH through deglutahionylation. Grxs can reduce the disulfides via dithiol or monothiol mechanism (Vlamis-Gardikas and Holmgren, 2002). In dithiol mechanism, a transient state between Grx and protein disulfides is achieved by the nucelophilic attack of N-terminal Cys of the Grxs. Next, the electron is donated by the second Cys of the active site and the protein gets reduced and Grxs get oxidized. Grxs with dithiol active site can perform the reduction of both protein disuphides and GSH-thiol disulfides (Vlamis-Gardikas and Holmgren, 2002).

Under oxidative stress conditions, the increased generation of ROS causes damage to macromolecules. One mechanism to protect proteins from such damage is protein glutathionylation, in which a reversible disulfide is formed between the glutathione and free accessible protein Cys. This reversible posttranslational modification not only protects specific Cys from irreversible oxidation but also modulates protein activities and thus constitutes a regulatory mechanism (rev. Zaffagnini *et al.,* 2012). Recently, it has been described that the activity of several enzymes, such as isocitrate lyase from *Chlamydomonas reinhardtii* (Bedhomme *et al.,* 2009) as well as methionine sulfoxide reductases B and glyceraldehyde-3-phosphate dehydrogenase from *A. thaliana* (Tarrago *et al.,* 2009; Bedhomme *et al.,* 2012) are regulated by this mechanism.

In addition to their oxidoreductase activity, an increasing number of experiments suggest that Grxs are actively involved in the assembly of Fe-S cluster proteins or act as a scaffold

protein for the assembly of Fe-S cluster proteins. These proteins are found in all kingdoms of life and they take part in many biological processes in the cells like photosynthesis, respiration, sulfur and nitrogen assimilation and chlorophyll catabolism (Jhonson and Smith, 2005). The role of Grxs in Fe-S cluster biosynthesis was well studied in *S. cerevisiae* (Rodríguez-Manzaneque *et al.*, 2002; Mühlenhoff *et al.*, 2003; Achebach *et al.*, 2004). Disruption of Grx5 in *S. cerevisiae* showed that the cells became impaired in Fe-S cluster biogenesis in mitochondria. The Grx5 mutants showed higher level of free iron accumulation in the cells and displayed deficiency in Fe-S cluster assembly for at least two Fe–S proteins (aconitase and succinate dehydrogenase) leading to impaired respiratory growth and increased sensitivity to oxidative stress (Rodríguez-Manzaneque *et al.*, 1999; 2002). Many Grx5 homologous from various organisms have been tested for their function in Grx5 defective yeast cells. Substitution studies with human Grx5 and chicken Grx5 and Grxs from *E. coli* and *Synechocystis spp* showed that they all could be able to perform the function of Grx5 in yeast (Molina-Navarro *et al.*, 2006). Plants Grxs were also transformed into yeast Grx5 mutants in order to study their function in Fe-S cluster biosynthesis. (Cheng *et al.,* 2006; Cheng 2008) showed that either *AtGRXcp* or *AtGRX4* from *A. thaliana* restored the functions of yeast Grx5 when transformed into yeast Δ*grx5* mutants. Both of them suppressed the iron accumulation and protected the yeast cells against oxidative damage.

1.4.3. Grx localization

Many Grxs reported from yeast, bacteria and mammals have been found to be localized in different compartments. The number of Grxs reported from yeast, mammals and *E.coli* were 7, 4 and 4 respectively. In yeast Grx1 and Grx2 are characterized to be in cytosol, whereas Grx3 and Grx4 are predominantly located at the nucleus, Grx5 targets to mitochondria, and Grx6 and Grx7 are found in the *cis*-Golgi (Mesecke *et al.,* 2008).

In plants, putative localization of the Grxs were also shown to be present in different compartments: cytosol, chloroplast, mitochondria and nucleus (rev. Lemaire, 2004; Rouhier *et al.,* 2004) and it is thought that these Grx proteins have specific functions in each compartment (Cheng *et al.,* 2006; Li *et al.,* 2009). As plant Grxs are encoded by multigene families, the sub-cellular localization study provided information about their possible functions. Most of the knowledge about plant Grxs is available from *Arabidopsis* and poplar. AtGRXcp (*AtGRXS14),* AtGRX4 (*AtGRXS15)* and AtGRXC5 were experimentally proven to be localized to

chloroplasts (Cheng *et al.*, 2006; Cheng, 2008; Couturier *et al.,* 2011). AtGrxS13 and AtGrxC10, were found to be diffused into the cell, having cytosolic localization (Couturier *et al.,* 2011). The CC-type Grxs, such as (GRXC7/ROXY1 and GRXC8/ROXY2) from *Arabidopsis* were found to be nucleo-cytoplasmic (Li *et al.,* 2009) and *Arabidopsis* GRXC9 was found to be localized in the nucleus (Ndamukong *et al.*, 2007). The confocal microscopy visualization of poplar Grxs showed that GrxS14 and GrxS16 were present in the chloroplast whereas GrxS15 was located in the mitochondria (Bandyopadhyay *et al.*, 2008). Grxs from *Ricinus communis* and poplar plants were shown to be very abundant in the phloem sap, which might indicate that Grx proteins are also secreted (Szederkenyi *et al.,* 1997; Rouhier *et al.,* 2001).

1.4.4. Grx functions in plants

The most documented functions of Grxs are their involvement in the oxidative stress response in bacteria, yeast, and mammals (rev. Meyer *et al.,* 2009). In spite of the high number of *grx* genes in plant genomes, the biological functions and physiological roles of most of them are at present unknown. In *Arabidopsis,* only 8 out of 31 Grxs have been functionally characterized by genetic methods (Laporte *et al.,* 2012). Several studies suggest that plant Grxs are also involved in protecting cells against oxidative damage. The *Arabidopsis* AtGRXcp and AtGRX4 have been shown to play a critical role in protecting seedlings against external oxidants (Cheng *et al.,* 2006, Cheng, 2008). Furthermore, the loss of AtGRXcp function leads to protein oxidation in chloroplasts which demonstrated that Grxs are involved in maintaining the redox state of chloroplasts (Cheng *et al.,* 2006). The *Arabidopsis* GRXS13 has been shown to be critical to limit basal and photo-oxidative stress-induced ROS production, thus protecting against oxidative cellular damage (Laporte *et al.,* 2012). Recently, new emerging functions are being described for plant Grxs (Rouhier *et al*., 2008). Grx plant proteins have been reported to be involved in plant protection against different abiotic stresses (Sundaram *et al*., 2009; Sundaram and Rathinasabapathi, 2010), as well as in plant development (Xing *et al*., 2005). Molecular genetic evidence suggests that ROXY1, encoding a CC-type Grx, is required for petal development in *Arabidopsis* (Xing *et al.,* 2005; Li *et al.,* 2009). Furthermore, it has been shown that along with ROXY1, another CC type Grx, ROXY2, plays an important role in anther initiation and differentiation (Xing and Zachgo, 2008).

Plant Grx proteins can also be involved in redox regulation of protein activity by reducing disulfide bridges or by reversible glutathionylation of the target proteins (Lemaire, 2004; rev. Zaffagnini *et al.,* 2012). It has been described that the activity of some transcription factors, such as PERIANTHIA (PAN) (Li *et al*., 2009), or TGA factors (Ndamukong *et al*., 2007) are regulated by their interaction with either Grxs ROXY1 or GRX480, respectively. Likewise, it has been shown that Methionine sulfoxide reductase B and glyceraldehyde-3-phosphate dehydrogenase from *A. thaliana* are regulated by the glutathionylation/deglutathionylation mechanism (Tarrago *et al.,* 2009; Bedhomme *et al.,* 2012). Finally, the involvement of plant Grx proteins in Fe-S cluster biosynthesis has also been described (rev. Rouhier *et al.,* 2009). Rouhier *et al.,* (2007) showed that poplar PtGrxC1 was able to dimerize *in vitro* by incorporating a relatively stable Fe-S cluster. Recent studies, by using yeast Δ*grx5* mutant cells, suggest that some *Arabidopsis* and poplar Grxs have an important role in Fe-S cluster biogenesis (Cheng *et al.,* 2006; Cheng, 2008; Bandyopadhyay *et al.,* 2008).

Many heterologous expression studies have been carried out to study the function of plant Grxs. Yeast Δ*grx5* mutants were used to assess the function of different plant Grxs. Expression of either *Arabidopsis* AtGRXcp or AtGRX4 into this yeast mutant showed that these Grxs were able to suppress the iron accumulation and protected the yeast cells against oxidants (Cheng *et al.,* 2006; Cheng, 2008). Likewise, complementation studies with poplar Grxs (GrxS14, S15, S16 and S17) in yeast Δ*grx5* mutants showed that only GrxS14 and S16 were able to restore the function of Grx5 in yeast Fe-S cluster biosynthesis (Bandyopadhyay *et al.,* 2008). Heterologous expression in plants also revealed the roles of Grx plant proteins. Expression of *Pteris vittata* Grx, PvGRX5, in *Arabidopsis* plants conferred much tolerance to temperature than the control plants (Sundaram and Rathinasabapathi, 2010). Likewise the ectopic expression of *Arabidopsis* Grx, AtGRX17, in tomato plants increased thermotolerance (Wu *et al.,* 2012). Over-expression of tomato Grx, SlGRX1, in *Arabidopsis* increases the plants resistance against oxidative, salt and drought stresses (Guo *et al.,* 2010). Furthermore the expression of rice Grxs, OsROXY1 and OsROXY2, in *Arabidopsis* complemented the function of *roxy1* mutant phenotype and it was found that over-expression of these two Grxs led to hypersensitivity to the infection caused by *Botrytis cinerea* (Wang *et al.,* 2009).

1.5. Pathogenesis of PMMoV-S and PMMoV-I in *N. benthamiana* plants

N. benthamiana plants belong to the *Solanaceae* family and are susceptible to both PMMoV-S and PMMoV-I viruses. This host plant was used in this work to study the effect of *Cch* Grx in PMMoV-I plant-virus interaction. The first steps of the infection are similar for the two viruses, but at later stages of infection, PMMoV-I infected plants show signs of symptom recovery. In 2003, Pérez Bueno observed that when *N. benthamiana* plants were inoculated with PMMoV-I virus at the 3-5 leaves stage, the plants start to show recovery from infection from 21 dpi onwards, developing a longer elongation in the stem, and with symptomless leaves in the recovered part of the plant, in contrast to those infected with PMMoV-S that do not recovered.

Thermoluminiscence analysis pointed to a higher lipid peroxidation in the PMMoV-S-infected plants than in the PMMoV-I-infected ones (Rahoutei *et al.,* 1999). In addition, the fluorescence image analysis and the non-photochemical quenching measures of the dissipated energy in other forms from the photo assimilates revealed characteristic patterns either in the asymptotic (Pérez Bueno *et al.,* 2006), or symptomatic leaves (Pineda *et al.,* 2011), that correlate to the viral accumulation pattern as revealed by tissue print analysis or after U.V. illumination of GFP-labelled TMV (TMV-1056) (Pineda *et al.,* 2011, unpublished data from the lab).

Furthermore, robotized thermal analysis and fluorescence image analysis of plants infected with either PMMoV-S or PMMoV-I revealed an increase of temperature at 7 dpi associated to the main veins. This increase has been associated to stomatal closure, being prior to the detection of viral accumulation and to the observed changes in the fluorescence emitted by chlorophyll. It has been proposed that the increase of temperature is a systemic defence mechanism regulated by the loss of water (Chaerle *et al*., 2006).

The infection by the S and I strains of PMMoV is associated to a diminished efficiency of the photosynthetic activity in the Photosystem II, as well as to a reduced accumulation of the 24K and 16K proteins from the Oxygen Evolving Complex (OEC) in the thylakoid membranes of the plants (Rahoutei *et al*., 1999). Furthermore, Pérez-Bueno *et al.,* (2004) showed, by means of protein 2-D gel analysis and immunodetection, a selective reduced accumulation of distinct isoforms of the 24K protein in the PMMoV-S-infected plants. The three proteins from the OEC are encoded by multigene families (Pérez-Bueno *et al*., 2011). A reduced accumulation of their mRNAs is observed along the viral infection, except for the recovery phase of the PMMoV-I

infection (Pérez-Bueno, 2003). The reduced accumulation is less significant when total protein extracts were analyzed, thus indicating that the three proteins are regulated both at the transcriptional and post-transcriptional levels (Hakmaoui *et al*., 2012). It has been proposed that the accumulation of either the 33K protein or 24K protein in the chloroplast maintain the redox poise of the cell (Peltier *et al*., 2000; Abbink *et al*., 2002).

The proteomic analysis of the chloroplast from PMMoV-S-infected plants corroborated the existence of isoforms of the 16K protein and revealed the diminished accumulation of proteins from the photosynthetic electron transport and Benson-Calvin cycle (Pineda *et al*., 2010).

Further studies (Tena, 2012) showed, by constructing chimera viruses containing different genomic regions from PMMoV-I in the context of PMMoV-S that the recovery phenotype was due to regions in the 126K protein from PMMoV-I being at present unknown whether it is due to either the methyltransferase domain or the entire 126K protein. In these studies Tena (2012) has determined that the recovery phenotype was not associated to a diminished viral accumulation as in the case of PMMoV-I and therefore, the data ruled out that plant recovery was due to post-transcriptional gene silencing (PTGS) resistance mechanism, although specific viral siRNAs were detected.

Furthermore, it has been shown that there are not much differences in the different hormones, enzymes and metabolites assayed in the plants infected with either viral strain at the earlier stage of infection, i.e. at 7 and 14 dpi, at variance what it has been determined from 21 dpi onwards, up to 28 dpi, the last time point analyzed, where there are significant differences (Hakmaoui *et al*., 2012; Tena, 2012). Tena (2012) has determined that ET accumulates as a host response against viral infection up to 14 and 28 dpi, in the plants infected with PMMoV-S and PMMoV-I, respectively, at variance to the described in TMV-infected tobacco plants, in which no ET was detected and that could be due to the stage of the infection (ref. in Goodman *et al*., 1986).

The recovery phenotype is associated to defence mechanisms such as the accumulation of nitric oxide, ROS, SA, increase in respiration, reduction in abscisic acid content, accumulation of pathogen-related proteins (PRs), increase in superoxide dismutase maintenance of the content of three peroxiredoxins and the glutathione pool. It is at present unknown, whether these defence mechanisms are due to their activation by either the PMMoV-I

methyltransferase domain or the 126K protein or because that protein is not able to suppress plant basal defence mechanisms as the helicase domain of TMV does in *A. thaliana* plants (Wang *et al*., 2009; Hakmaoui *et al*., 2012; Tena, 2012).

In addition, Tena (2012) has determined that the recovered part of the plants infected with PMMoV-I, are less susceptible to further reinoculation with either homologous or heterologous viruses, thus indicating that in this part of the plants defence mechanisms are activated as it could be also inferred from the higher accumulation of PR proteins in these part of the plant, an indicator of resistance mechanisms in susceptible interactions (Elvira *et al*., 2008).

1.6. PR proteins

PRs proteins are low molecular weight proteins produced by plants under pathological or related situations. PRs get accumulate in plants after pathogen attack by virus, viroids, bacteria, fungi, nematodes, insects and herbivores as well as after wounding and certain abiotic stress conditions (rev. van Loon *et al*., 2006).

PR proteins were first observed in tobacco plants infected with TMV (van Loon and van Kammen, 1970). On the basis of amino acid sequence data and biochemical functions, PR proteins have been classified into 17 families (PR-1 through 17) (Rev. van Loon *et al.,* 2006). Within each PR family, several isoforms exist as acidic and basic forms. Usually PR genes are expressed at basal level at normal conditions but upon pathogen attack the expression level get increased. Many PR protein mRNAs expressions were also altered under abiotic stress conditions such as cold and light (Hon *et al.,* 1995; Zeier *et al.,* 2004) and at different developmental steps such as leaf senescence (Morris *et al.,* 2000; Obregon *et al.,* 2001) and flowering (Lotan *et al.,* 1989). Over expression of PR genes in transgenic plants stated that plants showed better disease resistance when co-ordinately expressing a set of PR genes than when the individual genes were expressed (Zhu *et al.,* 1994).

Distinct sets of PR proteins are induced by different pathogens. It is currently accepted that in *Arabidopsis*, biotrophic and hemi-biotrophic pathogens mainly induce the SA-dependent defence signalling pathway that regulates the expression of acidic PR proteins such as PR-1, PR-2, and PR-5, often used as markers to monitor SAR induction (Ryals *et al.,* 1996), whereas the ET- or JA-dependent signaling pathways are mainly induced by necrotrophic pathogens,

which regulate the expression of basic PR proteins such as PR-2, PR-4, and PDF1.2 (Glazebrook, 2005; van Loon *et al*., 2006). Cross-talk among these signaling pathways provides the plant a regulatory way for fine tuning the defense response against pathogens (Pieterse *et al.,* 2012). The PRs analyzed in this work correspond to markers of the SA-dependent pathway (acidic PR-1, PR-2 and PR-5) and ET-dependent pathway (basic PR-2) (rev. van Loon *et al*., 2006).

SA brings about the expression of PR proteins through the activation of transcription factors. Transduction of the SA signal to activate PR gene expression and SAR requires the function of NON-EXPRESSER OF PATHOGENESIS-RELATED GENES 1 (NPR1) (rev. Pieterse and van Loon, 2004). Analysis of the loss-of-function of NPR1 revealed that it plays a central role in SAR mediated signalling (Bonas and Lahayae, 2002). NPR1 is devoid of DNA binding site and it activates the PR gene expression indirectly by interacting with sequence specific TGA transcription factors. According to the current model, NPR1 protein is located in the cytosol as an oligomer (Mou *et al.,* 2003). Changes in the redox state of the cell leads to the reduction of critical Cys residues in NPR1 giving the monomeric form (Tada *et al.,* 2008) and thus further facilitating its translocation to the nucleus from cytoplasm. NPR1 and TGA factors interact in the nucleus and activate defense gene expression, although this mechanism is still not well understood (Fu and Dong, 2013).

1.7. 9-Lipoxygenase (9-LOX)

Lipoxygenases (Linoleate: Oxygen reductase; EC 1.13.11.12) (LOX) are enzymes that catalyze the regio and stereo specific insertion of molecular oxygen into polyunsaturated fatty acids containing a (1*Z*, 4Z)-pentadiene system (i.e. linoleic and α-linolenic acid) to produce unsaturated fatty acid hydroperoxides (oxylipins). Oxygen insertion takes place either at C-9 (9-LOX) or at C-13 (13-LOX) of the carbon backbone of α-linolenic acid to form (9S)-hydroperoxyoctadecatrienoic acid (9-HPOT) and (13S)-hydroperoxyoctadecatrienoic acid (13-HPOT) (Siedow, 1991). LOX initiates the synthesis of either acyclic or cyclic compounds called oxylipins (rev. Porta and Rocha-Sosa 2002). The oxylipins produced through LOX pathways act as signals for plant defence and development (rev. López *et al.,* 2008). 9-LOX pathway induces plant defence response through a JA-independent signaling pathway (Vellosillo *et al.,* 2007).

Several studies have revealed that 9-LOX pathway plays an important role in the development of HR and disease resistance (Montillet *et al.,* 2005; López *et al.,* 2011; Vicente *et al.,* 2012). 9-LOX activity and expression increases with the induction of HR in tobacco (Rancé *et al.,* 1998, Montillet *et al.,* 2002), potato (Göbel *et al.,* 2002), cotton, (Sayegh-Alhamdia *et al.,* 2008) and pepper plants (Hwang and Hwang, 2010). Moreover, experiments in *Arabidopsis* showed that 9-HPOT produced by 9-LOX pathway was necessary for developing resistance against *Pseudomonas syringae* pv. *tomato* (*Pst*) (Vicente *et al.,* 2012).However, in compatible interactions, 9-LOX expression was delayed and reached much lower levels (Hwang and Hwang, 2010), except for plant-pathogen interactions leading to systemic necrosis (García-Marcos *et al.,* 2009; 2013). In this sense, it is important to note that 9-LOX derived oxylipins were found to be sufficient for the initiation of programmed cell death (PCD) and HR in tobacco plants infected with *Ralstonia solanacearum* (Cacas *et al.,* 2005).

Apart from taking part in plant defence, 9-LOX are also involved in plant developmental processes. The 9-LOX derived products have been found to play an important role in *Arabidposis* and maize root development, (Vellosillo *et al.,* 2007; Gao *et al.,* 2008), in potato tuber development (Kolomiets *et al.,* 2001) and in almond seeds development (Santino *et al.,* 2005).

1.8. Enzymes related to Grxs

1.8.1. Glutathione Reductase (GR)

GR is a member of flavoprotein oxidoreductase family found in both prokaryotes and eukaryotes. GR catalyzes the conversion of oxidized GSSG to the reduced form (GSH) using NAD(P)H as an electron donor (Meister and Anderson 1983). GR plays an important role in maintaining the antioxidant machinery of cells (Ansel *et al.,* 2006) and maintains the cellular redox state by utilizing the reducing power of GSH (Lillig *et al.,* 2008). In the Grx system, GR plays an important role by transferring the reducing equivalents from NADPH to oxidized glutathione (GSSG) and thus maintaining the reduced glutathione level for the reduction of Grx.

GR plays an important role in response to both biotic and abiotic stresses in plants. GR activity was found to decrease in tomato plants when infected with *Botrytis cinerea* (Kuzniak and Sklodowska, 2005) and in apricot seeds when infected with *Prunus necrotic ringspot rvirus* (PNRSV) (Amari *et al.,* 2007). However, GR level was found to increase in *Hibiscus*

cannabinus plants when infected with Mesta yellow vein mosaic disease (Sarkar *et al.,* 2011). GR activity was also found to vary at different abiotic stresses. An increase in GR activity was found in *C. annuum* plants in the presence of Cd (León *et al.,* 2002) and in chickpea seedlings roots following salt stress (Eyidogan and Oz, 2007).

Furthermore, the function of plant GR proteins was analyzed by heterologous expression either in yeast GR-deficient mutants (Chen *et al.,* 2007) or in plants (Kornyeyev *et al.,* 2003; Chen *et al.,* 2007). The results indicated that GR has a critical role in protecting cells against oxidative stress and showed that GR over expression enhanced resistance against abiotic stress (Kornyeyev *et al.,* 2003) and pathogens (Chen *et al.,* 2007).

1.8.2. Glutathione-S-transferases (GST)

GSTs are multifunctional dimeric proteins that catalyze the conjugation of reduced GSH to electrophilic centers found over a wide variety of hydrophobic compounds through the sulfhydryl group (Douglas, 1987; Cummins *et al.,* 2011). GST function was first reported as to degrade the herbicide chloro-S-triazine atrazine to a nontoxic form by conjugating GSH to the herbicide (Shimabukuro, 1971), thereby protecting the crop from this herbicide injury. The conjugation of GSH usually results in the detoxification of toxic compounds (Ketterer *et al.,* 1988; Mannervik and Danielson, 1988) playing a key role in cellular detoxification (rev. Marrs, 1996; Dixon and Edwards 2010).

The general mechanism of GST catalyzation is as follows:

$$GSH + R\text{-}X \longrightarrow GSR + HX$$

In plants, the number of genes encoding GSTs is relatively high with more than 50 members in *Arabidopsis*. This GST superfamily is subdivided into classes reflecting sequence, structural and functional diversification (Dixon and Edwards 2010). GST gene expression was induced under either biotic or abiotic stress conditions (rev. Moons, 2005; Sappl *et al.,* 2009; Jain *et al.,* 2010). In addition to herbicide application, plant GSTs are induced by H_2O_2, auxin and SA (Boot *et al.,* 1993; Levine *et al.,* 1994; Chen *et al.,* 1999; Sappl *et al.,* 2009) by wounding and temperature (Boot *et al.,* 1993; Vollenweider *et al.,* 2000) as well as by pathogens (Mauch and Dudler, 1993; Wagner *et al.,* 2002; Lieberherr *et al.,* 2003). The antioxidant activity of GSTs could limit symptom development during compatible pathogen

interactions, or restrict necrotic lesion development in non-compatible interactions (Alvares *et al.,* 1998). It has been suggested that GSTs may be induced in response to general cellular injury and oxidative stress caused by those different stresses (Marrs, 1996), thus protecting plants against oxidative damage (Dalton *et al.,* 2009). Thus, GST expression is used as a marker of plant response against oxidative damage.

1.9. Pyridine Nucleotides (PNs)

Redox reactions are fundamental metabolic processes by which cellular catabolic and anabolic processes proceed in order to convert and distribute the energy for plant growth and development (Noctor, 2006). Cellular redox state is a hypothetical state that comprises of both oxidized/reduced states of distinct redox-active metabolites. The three major redox determinants of the cells are ascorbate (ASC), GSH and the PNs (Queval *et al.,* 2007). Among them, PNs have a key role in the redox state of the cell as they are involved in maintaining the redox state of both ascorbate and GSH along with other systems. PNs include nicotinamide adenine dinucleotide (NAD) and its phosphorylated form, NADP. They are present in the cell as oxidized (NAD^+, $NADP^+$), and reduced forms (NADH and NADPH) and they are ubiquitous biomolecules found in both prokaryotic and eukaryotic living organisms. These biomolecules act as coenzymes in biochemical reactions as they transfer hydrogen atoms and electrons from one compound to another through redox reactions (Noctor, 2006).

The structure of β-Nicotinamide adenine dinucleotide (NAD), known as Nicotinamide adenine dinucleotide, consists of two nucleotides joined together by means of their phosphate group. The two nucleotides found in the structure are adenosine monophosphate (adenine plus ribose-phosphate) and nicotinamide ribotide (nicotinamide plus ribose-phosphate) (Fig.1.6). Nicotinamide is the active part of the structure which takes part in oxidation and reduction processes. The oxidized form NAD^+ has one hydrogen atom less than the reduced form (NADH), and has a positive charge on the nitrogen atom which allows it to accept a second electron upon reduction. NADP is the phosphorylated derivative form of NAD. NADP structure is identical to that of NAD but have an additional phosphate group at the ribose residue.

PNs are involved in many metabolic processes and are found in all of the plant compartments. They are transported within other compartments through different metabolite shuttles (Day and Wiskich, 1981; Journet *et al*., 1981; Heineke *et al*., 1991; Reumann *et al*.,

1994). The level of PNs were measured and their roles have been studied in mitochondria (Igamberdiev and Gardeström, 2003), chloroplast (Takahama *et al*., 1981) and peroxisomes (Reumann *et al*., 1994) where the active functions of respiration, photosynthesis and photorespiration take place. These biomolecules are involved in cellular energy metabolism, including glycolysis, TCA cycle and oxidative phosphorylation (Hunt *et al.,* 2004).

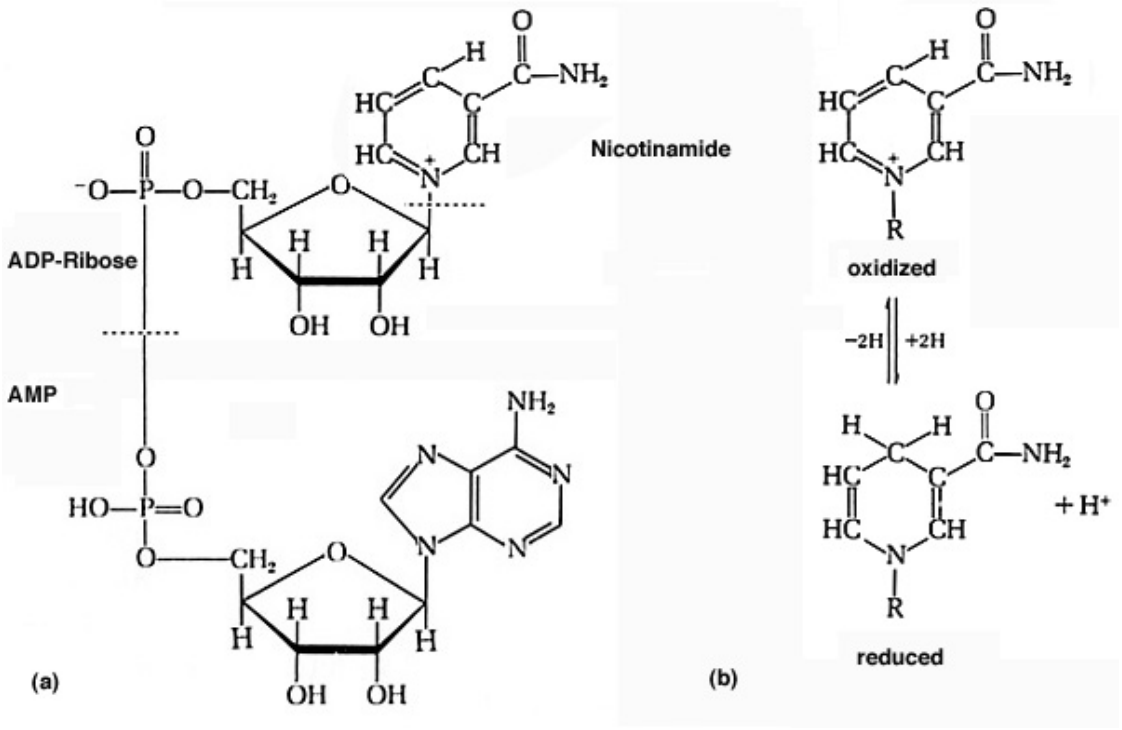

Fig.1.6.(a). Structure of NAD. NAD structure consists of Adenosine monophosphate (adenine plus ribose-phosphate) and nicotinamide ribotide. (b) Structure of NAD moiety in oxidized and reduced conditions.

PN levels get changed at different stage of plant growth (Yamamoto, 1963; Bonzon *et al.,* 1983; Queval and Noctor, 2007; Hunt and Gray, 2009) and they also play an important role in cellular development. Experiments with *Arabidopsis* cell culture showed that PNs are involved in maintaining the redox homeostasis of the cells during the growth cycle (Pellney *et al.,* 2009).

PNs play an important role in the activation of redox dependent transcription of genes. Induction of NAD contents in the leaves cause increased accumulation of *GLIP1,* RPM1-

interacting protein 4, chitinases, several genes involved in glucosinolate metabolism and WRKY transcription factors (Pétriacq *et al.,* 2012).

Recently, PN pools have been found to correlate with cellular processes that are involved in stress responses both in animals and plants (Berger *et al.,* 2004; Hunt *et al.,* 2004) as well as in plant response against pathogens (Pétriacq *et al.,* 2013). Thereby, an increase in NAD accumulation, as it is produced in the CMSII mitochondrial mutant of *N. sylvestris*, improved plant ozone tolerance and resistance to virus infection, thus suggesting that NAD may be involved in plant defence responses (Dutilleul *et al.,* 2003, 2005; Djebbar *et al.,* 2012). Several lines of evidence corroborated that an increase in NAD accumulation in Arabidopsis plants, either by exogenous application of PNs or by over expression of *nadC* gene from *E. coli,* modulates plant responses through gene expression and mainly influences the induction of various pathogen-related genes and also stimulates plant resistance against *Pseudomonas syringae* (Zhang and Mou, 2009; Pétriacq *et al.,* 2012).

2.OBJECTIVES

Objectives

The most documented functions for Grxs are their involvement in the oxidative stress response (Holmgren 2000; Cheng *et al*., 2006), but recently, new emerging functions are being described for plant Grxs (Rouhier *et al*., 2008). Grx plant proteins have been reported to be involved in plant protection against different abiotic stresses (Sundaram *et al*., 2009), in protein activity regulation (Lemaire, 2004; Ndamukong *et al*., 2007; Li *et al*., 2009) as well as in plant development (Xing *et al.*, 2005: Xing *et al*., 2008). The main aim of this work was to functionally characterize the *C. chinense* Grx (*Cch* Grx) protein and to study its relationship with the infection caused by the plant virus PMMoV-I.

In this study we took the following tasks to functionally characterize the protein:

1. **Molecular, cellular and enzymatic characterization of *C. chinense* Grx protein.**
2. **Analysis of the effect of *Cch* Grx constitutive expression over PMMoV-I viral accumulation.**
3. **Study of the underlying resistance mechanism/s mediated by *Cch* Grx against PMMoV-I viral infection.**
4. **Analysis of *Cch* Grx contribution in maintaining the redox state of pyridine nucleotides in the cell.**
5. **Analysis of the role of *Cch* Grx in tolerance against abiotic stress.**
6. **Elucidating *Cch* Grx involvement in Fe-S cluster assembly mechanism.**

Work approach:

To address these objectives we expressed *Cch* Grx protein in different biological systems, bacteria, yeasts and plants. For the study of *Cch* Grx expression in plants, we used *N. benthamiana* Domin transgenic plants, previously obtained in our group, that constitutively express the native *Cch* Grx choroplastic protein of *C. chinense* (Grx Exp), *Cch* Grx fused to GFP (Grx:GFP) and a protein with a deletion of 63 aa at its amino terminus fused to GFP (Δ2M:Grx:GFP) that does not located to the chloroplasts but to the nuclei. This plant host is susceptible to all the tobamoviruses and it will be appropriate to study the role of Grx in a plant-virus compatible interaction. The Italian strain of *Pepper mild mottle virus* (PMMoV-I) was chosen to carry out this study, because preliminary experiments from our lab had shown a

reduction in the accumulation levels of virus at late times of infection (Montes-Casado *et al*., 2010).

The constructs of *Cch* Grx used for *N. bentamiana* transformation are shown below:

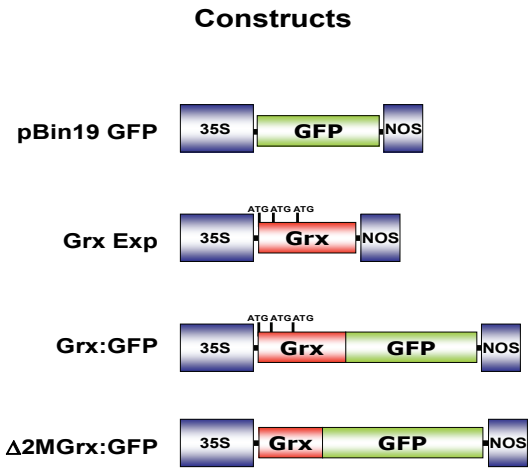

Fig. 2.1. Constructs used for transformation of *N. benthamiana* plants were cloned in the vector pBIN 19. pBIN 19:GFP, native *Cch* Grx (Grx:Exp), *Cch* Grx fused to GFP (Grx:GFP) and a N-deleted 63 aa *Cch* Grx fused to GFP (Δ2M:Grx:GFP) constructs were used. 35S: *Cauliflower mosaic virus* promoter; GFP: Green fluorescent protein; NOS: Nopaline synthase terminator.

3.MATERIALS & METHODS

3.1. Virus

The tobamovirus used was the Italian strain of Pepper Mild Mottle Virus (PMMoV-I) described by Wetter *et al.,* (1984) and was a kind gift from Dr. M. Conti (Italy).

3.2. Plants

Nicotiana benthamiana Domin wild type plants and the transgenic *N. benthamiana* plants constitutively expressing GFP (*Nb:GFP* line 11), native *Cch* Grx (*Nb:Grx* line 3), a *Cch* Grx:GFP fusion protein (*Nb:Grx-GFP* line 16) and a 63 aa truncated *Cch* Grx fused to GFP (*Nb:Δ2MGrx-GFP* line 40) were used in this work. These transgenic lines were selected from previous experiments in our laboratory and analyzed for their constitutive expression of the corresponding Grx.

3.3. Bacterial strains

Escherichia coli strains DH5α (*supE44 ΔlacU169, (8fi80lacZΔM15*) *hsdR17 recA1 end A1 gyr A96 thi-1 rel A1 DE(argF-lac) 169)* (Hanahan, 1983), and M15(pREP4) derived from *E. coli* K12 and have the phenotype Nal^S, $Str^{S,}$ Rif^S, Thi^-, Lac^-, Ara^+, Gal^+, Mtl^-, F^-, $RecA^+$, Uvr^+, Lon^+ (QIAexpressionist™)

3.4. Yeast strains

***Saccharomyces cerevisiae* strain**	**Description**	**Reference**
W303-1B	*MAT* alpha *his3 ura3 leu2 ade2 trp1*	Rodriguez-Manzaneque *et al.,* 2002
MML100	*MAT***a** *his3 ura3 leu2 ade2 trp1 Δgrx5*::*GEN R*	Rodriguez-Manzaneque *et al.,* 2002
MML240	*MAT***a** *his3 ura3 leu2 ade2 trp1* [pMM54(*GRX5-3HA*)]::*LEU2+ Δgrx5*::*GEN R*	Molina *et al.,* 2004
T11	*MAT***a** *his3 ura3 leu2 ade2 trp1* [pMM1025(*Cch Grx-3HA*)]::*LEU2+ Δgrx5*::*GEN R*	This work

3.5. Immunosera

Anti PMMoV-CP: The immunosera against the PMMoV coat protein (CP) was obtained in our laboratory (Alonso *et al*., 1989). For the detection of PMMoV CP by Western blot and by immunofluorescence dilutions 1/1000 and 1/100 were used, respectively.

Anti-Grx: Immunosera against the *C. chinense* glutaredoxin was obtained in our laboratory by using *E. coli*-expressed 6xHistidine tagged *Cch* Grx protein (His-Grx). The purified protein was used for rabbit immunization. The *Cch* Grx specific inmunoserum was used at 1/1000 dilution for detection of Grx protein expression by Western blot analysis.

GFP specific polyclonal antibodies: GFP (FL): sc-8334 from Santa Cruz Biotechnology, INC (Heidelberg, Germany) was used at 1/250 dilution for GFP detection by Western blot analysis.

HA epitope specific monoclonal antibody: 12CA5 anti-HA mAb (Roche Diagnostics, Mannheim, Germany) was used at 1:2500 dilution.

Anti-Digoxigenin alkaline phosphatase (AP) conjugated Fab fragments (Roche Diagnostics GmbH, Mannheim, Germany) was used at 1:10,000 dilution.

Secondary antibodies:

Horseradish Peroxidase-Linked Goat anti-rabbit IgGs (Santa Cruz Biotechnology)

Anti-Mouse IgG, Horseradish Peroxidase-linked species-specific whole antibody (GE Healthcare).

Alexa 488 labelled Goat anti-rabbit IgG antibodies (Molecular Probes)

AP-labelled Goat anti-rabbit IgG antibodies (Sigma)

3.6. Cultivation of plants on soil

N. benthamiana plants were grown in growth chambers at 25ºC, with 65% relative humidity and a photoperiod of 16 hrs light with a light intensity of 6,500 lux.

3.7. Cultivation of plants in selection media

R1 and R2 seeds from the *N. benthamiana* transgenic lines were surface sterilized in 10% bleach for 15 minutes and washed 3-4 times with sterile water. Subsequently, they were cultured in solid Murashige and Skoog media (MS) with 3% sucrose (Murashige and Skoog, 1962) containing 50 μg/ml of kanamycin as selection medium. The plants were grown in growth

chambers at 25ºC under sterile condition with a photoperiod of 16 hrs light and a light intensity of 10,000 lux.

After grown for 14 days in *in vitro* conditions, the plants were transplanted to pots containing soil, and they were grown as above described.

3.8. Analysis of *C. chinense* Grx expression in *N. benthamiana* transgenic plants

In order to determine the accumulation level of *Cch* Grx in *N. benthamiana* transgenic plants harbouring each construction, systemic leaves from 6 week-old plants were sampled and total proteins were extracted by using 2x Laemmli buffer (100 mM Tris-HCl, pH 6.8; 4% SDS; 200 mM DTT; 0.6 mM PMSF; 20% glycerol and 0.05% bromophenol blue) (Laemmli, 1970) in the proportion of 5 µl of buffer/1 mg of fresh tissue. Samples were heated at 95^{o}C for 5 min followed by sonication for 5 min in a water sonicator (JP Selecta, Barcelona Spain) and then centrifuged at 20,000 g for 5 min. Protein content of *Cch* Grx, *Cch* Grx-GFP and *Cch* Δ2MGrx-GFP was assayed by Western blot analysis. Proteins from 5 µl of total extracts (1 or 0.1 mg of fresh tissue, depending on the transgenic line) were separated by electrophoresis on SDS polyacrylamide gels (SDS-PAGE) according to Laemmli (1970), by using 17.5% and 5 % polyacrylamide as resolving and stacking gels, respectively. Western blot analysis was performed as described in Ruíz del Pino *et al*., (2003) by using *Cch* Grx specific immunoserum diluted at 1/1000. The immunoreactions were visualized with the ECL chemiluminescence kit (GE Healthcare Amersham) following manufacturer's instructions**.** The enzymatic reaction produces a luminescent compound that is detected by visible light sensitive films (Hyperfilm, Pharmacia).

3.9. Plant virus inoculation and purification

In order to purify the virus, PMMoV-I was propagated in *N. benthamiana* Domin plants. The first pair of developed leaves from 6 week-old plants were mechanically inoculated with purified PMMoV-I virion preparation at the concentration of 50 µg/ml in inoculation buffer (0.02 M sodium phosphate buffer, pH 7), by using carborundum as abrasive. Ten days after inoculation, virus was purified by the method described by García-Luque *et al*., (1990). The viral concentration was calculated by spectrophotometric methods using a $\xi_{260,\ 0.1\%} = 3$ (Wetter *et al*., 1984).

3.10. Purification and analysis of viral RNA

The viral RNA was purified by following the method described in García-Luque *et al.,* (1990). The purified viral RNA was quantified in a spectrophotometer NanoDrop™ 1000 (Nanodrop Technologies) and analyzed by 0.8% agarose gel electrophoresis as described in 2.16 paragraph. The RNA was kept at -80ºC.

For either viral or plant RNA analysis, buffers were sterilized and equipment was treated with 10% SDS solution before electrophoresis in order to avoid ribonuclease contamination.

3.11. Cultivation of *E. coli*

Bacterial strain of *E. coli DH5α* was used for cloning and purification of plasmids and the strain M15 (pRep4) was used to express the *C. chinense* Grx protein. Bacteria were cultivated at 37°C in Luria-Bertani (LB) media (Sambrook *et al*., 1989). Media were supplemented with the required antibiotics for selection of transformants, 50 μg/ml ampicillin for selection of *E. coli DH5α* clones, and 100 μg/ml ampicillin plus 25 μg/ml kanamycin for selection of M15(Rep4):*Cch* Grx clones. Bacterial clones were stored at -80°C in the same medium in the presence of 20% glycerol (v/v). Growth in solid medium was carried out in LB medium with 1.5% agar, supplemented with the corresponding antibiotics for the selection of transformants.

3.12. Preparation of *E. coli* electro-competent cells and transformation

The bacterial transformation was carried out by electroporation. To prepare electro-competent cells, a single bacterial colony was grown in 10 ml of LB medium for 12 hours. 2.5 ml of this culture was used to inoculate 500 ml of LB medium without NaCl and the culture was grown until the bacterial density reached 0.4-0.5 OD at 600 nm. The bacteria were collected by centrifugation for 15 min at 2600 g at 4°C, and the pellet was resuspended in 450 ml of ice-cold sterile 10% glycerol. The centrifugation was repeated 3 times and the pellet was resuspended in in 250, 10 and 2 ml of ice-cold sterile 10% glycerol. Finally, the bacterial suspension was distributed onto aliquots of 50 μl, frozen in liquid nitrogen and stored at -80°C.

For bacteria transformation, DNA ligation reaction mix was dialyzed against sterile distilled water with Nitrocellulose filters 0.025 μm (Millipore Corporation, Bedford, MA) and mixed with a bacterial aliquot. Transformation was performed by electroporation in a Gene-

pulser unit (Bio-Rad Laboratories) set at 2.2 KV, 25 μF and 200 Ω in 0.2 cm cuvettes (Bio-Rad Laboratories).

3.13. Manipulation of DNA

3.13.1. Plasmid Purification

For the purification of plasmid DNA, bacteria were grown in 500 ml of LB medium supplemented with the required selection antibiotics and the plasmids were purified using the "Qiagen Plasmid Midi Kit" (Qiagen), following the protocol described by the manufacturer.

DNA concentration was determined spectrophotometrically using a $\xi_{260\ 0.1\%} = 21$ (Billeter *et al*., 1966).

3.13.2. Enzymatic treatment of plasmid DNA

The manipulation of DNA with restriction enzymes was carried out by following the instructions provided by the suppliers and according to established protocols (Sambrook *et al*., 1989).

3.13.3. PCR DNA amplification

DNA fragment amplification was performed by polymerase chain reaction (PCR) essentially as described in Tenllado *et al.*, (1994), using plasmid DNA (0.5 μg) as template. The reaction mixture contained, in a final volume of 50 μl, 1x enzyme buffer, 0.2 mM each dNTPs (Promega), specific primers for the fragment amplification at a final concentration of 0.5 μM and 0.01 U of High-Fidelity DNA Polymerase (Finnzymes). The annealing temperature was calculated based on the AT-GC percentage of the primers (nº AT bases x2 + nº GC bases x4).

3.13.4. Electrophoretic analysis of DNA

DNA samples were analyzed by 0.8% agarose gel electrophoresis containing ethidium bromide (0.5 μg/ml). Samples were diluted with 0.2 volumes of loading buffer (30% glycerol, 0.25% bromophenol blue and 0.25% Xylene cyanol) before loading onto the well. The buffer used for electrophoresis was TAE buffer (40 mM Tris-acetate, 1 mM EDTA, pH 7.8) and the voltage applied was 5 V/cm. The bands were visualized by UV illumination. *Eco*RI/*Hind*III

digested- λ phage DNA and the *Sau*IIIA-digested pUC18 plasmid were used as DNA size markers.

3.13.5. Recovery of DNA from agarose gels

In order to purify either DNA fragments or digested plasmids, an electrophoresis in low-melting-temperature agarose (Seakem GTG agarose, BMA) was performed. Once the DNA fragments were separated, DNA bands were visualized under UV, cut and eluted from the agarose gel by freezing and thawing in the presence of phenol. For this purpose, the agarose containing the DNA band of interest was grinded with a volume of 0.1 M Tris pH 8-saturated phenol. The homogenate was frozen at -80^{o}C for 3 min and then centrifuged at 20,000 g for 15 min. The aqueous phase was collected and subjected to two consecutive extractions with phenol:chloroform:isoamyl alcohol (25:24:1). Subsequently, the DNA was precipitated by adding 0.1 volumes of 3 M Sodium acetate pH 5.2 and two volumes of 100% ethanol. The DNA was collected by centrifugation and resuspended in sterile deionised water.

3.13.6. Ligation and cloning of DNA fragments into plasmid vectors

Digested DNA fragments were ligated to the plasmid vector, digested with the same restriction enzymes, with 5 U of T4 DNA ligase (5 U/µl) (Promega) following the manufacturer's instructions. The recombinant plasmid was introduced in to *E. coli* DH5α competent cells by electroporation as described in the 2.12 paragraph.

3.13.7. Nucleotide sequence determination and analysis

The sequence of the recombinant plasmids were obtained by automated DNA sequencing at Secugen S.L. (Madrid, Spain). DNA sequence analysis was performed by BLASTN 2.2.27 program (Altschul *et al.,* 1997).

3.14. *Cch* Grx protein expression in *E. coli*

In order to *in vitro* express the *Cch* Grx protein, we used *E.coli* M15(pREP4):Grx clones containing the sequence coding the Grx mature protein cloned in the sites *Pvu*II and *Sal*I of the plasmid pQE-1 (Qiagen), obtained previously in our laboratory. The protein obtained is an N-terminal 6xHis-tagged Grx protein (His-Grx).

3.14.1. Purification of *Cch* Grx protein under denaturing condition

Three bacterial colonies of *E.coli* M15 (pREP4): *Cch* Grx (no.10, 18 and 26) transformed with the pQE-1-*Cch* Grx plasmid were selected to analyze the expression level of the His-Grx by a minipreparation assay under denaturing condition. The buffers and reagents used were as described (The QIAexpressionist).

To start-up the initial culture, a single colony was inoculated in 5 ml of LB media containing ampicillin (100 µg/ml) and kanamycin (25 µg/ml) and grown overnight at 37^{o}C. Around 500 µl of this culture were inoculated onto two 10 ml LB media supplemented with antibiotics and grown at 37^{o}C until it reaches an OD_{600} between 0.5 to 0.7. In one tube the protein expression was induced by adding Isopropyl β-D-1-thiogalactopyranoside (IPTG) at a final concentration of 1mM, while in the other tube no IPTG was added and taken as non-induced control. After 4-5 hours of growth, 1 ml of culture from both induced and non-induced cultures were centrifuged and the bacteria were lysed with 400 µl of buffer B (100 mM NaH_2PO_4, 8 M Urea, 10 mM Tris-Cl pH 8). The lysate obtained was centrifuged at 15,000 x g for 20 min to get the supernatant. The His-Grx expressed protein was affinity purified from the lysate supernatant by using 25 µl of activated HIS-Select Nickel affinity Gel resin (Sigma) as described in (The QIAexpressionist). The resin was activated according to the manufacture's instruction.

Purified proteins and bacterial extracts were analyzed by SDS-PAGE analysis. 10 µl of purified protein solution was diluted with 2.5 µl of 5x Laemmli sample buffer and the bacteria pellet from 1 ml of culture was diluted with 100 µl Laemmli buffer. Both samples were heated to 95^{o}C for 5 min and then, 10 µl of each sample were loaded onto SDS-PAGE gels (Laemmli, 1970) containing 17.5% and 5% polyacrylamide as resolving and stacking gels respectively. Gels were stained with Coomassie brilliant blue-R250.

3.14.2. Expression and purification of His-Grx soluble protein under native conditions

E.coli M15 (pREP4): *Cch* Grx colony no 10 was used for protein expression and purification of native soluble His-Grx protein.

A single colony was inoculated in 20 ml of LB media containing ampicillin (100 µg/ml) and kanamycin (25 µg/ml) and grown overnight at 37^{o}C. The entire culture was used to inoculate

2 l of LB media and allowed to grow until it reaches an OD_{600} of 0.5. A sample of 1ml culture was centrifuged and stored at -20°C as control before His-Grx induction. Grx expression was induced by adding 1mM IPTG and the cells were grown for additional 4-5 hours at 37°C with agitation. Then 1 ml sample was centrifuged and stored at -20°C for further analysis. The remaining cells were harvested and stored overnight at -80°C.

Purification of the protein was performed under non-denaturing (native) conditions using HIS-Select® Nickel Affinity Gel purification resin (Sigma-Aldrich). All the buffers and reagents used were as described (The QIAexpressionist). All purification steps were carried out at 4ºC. The bacterial pellet was thawed for 15 min on ice and resuspended in 40 ml of cold lysis buffer (50 mM NaH_2PO_4, 300 mM NaCl pH 8) and the bacterial cells were broken by French press (Spectronic Instruments) at 1000 psi for three times. About 100 µl of broken cells were taken and stored at -20°C for further analysis. Then, the lysate was centrifuged at 10000 g for 30 min. and the supernatant was used to purify the soluble His-Grx protein. To 30 ml of the supernatant lysate, 5 ml of the activated HIS-Select® Nickel Affinity resin were added and mixed at 200 rpm on a rotary shaker at 4°C for 60 min. The lysate–resin mixture was loaded into a column and once the resin settled down, it was washed with washing buffer (50 mM NaH_2PO_4, 300 mM NaCl 15 mM imidazole, pH 8). The bound protein was eluted off from the column with 10 ml of native elution buffer (50 mM NaH_2PO_4, 300 mM NaCl 250 mM imidazole, pH 8) and collected in several different fractions of 1 ml each. The purified protein was dialyzed using the dialysis buffer (Tris-HCl 30 mM pH 7.9) at 4°C for 24 hours with two buffer changes. Samples were collected from each purification step for SDS-PAGE analysis and the purity of purified His-Grx was checked by SDS-PAGE analysis.

His-Grx protein concentration was determined spectrophotometrically using an extinction coefficient $\xi_{280,\ 0.1\%} = 0.698$ calculated according to Gill and von Hipple (1989).

3.14.3. Determination of Grx activity by β-Hydroxyethylene Disulfide Assay (HED assay)

The β-hydroxyethyl disulfide (HED) assay was performed essentially as described by Holmgren and Åslund (1995). In this assay, Grx activity was measured by following nicotinamide adenine dinucleotide phosphate (NADPH) oxidation as a decrease in absorbance at 340 nm in a coupled enzyme reaction with 1 mM reduced glutathione (GSH) and glutathione reductase. In a final volume of 1ml, 1 mM GSH, 0.7 mM β-hydroxy ethyl disulfide (HED), 0.25

mM NADPH and 6.4 μg/mL glutathione reductase were mixed in 0.1 M Tris-Cl pH 7.4. The reaction mixture was incubated at room temperature for 2 min to allow HED substrate and the GSH to form mixed disulfides and then, the decrease in OD at 340 nm was recorded in a SpectroMax micro-plate reader for 1 min at room temperature. His-Grx protein was added to the same cuvette and the decrease in absorbance at 340 nm was recorded as above. Measured activities in all assays were corrected by subtracting the absorbance before adding the His-Grx protein. One unit of activity is defined as the consumption of 1 μmol of NADPH per minute calculated from the expression $(\Delta A_{340} \times V) / (min \times 6.2)$, where V is the cuvette volume in ml and 6.2 is the mM extinction coefficient for NADPH. The K_m value for glutathione was determined using varying concentrations of GSH (0.5-5.0 mM). Two independent experiments were performed at each substrate concentration, and the apparent K_m and K_{cat} values were calculated by non-linear regression using the program SigmaPlot 12.0.

3.15. Analysis of PMMoV-I viral coat protein (CP) accumulation in *N. benthamiana* transgenic plants

To study viral CP accumulation in *N. benthamiana* transgenic plants, the plants were inoculated with PMMoV-I at a viral concentration of either 5 or 50 μg/ml by using the same conditions as described in paragraph 3.9. Control plants were inoculated with inoculation buffer. Five to ten plants were used in each experiment and the experiment was repeated three times.

Samples were taken at 7 dpi from the inoculated leaves, and also from the systemic leaves of both mock-inoculated and PMMoV-I-infected plants at 7, 14 and 28 dpi.

Total proteins were extracted from the sample leaves as described above (3.8). Total protein extracts were analyzed electrophoretically on SDS polyacrylamide gels (SDS-PAGE) according to Laemmli (1970) by using 17.5% and 5 % polyacrylamide as resolving and stacking gels respectively. For 7 dpi, 5 μl sample of total protein extracts corresponding to 0.4 mg of fresh tissue were loaded. For the rest of analyzed time points total protein extracts corresponding to 0.2 mg of fresh tissue were loaded onto the gels. A standard curve of virus (0.25, 0.5 and 1 μg) was loaded onto each gel. The proteins were stained with Coomassie Blue R250 (Sambrook *et al.,* 1989) and PMMoV-I coat protein was quantified by using a densitometer and the Quantity One software (Bio-Rad, Hercules, CA, USA), as described in Tena *et al.,* (2012).

3.16. PMMoV-I infection of *N. benthamiana* protoplasts

N. benthamiana protoplasts were prepared from 6-8 week old plants. The leaves selected for these assays were about 4-5 cm long in size. The leaves were surface sterilized by immersing them in 10% bleach solution for 15 min and followed by 3 times wash with sterilized water. Protoplasts were obtained as described in Ruíz del Pino *et al.,* (2003), except that protoplasts were washed 2 times with ice-cold solution of 12% mannitol containing 6 mM $CaCl_2$. Protoplasts were counted in a haemocytometer and resuspended in ice-cold electroporation buffer (12% mannitol, 6 mM $CaCl_2$, 80 mM KCl pH 7.2) at a concentration of 1.3 $x10^6$ protoplasts/ ml.

Protoplasts were transfected with PMMoV-I RNA by electroporation using a Gene-pulser apparatus (Bio-Rad laboratories). For electroporation, $4x10^5$ protoplasts in a final volume of 300 µl were taken in 0.2 cm electroporation cuvettes (Bio-Rad laboratories) and kept on ice. 20 µg of PMMoV-I RNA were added to the cuvette, mixed with protoplasts and immediately used for electroporation. The conditions set for electroporation were: 125 µF and 0.12 kV. The infected protoplasts were kept on ice for 15 min in order to get recovered from the shock. Then, the protoplasts were incubated in CPW-13% Mannitol pH 5.6 in a growth chamber at 25^{o}C with a 16 h photoperiod. Samples were taken at 16, 24 and 48 hpi, collected by centrifugation at 134 g and resuspended in 5x Laemmli buffer (Laemmli, 1970) and kept at -80^{o}C until they were analyzed.

To analyze the protoplast infection, 10^4 protoplasts were loaded onto the gel and analyzed by Western blot for the accumulation of PMMoV-I CP as described in paragraph 3.8. except that a PMMoV CP-specific immunoserum at 1/1000 dilution was used.

3.16.1. Protoplast immunofluorescence assay

At 24 hpi, control and PMMoV-I infected protoplasts were collected by centrifugation at 134 g and analysed for infection as described in Ruíz del Pino *et al.*, (2003), with some modifications. Briefly, 10^5 protoplasts were fixed in 4% paraformaldehyde in 9% mannitol (pH 7.2) for 30', after washing, they were resuspended in 1 ml of PBS (3.2 mM Na_2HPO_4, 0.5 mM KH_2PO_4, 1.3 mM KCl, 135 mM NaCl, pH 7.2)-9% mannitol and 10^4 protoplasts were fixed over the poly-L-Lysine (0.01%) (Sigma)-coated glass slides by cytospin centrifuge (Shandon), and kept at -20ºC. Before the assay, protoplasts were rehydrated with PBS for four times. Primary immunoserum was anti-PMMoV-S-CP diluted 1/100 in incubation buffer [PBST (PBS +0.05%

Tween 20), containing 2% BSA and 1% (v/v) of goat serum] and secondary antibody was goat anti-rabbit IgG antibodies conjugated to Alexa 488 (Molecular Probes) diluted 1/100 times in incubation buffer. Samples were mounted with Vectashield (Vector laboratories, Inc. Burlingame, CA, USA) after washing with PBST for 3 times. The percentage of infection was counted under a Leica AF6000 LX multidimensional microscope and observed under a Leica TCS SP5 confocal laser microscope. For antibody detection imaging, excitation at 488 nm and collection at 519 nm was used. For chlorophyll autofluorescence imaging, excitation at 633 nm and collection at 670 nm was used. At least 200 cells were analysed for specific fluorescence to calculate infection percentages.

3.16.2. Immuno-staining of protoplasts with AP-labelled antibodies

Goat anti-rabbit IgG antibodies conjugated with alkaline phosphatase (AP) were used as secondary antibodies to analyze the protoplast infection rate in the GFP expressing lines of *Nb:GFP, Nb:Grx-GFP and Nb:Δ2MGrx-GFP*. The samples were prepared as mentioned above up to primary antibody incubation except that TBS (10mM Tris-HCl, 160 mM NaCl, pH 7.2) was used. For secondary antibody treatment, the samples were incubated with AP-conjugated anti-rabbit IgG antibodies (Sigma) [diluted 1/100 times in TBST (TBS+0.05% Tween 20), 2% BSA and 1% (v/v) of goat serum] for 1 hr at room temperature under dark. Slides were washed with TBS for 10 times and then incubated with AP buffer (100 mM Tris-ClH, pH 9.5, 100 mM NaCl, 5 mM $MgCl_2$) twice, 5 min each. The colour was developed by incubating with the alkaline phosphatase substrate SIGMA *FAST*™ BCIP/NBT (5-Bromo-4-chloro-3-indolyl phosphate/Nitro blue tetrazolium) (Sigma) (prepared according to manufacturer's instructions) for 30 min at room temperature under dark. The reaction was stopped by adding TBS containing 20 mM EDTA and washed with water and mounted with glycerol/PBS (v/v). The purple colour developed in the infected protoplasts was examined under a Zeiss microscope in order to calculate the percentage of infection as above.

3.17. Subcellular localization of *Cch* Grx protein

For the subcellular localization of *Cch* Grx, the protoplasts obtained from *Nb:GFP, Nb:Grx-GFP* and *Nb:Δ2MGrx-GFP* lines were visualized with confocal microscope. 10^5 protoplasts from each line were fixed with 4% paraformaldehyde in 9% mannitol (pH 7.2) as

described in 2.26, and stained with 4', 6-Diamidino-2-phenylindol dihydrochloride (DAPI), in order to label the nuclei. DAPI staining was performed as follows: around 10^4 protoplasts were incubated with 100 µl of 2 µg/ml DAPI solution in PBS-9% mannitol for 5 minutes. Afterwards, 900 µl of PBS-9% mannitol was added and kept for another 15 minutes. The protoplasts were collected and washed with PBS-9% mannitol twice and finally suspended in 100 µl of PBS-9% mannitol. Around 20 µl of these samples were loaded over poly-L-Lysine (0.01%) (Sigma)-coated glass slides and kept until the protoplast settled. The samples were mounted with Vectashield (Vector laboratories, Inc. Burlingame, CA, USA) and cover slips were sealed with nail polish. For GFP confocal microscopy imaging, the protoplasts were excited at 488 nm (the peak of GFP) and emission was recorded at 520 nm. The auto fluorescence of chlorophyll was detected as described in 3.16.1. Nuclei labelled with DAPI were imaging with excitation at 365 nm and emission at 460 nm. Samples were examined by Leica TCS SP2 confocal laser-scanning microscope at ×40 oil immersion objective lens.

3.18. Extraction of total RNA from *N. benthamiana* plant leaves

For RNA extraction, about 2 g of plant leaf tissue were taken at 7, 21 and 28 dpi, from control mock- and PMMoV-I-inoculated plants. At 7 dpi, samples were taken from both the inoculated and systemic leaves; at 21 dpi, samples were taken from systemic leaves and at 28 dpi, samples were taken from symptomatic (infected) and asymptomatic (recovered) systemic leaves. Total leaf RNA was extracted according to the method based on Chomcynski and Sacchi (1987) by using TRI reagent (Sigma-Aldrich Co.) and following the manufacturer's instructions with the following modifications: an additional centrifugation at 12000 g for 10' at 4ºC after plant tissue homogenization and an additional final RNA precipitation step in 0.3 M Sodium acetate pH 5.2 and 2.5 volumes of 100% cold ethanol were performed.

RNA concentration was determined by spectrophotometric methods using the NanoDrop™ 1000 spectrophotometer (Nanodrop Technologies). 260/230 ratios and 260/280 ratios were taken into consideration. RNA samples were conserved at - 80ºC until their analysis.

3.19. Synthesis of Digoxigenin-labelled RNA probes

The probes used in this work were: PMMoV RNA of negative polarity; glutathione Reductase (GR), an enzyme involved in the glutaredoxin-GSH cycle; glutathione S-transferase

(GST), an enzyme catalyzing the conjugation of glutathione (GSH) to a wide range of phytotoxic substrates, pathogenesis related proteins (acidic PR-1, PR-2a, PR-5), (basic PR-2b) which are involved in the defence mechanism against pathogens through salicylic acid, and ethylene pathways and 9-LOX, involved in the synthesis of oxylipins which took part in defence against pathogens.

PMMoV probe:

For viral RNA detection, the clone pT-CPS containing a cDNA fragment of 694 bp corresponding to PMMoV-S CP and 3' non-coding region of the virus (Gilardi *et al*., 1998) was used. The plasmid was linearized by digestion with *Hind*III and transcribed by T7 RNA polymerase. Because viral RNAs are 3´ co-terminal, this probe detects PMMoV genomic RNA and CP subgenomic RNA.

Pathogenesis Related proteins (PR probes):

The probes used for the detection of mRNA coding for acidic PR-1, PR-2 and PR-5 proteins of *N. tabacum* were obtained from Dr. Carmen Castresana (CNB, CSIC. Madrid). Plasmids were linearized with *Hind*III and transcribed by using either T3 or T7 RNA polymerase.

The probe used to detect the mRNA coding for the basic PR-2b protein was specific for basic β-1, 3-glucanase *gn2* from *N. plumbaginifolia* and was a kind gift from Dr. C. Castresana (CNB, CSIC. Madrid). The plasmid was linearized with *Eco*R1 restriction enzyme and transcribed with T3 RNA polymerase.

9-LOX Probe:

The cDNA cloned from *N. tabacum* 9-LOX (kindly provided by Dr.C.Castresana, CNB, CSIC) was used to detect the 9-LOX expression. The plasmid was linearized with *Hind*III restriction enzyme and transcribed with T7 RNA polymerase.

GR probe:

The tobacco Glutathione reductase (GR) clone pGRT4 was a kind gift from Dr Mullineaux (Creissen and Mullineaux, 1995). It contains the 2 kb tobacco GR cDNA cloned into the pBluescriptII plasmid. The plasmid was linearized with *Eco*R1 enzyme and transcribed with the T7 RNA polymerase.

GST probe:

GST riboprobe was prepared from pCNT 103 pBK (kindly provided by Dr. C. Castresana, CNB, CSIC). The plasmid was linearized with *Hind*III restriction enzyme and then transcribed with T3 RNA polymerase.

To prepare non-isotopic probes, the linearized vectors were used as templates for *in vitro* synthesis of RNA transcripts. The MAXIscript kit (Ambion) was used for *in vitro* transcription following manufacturer's instructions. Nucleotides ATP, GTP and CTP were used at 1 mM final concentration in the reaction mixture. The labelled nucleotide Digoxigenin-11-UTP (Roche Diagnostics GmbH, Mannheim, Germany) at 0.35 mM and unmodified UTP at 0.65mM were added to the reaction mixture. In all hybridization experiments the probes were denatured by heating at 95^{o}C for 10 min and cooled on ice for 3 min before being added to the membrane for hybridization.

3.20. Detection of RNA sequences by Northern blot analysis

For Northern blot analysis, 10 µg of sample RNAs were denatured at 65°C for 4 min in 3-morfolino-propanosulfónico (MOPS)-Acetate-EDTA buffer (2 mM MOPS, 1.5 mM sodium acetate, 1.6 mM EDTA pH 7.0) containing 10.2% formamide, 0.9% formaldehyde, and 0.06 mg/ml ethidium bromide. Then, the samples were electrophoresed onto 1.5% agarose-formaldehyde gels containing MOPS buffer (50 mM MOPS, 0.4 mM EDTA pH 7) and 6% formaldehyde, using the same buffer as electrophoresis buffer and applying a current of 5 V/cm. RNAs were visualized under UV light illumination and then transferred onto nylon membranes (Hybond-N, Pharmacia) by capillarity, in 10x SSC buffer (1.5 M NaCl, 0.15 M sodium citrate pH 7) overnight as described in Sambrook *et al*., (1989). The RNA was fixed to the membrane by irradiation with UV light (120 mJ) in a UV Stratalinker apparatus (Cultek). The membranes with transferred RNA were stored in cold condition for later use.

For hybridization with Digoxigenin-labelled RNA probes, described in paragraph 3.19, the DIG Luminescent Detection Kit (Roche Diagnostics GmbH, Mannheim, Germany) was used. The membranes were incubated with standard buffer (50% formamide, 5xSSC, 0.1% sodium-lauroylsarcosine, 0.02% SDS and 2% blocking reagent (Roche Diagnostics GmbH, Mannheim, Germany) for 2 hrs at 65^{o}C. Then, they were hybridized overnight at 68^{o}C with the standard buffer containing the corresponding probe. Once the hybridization was finished, the membranes were first washed in a buffer containing 2xSSC, 0.1% SDS for two times, 15 min each at room

temperature (RT) and again washed two times with 0.1xSSC, 0.1% SDS for 15 min at 65^{o}C. Probe detection was performed using the DIG Luminescent Detection Kit (Roche Diagnostics GmbH, Mannheim, Germany) according to manufacturer's protocol. In brief, the membranes were incubated with blocking solution [Maleic buffer (0.1M Maleic acid, 0.15M NaCl pH 7.5) containing 1% blocking reagent] for 30 min followed by incubation with anti-Digoxigenin AP-conjugated antibody at 1:10,000 for 30 min. Then, the membranes were washed for two times in washing buffer (Maleic buffer containing 0.3% (v/v) Tween 20) and equilibrated with detection buffer (0.1 M Tris-HCl pH 9.5, 0.1 M NaCl). The membranes were incubated with chemiluminescent substrate CSPD (Disodium 3-(4-methoxyspiro {1, 2-dioxetane-3, 2'- (5'-chloro) tricyclo(3.3.1.1^{3,7}) decan}-4-yl) phrnyl phosphate) (Roche Diagnostics GmbH, Mannheim, Germany) and then exposed to X-ray sensitive films (Hyperfilm, Pharmacia) for developing.

3.21. Extraction of pyridine nucleotides from leaf samples

To analyze the pyridine nucleotide (PN) content in mock- and PMMoV-I-infected plants, samples from plant leaves at 21 and 28 dpi were taken. About 30 mg of fresh leaf samples from 5 different plants were taken in two separate eppendorfs and grinded into powder form by agitating with ball bearing (0.6 mm diameter; Sigma) at 10000 rpm for 1 min. The PNs were extracted by selective hydrolysis of NADH and NADPH in acid medium and NAD^+ and $NADP^+$ in alkaline medium according to Hajirezaei *et al.,* (2002) except that the final pH of the neutralized supernatants was between 8.0 to 8.5. 100 µl aliquots were taken and frozen at -80^{o}C for later analysis.

PNs in the neutralized extracts were determined based on Gibon *et al*. (2004) with some modifications.

3.21.1. Determination of NAD^+ and NADH content in the plant extracts

For the determination of NAD^+ and NADH, 25 µl of the extracts mentioned above were diluted up to 100 µl with water and standard solutions in the range of 0-25 picomoles were freshly prepared. Triplicate aliquots of 100 µl of the extracts as well as the standards were added to 50 µl of detection mix which contained 0.3 M Tricine/KOH pH 9.0, 12 mM Na_2-EDTA, 0.3 mM phenazine ethosulfate (PES) (Sigma), 1.8 mM thiazolyl blue tetrazolium bromide (MTT)

(Sigma), 1.5 M ethanol, and 18 U/ml alcohol dehydrogenase (Roche). Along with the extracts mentioned above, a blank measurement was also performed. The absorbance was read at 550 nm in a microplate reader (Model 680, Biorad) for 40 min at 30°C. The concentration of NAD^+ and NADH in the extracts was determined from the standard curves generated in each assay after subtracting the blank value.

3.21.2. Determination of $NADP^+$ and NADPH content in the extracts

For the determination of $NADP^+$ and NADPH, 25 µl of the extracts mentioned above were diluted up to 100 µl with water and standard solutions in the range of 0-25 picomoles were freshly prepared. The assay was performed as above described, except that the detection mix contained 0.3 M Tricine/KOH pH 9.0, 12 mM Na_2-EDTA, 0.3 mM phenazine methosulfate (PMS) (Sigma), 1.8 mM MTT, 9 mM glucose-6-phosphate, and 9 U/ml glucose-6-phosphate dehydrogenase. The absorbance was read as above. The concentration of NADPH and $NADP^+$ in the extracts was determined by comparing the sample values to standard curves generated in each assay.

Statistic analysis was performed by SAS 9.1 programme (SAS 9.1 Inc.) using 1-way analysis of variance (ANOVA).

3.22. Oxidative stress tolerance test

To investigate the effect of constitutive expression of *Cch* Grx protein on oxidative stress tolerance*, N. bentahamiana* transgenic plants were grown over one-half MS media in the presence and absence of 3 mM H_2O_2 and 1 µM paraquat. The seedlings were grown horizontally for the first 3 days and then grown in vertical position for another one week. The conditions set for the growth of seedlings were 25^{o}C and 16 hrs of photoperiod. Root length was measured after 10 days. The experiments were performed with three replicas each containing 30 seedlings and repeated for 3 times.

Statistical analysis was performed by one-way ANOVA by using SPSS software programme (SPSS Inc, 1999).

3.23. Protein sequence analysis and structure prediction

Theoretical isoelectric point (pI) and Mr for the mature *Cch* Grx protein was calculated by ExPASY server (http://www. expasy.org/ tools/). Homologues of *Cch* Grx protein, with

CSYS active site were selected through BLASTp programme at NCBI server (http://blast.ncbi.nlm.nih.gov /Blast.cgi). To find the chloroplast targeting region in the protein sequence, ChloroP 1.1 programme was used (Emanuelsson *et al.,* 1999). Structure of *Cch* Grx was predicted by I-TASSER server, which uses the PDB template models of poplar GrxS12 (3fzaA), human GLRX3 (3zywA), human thioredoxin reductase (3h8qA), Zebrafish apo Grx2 (3uiwA) and yeast mutant Grx1p C30S (2jadA).

3.24. Multiple Sequence alignment and phylogenetic analysis

Proteins selected through BLASTp were subjected to multiple sequence alignment using ClustalW Program (www.ebi.ac.uk/Tools). The aligned sequences were further subjected to Phylogenetic analysis using MEGA 5.1 software (Tamura *et al.,* 2011), which uses the Maximum-likelihood method for the constructing of phylogenetic tree.

3.25. Heterologous expression of *Cch* Grx in *S. cerevisiae*

3.25.1. Cloning of *Cch* Grx protein cDNA in *S. cerevisiae*

To express *Cch* Grx mature protein in yeast cells, the yeast integrative plasmid pMM221 (Molina *et al*., 2004) (a gift from Dr. E. Herrero, Universitat de Lleida, Lérida, Spain), was used to clone *Cch* Grx coding sequence. This plasmid contains the mitochondrial targeting sequence of yeast *GRX5* at the 5' end of the multiple cloning site and 3HA/His_6 tags at its 3' end. The full length cDNA of *Cch* Grx was already cloned in our laboratory in pGEM-T Easy vector (pGEM-Grx). To remove the *N*-terminal signal peptide of the *Cch* Grx protein, a truncated form of the protein was amplified by PCR by using pGEM-Grx plasmid as template. The forward primer (5´-ATAAGAATGCGGCCGCgTCGGGTTCATTCG GGTCC-3´) contained the *Not*I site sequence (underlined). In order to prevent the codon breakage while expressing in yeast, an additional nucleotide (lower case) was added, what introduced an extra alanine at the end of the mitochondrial targeting sequence of *GRX5* in the fusion *Cch* Grx protein. The reverse primer (5´-GAAGATCTGCTTTCTGTTTTTCCAGGATTA-3´) contained the *Bgl*II site sequence (underlined). The PCR reaction was performed as described in paragraph 2.15, with 5 cycles at an annealing temperature of 60ºC, followed by 25 cycles at 68ºC. The amplified fragment of 364 nt was digested with the restriction enzymes *Not*I and *Bgl*II, purified by elution from agarose gels as described (paragraph 2.17) and cloned into pMM221 plasmid previously digested with

the same enzymes. The resulting plasmid (pMM1025), LEU+ and Ampicillin resistant (*Amp R*), was transformed into *E. coli* DH5α bacteria by electroporation (paragraph 2.12). Transformed clones were selected on LB media supplemented with 50 µg/ml ampicillin. The cloned nucleotide sequence was corroborated by nucleotide sequencing.

3.25.2. Growth conditions for *S. cerevisiae*

The yeast strains employed in this work are described in 2.4. paragraph. YPD medium (1% yeast extract, 2% peptone, 2% dextrose) was used for the growth of yeast cells by incubation at 30°C. YPGly and YPGal media are similar to YPD except that they contain 3% glycerol and 2% galactose instead of dextrose. Synthetic SD medium contains 0.67% yeast nitrogen base, 2% glucose, and the auxotrophic requirements Kaiser *et al*., (1994).

3.25.3. Expression of *Cch* Grx protein in yeast strains

The plasmid pMM1025, containing the *Cch grx* sequence coding for the mature protein, was linearized with *Cla*I and transformed onto the wild type mat alpha strain W303-1B and the integrated plasmid was selected by growing in Leu auxotrophic medium. Then crossing over was carried with the opposite mating partner having *Δgrx5* background, strain MML 100, having Geneticin resistance marker (*GEN R*). The resulted diploid strain was selected over Leu auxotrophic and Geneticin containing media in order to have *Cch grx* sequence transformed in *Δgrx5* strain. In order to produce the haploid cells, sporulation was induced in the crossed over diploid cells. The spores were micro manipulated to obtain the tetrads and again grown over the Leu auxotrophic and Geneticin media in which the yeast haploid strain containing *Cch grx* gene in the *Δgrx5* background could be selected. DNA transformation, selection over media, crosses between the yeast strains, sporulation, and tetrad analyses were carried out as described by Kaiser *et al*., (1994).

In order to select the yeast strains expressing the HA-tagged- *Cch* Grx mature protein the different transformed yeast colonies (T1, T7, T9, T11, T12, T14) were grown exponentially on YPD medium supplemented with Geneticin and Ampicillin at 30ºC and were assayed for *Cch* Grx expression. Cells were harvested around the OD_{600} of 0.7 and the pellets were resuspended in 15 µl of 5M urea and boiled for 2 min. The cells were broken by adding an equal volume of glass beads (0.6 mm diameter, Sigma), mixed with 50 µl of 2% SDS in 0.125M Tris-HCl buffer,

pH 6.8, and vortex for 1 min. The resulting lysates were boiled for 2 min and the supernatants were collected. The proteins in the sample were quantified by Micro DC protein assay (BioRad). The proteins were immunodetected by Western blot analysis in which the HA-tagged proteins were detected by using 12CA5 anti-HA monoclonal antibody (Roche Diagnostics, Mannheim, Germany) at 1:2500 dilution and it was further detected with the secondary antibody Anti-Mouse IgG, Horseradish Peroxidase-linked species-specific whole antibody (GE Healthcare). The signals were detected by ECL (GE Healthcare Amersham). Yeast strain MML240 expressing the Grx5-3HA protein under its promoter was taken as positive control.

3.25.4. Sensitivity to oxidants

Wild type strain (W303-1B), Grx5 defective strain (MML100), Grx5 revertant strain (MML240) and *Cch* Grx expressing strain (T11) were assayed for sensitivity to oxidants. *S. cerevisiae* cells, grown exponentially for at least 10 generations at 30°C, were taken for the oxidant sensitivity tests. The grown cultures were spotted at 1:10 serial dilutions over YPD plates containing either 0.3mM tert-butyl hydroperoxide (t-BOOH) (Sigma Aldrich) or 1.25mM diamide (Sigma Aldrich) and recording growth after 2 days of incubation at 30°C.

3.25.5. Determination of iron accumulation in the yeast cells

The aforementioned yeast strains were grown exponentially on the YPD media and harvested at the OD_{600} of 0.8. After acid digestion, whole cell and mitochondrial iron were determined under reducing conditions with bathophenanthroline sulfonate (BPS) as chelator as described by Fish (1988).

3.25.6. Determination of aconitase and malate dehydrogenase (MDH) activities

Yeast strains mentioned above were grown exponentially in YPGal media and harvested at the OD_{600} of 0.8. The samples were digested by treating them with 100 µl of Tris 100 mM pH 8.0 with protease inhibitors (2 mM phenylmethylsulfonyl fluoride, 0.2 mM tolylsulfonyl phenylalanyl chloromethyl ketone [TPCK], and 2 µM pepstatin, final concentrations) along with glass beads. The supernatant was collected and the concentration of proteins was estimated by the Micro DC Protein Assay method (BIO-RAD) according to the manufacturer's instructions.

To measure the aconitase activity, 4 µl of protein extract were added to 500 µl of Tris HCl 50 mM pH 7.5 plus NaCl 1.7 mg/ml. OD was measured at 240 nm without adding the substrate cis-aconitate (time 0 OD) and then OD was measured again after adding the substrate (4 µl from an stock solution at 7 mg/ml). Specific activity (units/mg) was calculated from the formula.

$$\text{Specific activity} = \frac{\frac{\left(\text{OD(After aconitate)} - \text{OD(Before aconitate)}\right) \times 125}{4.28}}{\text{Protein concentration (mg/ml)}}$$

Where 125 in the formula represent the dilution of the sample and 4.28 is extinction coefficient of cis-aconitate ($mM.cm^{-1}$)

For the determination of MDH activity, 10 µl of protein extract were added to 970 µl of potassium phosphate buffer 0.1 M pH 7.4 containing 100µg of NADH. OD at 340 nm was measured (time 0), and the reaction started by adding the substrate oxalacetate (20 µl from the stock solution of 3.2 mg/ml). OD was then recorded after 1 min. Specific activity (units/mg) was calculated from the formula:

$$\text{Specific activity} = \frac{\frac{\left(\text{OD}(1\,\text{min}) - \text{OD}(0\,\text{min})\right) \times 100}{6.22}}{\text{Protein concentration (mg/ml)}}$$

Where 100 in the formula represent dilution of the sample and 6.22 is extinction coefficient of NADH (mM)

Relative ratio for aconitase to malate dehydrogenase was determined for all the four strains.

4.RESULTS

4.1. Molecular characterization of *C. chinense* Grx protein

The deduced amino acid (aa) sequence analysis of *Cch* Grx protein revealed that it encoded a 177 aa long protein, with a predicted 63 aa long N terminus chloroplastic targeting sequence. The sequence of *Cch* Grx without the plastid targeting sequence was analyzed. The mature protein contains 113 aa with a predicted Mr of 12.3 kDa and a theoretical pI value of 7.17.

Sequence analysis of *Cch* Grx protein showed that it belongs to the group of monothiol glutaredoxins with a CSYS active site, and thus it belongs to Class I group and positioned in the S12 subgroup according to the classification made by Couturier *et al.,* (2009a), therefore we name it as *Cch* GrxS12. (Fig.4.1 and 4.2).

To perform multiple sequence alignment, all Grx protein sequences retrieved by BLAST search were deleted for their targeting regions (Fig.4.1). On performing multiple sequence alignment, it was found that apart from CSYS active site, other conserved regions, ^{51}ELD^{53}, ^{74}TVPN^{77}, and ^{87}GCT^{89} are present in most of the selected proteins. A Try residue was present at the N-terminus of the active site (WCSYS) in all of the plant Grxs analyzed, whereas in the Grx6 from fungi *S. cerevisiae,* Thr was placed at that position.

Cch GrxS12 protein reported in this work showed high identity (97%) with GrxC5 (XP_004242377.1) from *Solanum lycopersicum*, 85% with GrxC5 (XP_002267052.1) from *Vitis vinifera*, 81% with GrxS12 (ACJ60637.1) from (*Populus tremula* x *Populus tremuloides*), 80% with GrxC5 (XP_003542446.1) from *Glycine max,* 84% with GrxC5 (XP_004140671.1) from *Cucumis sativus,* 79% with GrxC5 (XP_004290010.1) from *Fragaria vesca* subsp. vesca, 69% with GrxS12 (NP_179617.1) from *A. thaliana* and 78% with GrxS12 (NP_001148595.1) from (*Zea mays*). Lower identity (38%) was found with Grx6 (NP_010274.1) from *S. cerevisiae*.

A phylogenetic tree was constructed with the selected sequences. *Cch* GrxS12 was found to exhibit very close relationship with the GrxC5 reported from *S. lycopersicum* and *V. vinifera*. But *Cch* GrxS12 exhibits higher distance with the proteins reported from fungi *S. cerevisiae* (Fig.4.2), revealing the conservation in the biological system.

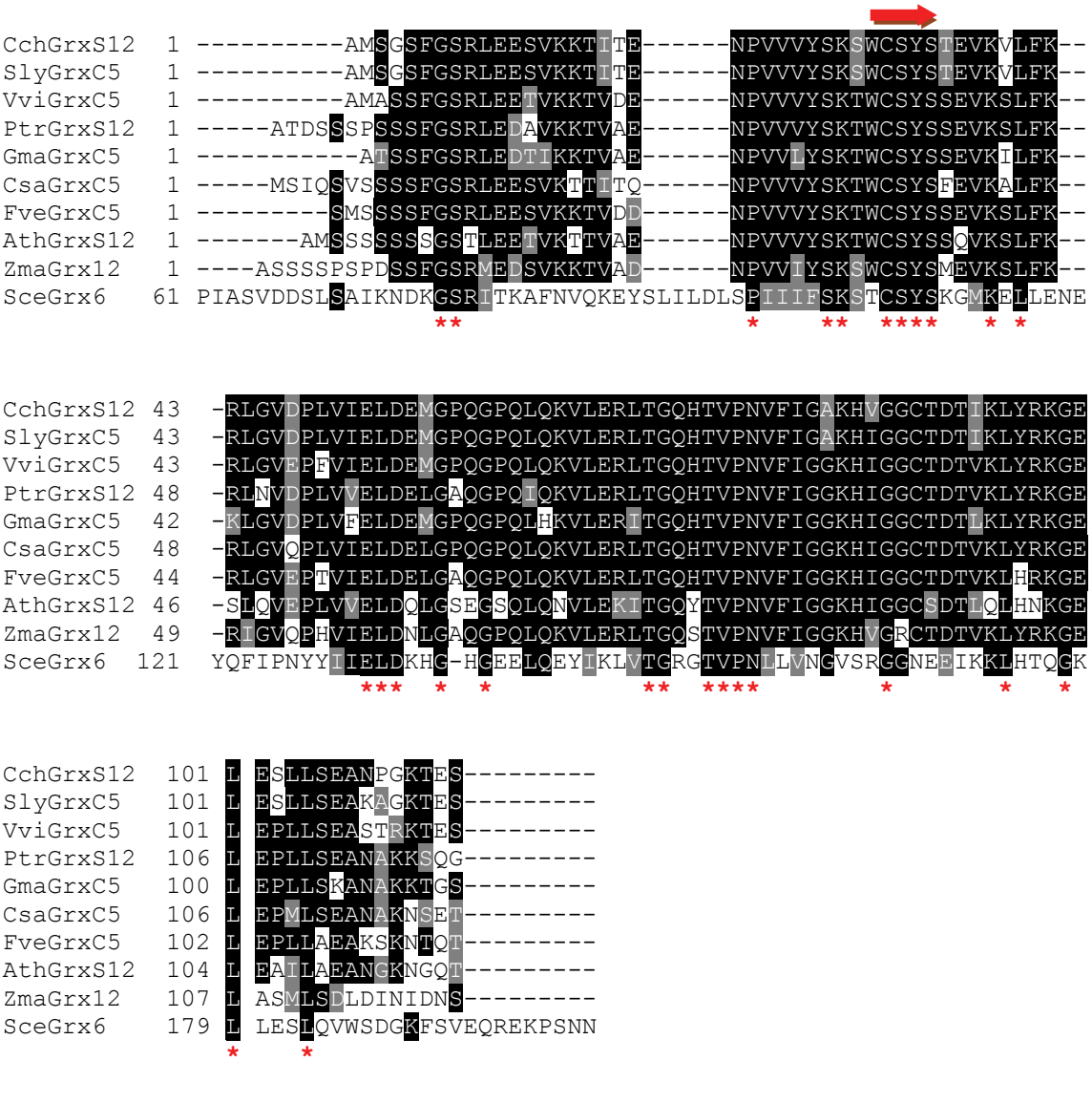

Fig.4.1. Multiple amino acid sequence alignment of the predicted mature form of CSYS active site Grxs. The conserved CSYS active site motif is indicated by a red arrow. Asterisks: conserved amino acids. Accession numbers are as follows: CchGrxS12 (this work), SlyGrxC5 (XP_004242377.1), VviGrxC5 (XP_002267052.1), PtrGrxS12 (ACJ60637.1), CsaGrxC5 (XP_004140671.1), GmaGrxC5 (XP_003542446.1), FveGrxC5 (XP_004290010.1), Ath GrxS12 (NP_179617.1), ZmaGrxS12 (NP_001148595.1), SceGrx6 (NP_010274.1). Where Cch is *Capsicum chinense*, Sly is *Solanum lycopersicum*, Vvi is *Vitis vinifera*, Ptr is *Populus tremula* x *Populus tremuloides*, Csa is *Cucumis sativus*, Gma is *Glycine max*, Fve is *Fragaria vesca* subsp. vesca , Ath is *Arabidopsis thaliana*, Zma is *Zea mays*, and Sce is *Saccharomyces cerevisiae*. The targeting sequences have been removed.

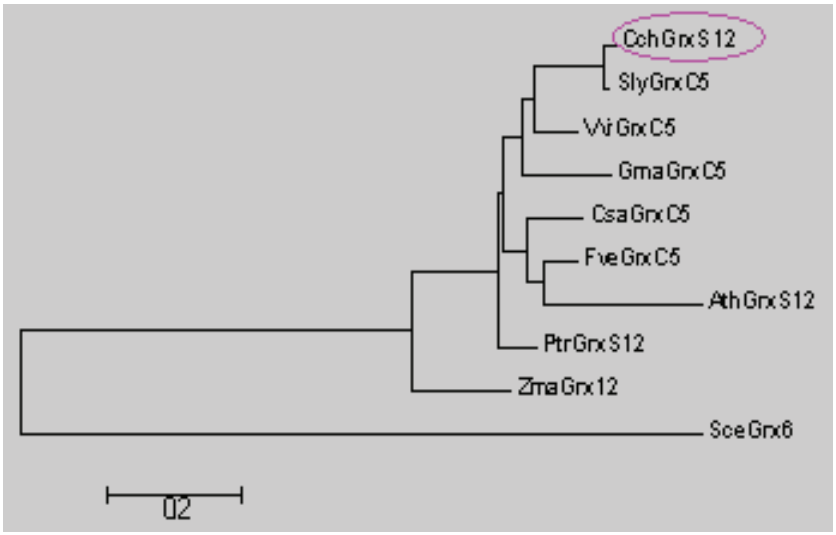

Fig.4.2. Phylogenetic analysis of *Cch* GrxS12 and Grx proteins, containing CSYS active site, from different organisms.

In the predicted 3-D protein structure, four β- strands are surrounded by five α-helix and coiled regions. The active site (CSYS) is located in the second α-helix. The secondary structure of the protein follows the pattern of α2 (residues 7-18), β-1(residues 22-26), α3 (residues 31-42), β-2 (residues 48-51), α4 (residues 60-70), β-3 (residues 79-80), β-4 (residues 83-85), α5 (residues 88-96), and α4 (residues 100-106) (Fig.4.3). Among the four strands, β1, β2 and β4 are running in the parallel direction whereas β3 runs in antiparallel direction.

Computer analysis revealed good similarity with the 3-D structure of poplar glutaredoxin S12 complexed with β-mercaptoethanol (Fig.4.4). Structural studies with poplar GrxS12 complexed with glutathione showed that among the conserved regions, WCSY, TVP and GCT are playing important roles for GSH binding (Couturier *et al.,* 2009b).

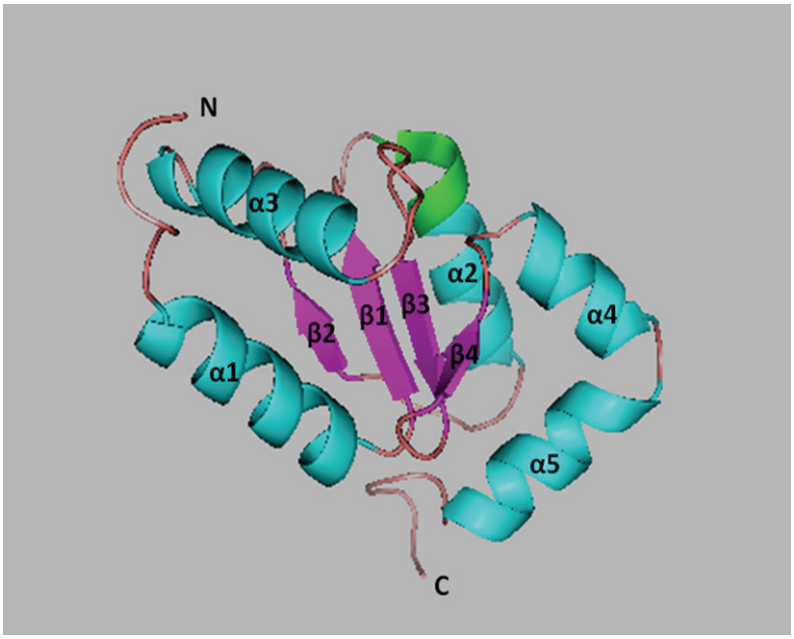

Fig.4.3.Overall fold of *Cch* GrxS12 protein. The backbone is represented with the secondary structural elements labelled as follows: α-helices are α1–α5, labelled in blue; β-strands are β1–β4, labelled in purple. The N- and C-terminals are indicated with N and C, respectively. The active site of the protein is labelled in green colour.

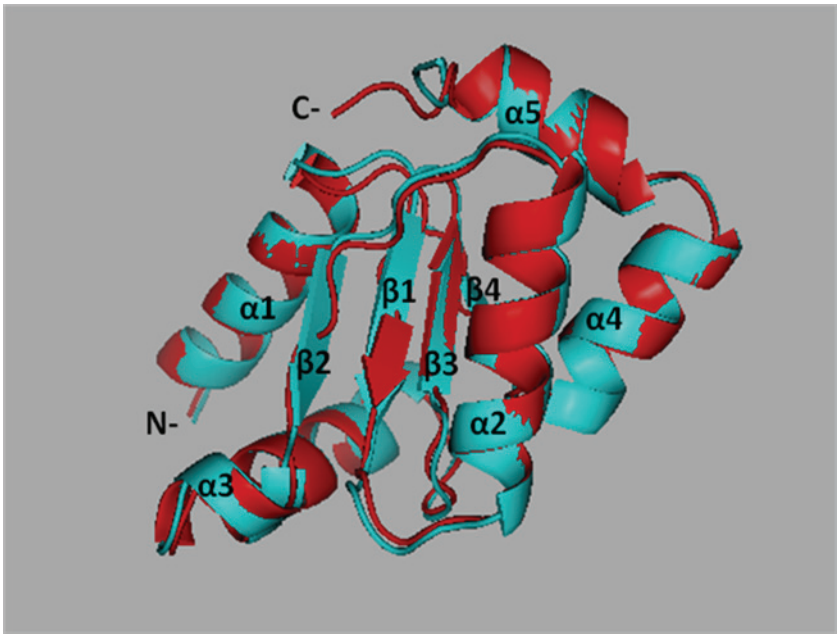

Fig.4.4. Superposition of *Cch* GrxS12 structure with GrxS12 from *Populus*. The red colour indicates the structure of *Cch* GrxS12 whereas the blue colour indicates GrxS12 from *Populus*.

4.2. Enzymatic characterization of *Cch* GrxS12 protein

To analyze the GSH-disulfide-oxidoreductase activity of the *Cch* GrxS12 protein, the mature protein was expressed *in vitro* in *E. coli*. The recombinant protein was 124 aa long and contained 114 amino acids from *Cch* GrxS12 protein sequence, from aa 63 to aa 177, with 8 His residues at the N terminus of the recombinant protein, fused to the Alanine 63 residue from the *Cch* GrxS12. The predicted molecular mass and pI of His-Grx protein were 13.8 kDa and 8.24, respectively.

For selection of the *E. coli* M15(pREP4):Grx clone that expressed high level and high quality *Cch* GrxS12 mature protein, three positive clones (no. 10, 18 and 26) were selected and analyzed by a minipreparation assay under denaturing condition. Protein expression study was carried out under inducing (with IPTG) and non-inducing (without IPTG) conditions and purified with HIS-Select Nickel affinity Gel resin (Sigma).

Purified proteins were analyzed by SDS-PAGE electrophoresis and were stained with Coomassie brilliant blue (Fig.4.5). The results showed that the recombinant protein His-Grx was only induced in the IPTG-treated bacterial culture. After analyzing the protein expression profiles of His-Grx from the three colonies (Fig.4.5), colony no. 10 was selected for further protein expression and purification and to study the enzyme kinetic assays, because His-Grx showed up as a single protein band while in the other two colonies, His-Grx protein showed up as double band.

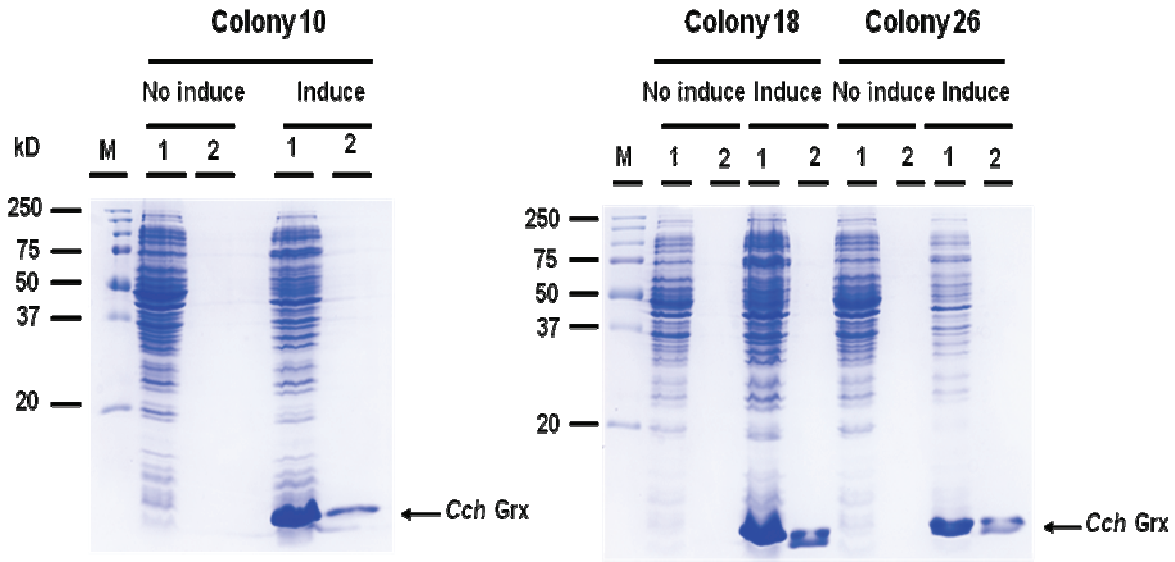

Fig.4.5.Purification of *Cch* GrxS12 from *E. coli* colonies under denaturing condition. The proteins were expressed and purified under induced (induce) and non-induced (No induce) conditions. M. Mr. Markers 1. Crude extracts 2.Purified protein.

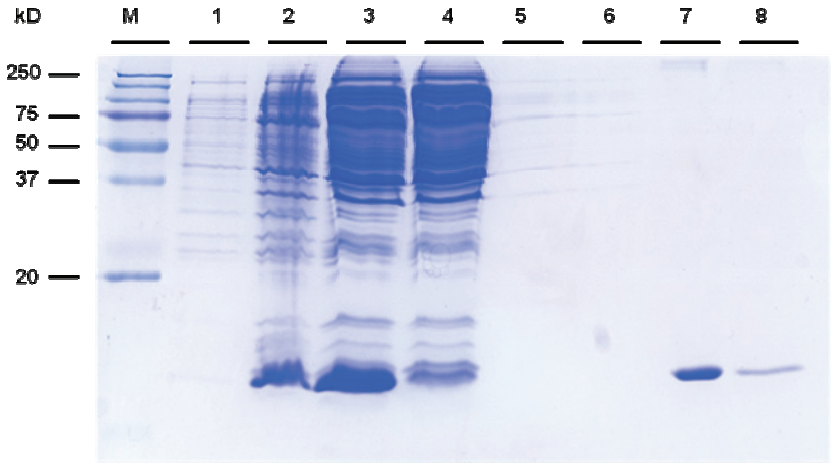

Fig.4.6. His-Grx soluble native protein purification using Nickel affinity gel column (Sigma) under native condition. M. Mr. Markers; 1 Expression under non-induced condition; 2. Total protein extract from induced bacterial cells; 3. Soluble total protein fraction; 4. HIS-Select Nickel affinity Gel resin (Sigma) no retained protein fraction; 5. 1st column wash; 6. 2nd column wash; 7. 1st His-Grx eluted fraction; 2nd His-Grx eluted fraction.

Native *Cch* His-Grx protein was purified from the soluble fraction of the total protein extracts from bacterial cells.

In figure 4.6, the SDS-PAGE protein analysis from the different purification steps of native His-Grx protein is shown. A high amount of the expressed His-Grx protein was in the form of soluble protein (Fig.4.6, lane 3) and most of it was retained by the HIS-Select Nickel resin (lane 4). The unbound bacterial proteins were removed by several washing steps (Fig.4.6, lanes 5 and 6). Most of the His-Grx purified protein was eluted from the resin with 250 mM Imidazole in the first 4 ml of elution buffer (lane 7) while in the next 4 ml elution fraction (lane 8), very little amount of protein was eluted. Both His-Grx protein preparations were free from visible protein contaminants (lanes 7 and 8).

The proteins collected from the two eluted fractions were pooled together and dialysed. The dialyzed protein was used for the enzymatic assay of the protein.

The calculated apparent Mr of the recombinant protein was 12.9 kDa well in accordance to the predicted one.

The yield of native *Cch* His-Grx purified protein was between 0.13 and 0.2 mg/100 ml of bacterial culture depending on the purification experiments.

A

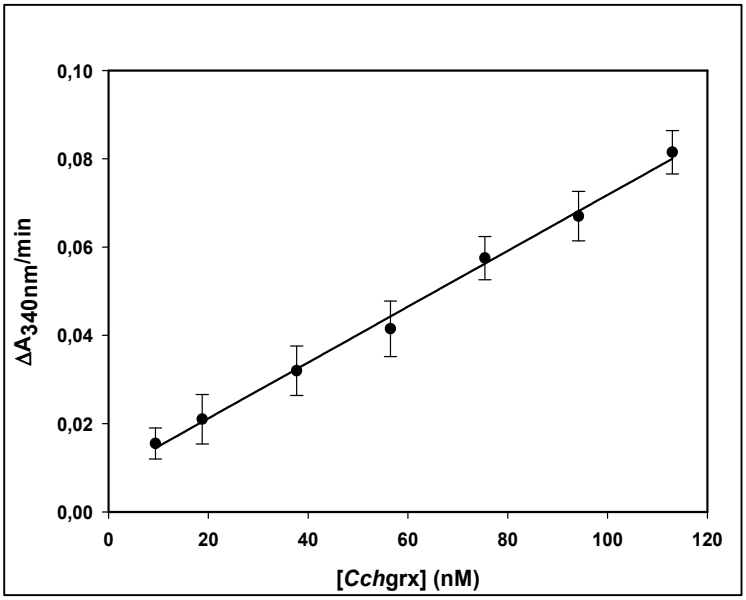

B

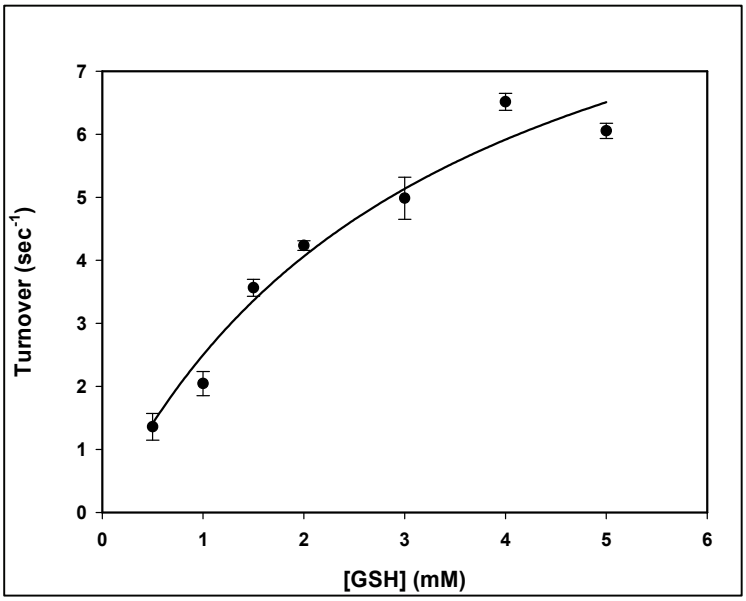

Fig.4.7.A. Linear dependence of HED activity on *Cch* GrxS12 concentration expressed as ΔA_{340}/min. The data are represented as mean ± S.D. B.Variations of the apparent turnover number during HED assay catalyzed by 84 nM of *Cch* GrxS12 in varying concentrations of GSH ranging from 0.5 to 5mM. The data are represented as mean ± S.D. The best fit was obtained using the Michaelis-Menten equation using non-linear regression equation.

The activity of *Cch* GrxS12 purified protein was determined by Grx HED assay as described under Materials and Methods. To determine the correlation between *Cch* His-Grx concentration and Grx activity, the concentration of Grx in the assay was varied from 10 nM to 125 nM. maintaining the GSH concentration at 1 mM. In this assay, it was displayed a linear relationship with increasing protein concentration (Fig. 4.7A). The specific activity was calculated as 0.12 U/nM. To determine the kinetic correlation between *Cch* His-Grx Grx activity and GSH concentration, the concentration of GSH was varied from 0.5 mM to 5 mM by maintaining the concentration of His-Grx protein at 84 nM in the presence of 0.7mM HED. The apparent K_m and apparent turnover (K_{cat} (Sec^{-1})) values for GSH were calculated by nonlinear regression using the Michaelis-Menten equation. Turnover number represents the moles of NADPH oxidized per second in the presence of 1 mol of *Cch* GrxS12. The apparent K_m (4.9 ± 1.9 mM) and apparent turnover K_{cat} (14.63 ± 4.8) values were obtained. The catalytic efficiency value (K_{cat}/ K_m $(M^{-1} Sec^{-1})$) was found to be 3.05×10^3. These experiments revealed that *Cch* GrxS12 monothiol glutaredoxin possessed GSH-disulfide oxidoreductase activity.

4.3. *Cch* GrxS12 derivatives constitutively expressed in plants are targeted to different subcellular compartments

Previous analysis in our working lab revealed that *Cch* GrxS12-GFP, and *Cch* Δ2MGrxS12-GFP proteins localized to the chloroplast and to the nuclei, respectively. To further expand these data, protoplasts from *N. benthamiana* transgenic plant lines that constitutively expressed these two constructs as well as those expressing free GFP were assayed under confocal microscope. The results (Fig.4.8) showed that while free GFP was located to the cytoplasm and the nucleus, the fluorescent signal due to the GrxS12-GFP fused protein was detected in the chloroplast confirming the chloroplast targeting of the protein. To experimentally verify the nuclear localization of Δ2MGrxS12-GFP protein, DAPI staining was performed. Thus it was possible to visualize the protein in both the nucleus, as detected in the merged image of both DAPI and GFP signals, and dispersed in the cytoplasm, thus confirming previous data and expanding them to the cytoplasm localization. That localization was similar to that of free GFP.

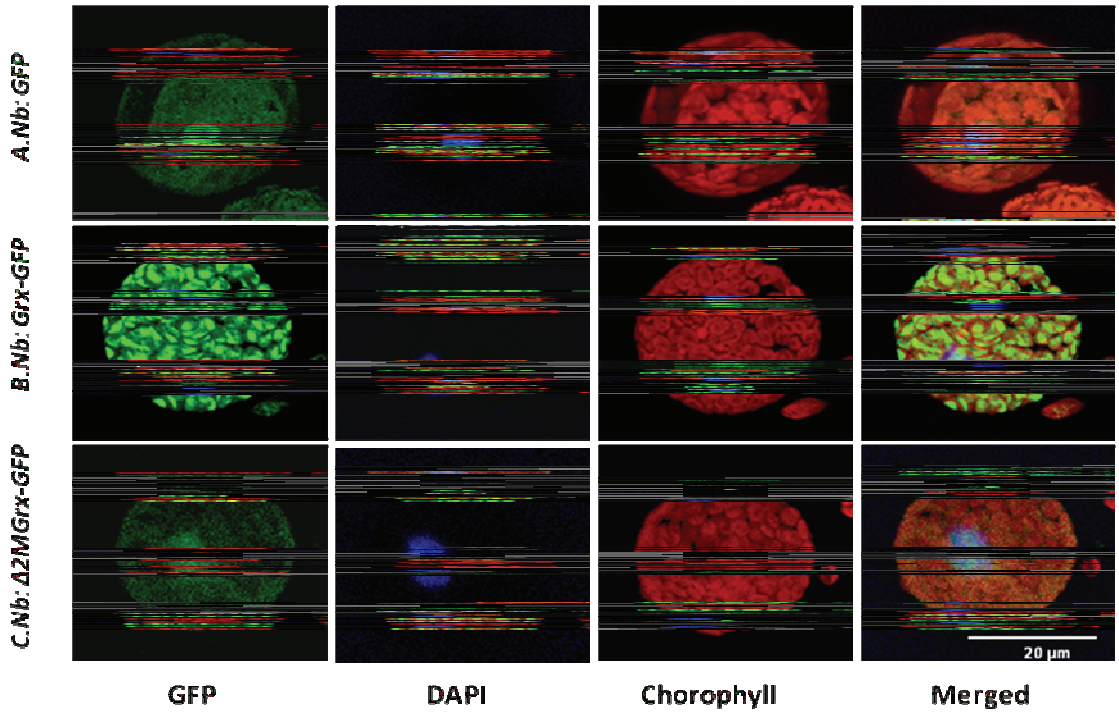

Fig.4.8. Subcellular localization study of *Cch* GrxS12 in *N. benthamiana* plant protoplasts from transgenic plants indicated on the left. A. *Nb:GFP,* plants expressing free GFP. B. *Nb:Grx-GFP*: plants expressing *Cch* GrxS12 fused to GFP. C. *Nb:Δ2MGrx-GFP*: The N-terminal 63 aa truncated *Cch* Grx fused to GFP. Merged images of GFP, DAPI and Chlorophyll are shown on the right. The nuclei were visualized by DAPI staining, Scale bar = 20 µm.

To rule out the possibility that the co-localization of *Cch* Δ2MGrxS12-GFP protein with DAPI was due to the existence of free GFP in the transgenic plants, total protein plant leaf extracts from transgenic plants *Nb:Grx-GFP* and *Nb:Δ2MGrx-GFP* were analyzed by Western blot analysis. *Nb:GFP* total protein plant leaf extracts were used as control of free GFP expression. Detection of both *Cch* GrxS12-GFP fused proteins and GFP free protein was carried out in the same membranes. The results obtained by using the Grx specific immunoserum indicated that *Cch* GrxS12-GFP and Δ2MGrxS12-GFP fused proteins were expressed in *Nb:Grx-GFP* (Fig.4.9A) and *Nb:Δ2MGrx-GFP* plants (Fig.4.9B), respectively. By using the GFP specific immunoserum, both GFP fused proteins were also detected and no free GFP was present in either *Nb:Grx-GFP* or *NbΔ2MGrx-GFP* plants (Fig.4.9 A and B). Therefore, these results confirm that the 63 N-terminal aa peptide of the *Cch* GrxS12 is the chloroplast signal peptide and

that the deletion of these 63 aa in construct *Cch* Δ2MGrxS12-GFP fused protein brings about a protein that is targeted to the same sites as free GFP.

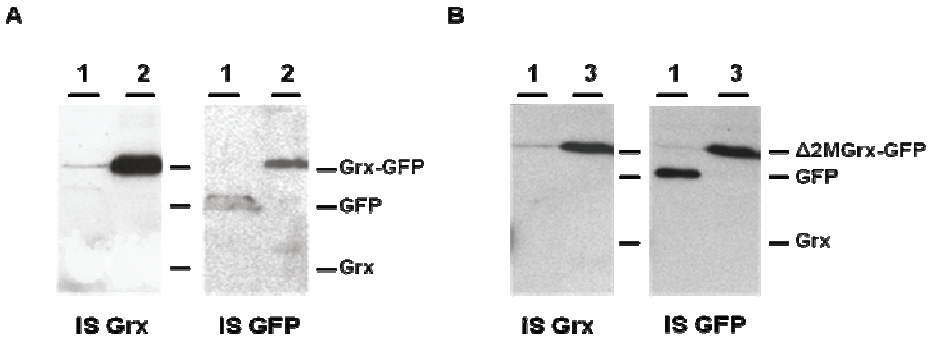

Fig.4.9.Western blot analysis of *Cch* GrxS12-GFP and *Cch* Δ2MGrxS12-GFP fused proteins and free GFP protein in transgenic *N. benthamiana* lines of *Nb:GFP*; *Nb:Grx-GFP*; *Nb:Δ2MGrx-GFP*. A. Analysis of *Nb:Grx-GFP* protein extracts; B. Analysis of *Nb:Δ2MGrx-GFP* protein extracts. 1. *Nb:GFP* 2. *Nb:Grx-GFP* 3. *Nb:Δ2MGrx-GFP*. The different immunosera (IS) are indicated at the bottom of the figure.

4.4. Expression analysis of *Cch* GrxS12 protein and its derivatives in *N. benthamiana* transgenic plants

N. benthamiana plants constitutively expressing GFP (*Nb:GFP*, line 11), native *Cch* GrxS12 (*Nb:Grx*, line 3), a GrxS12:GFP fusion protein (*Nb:Grx-GFP*, line 16) and a 63 aa truncated GrxS12 fused to GFP (*Nb:Δ2MGrx-GFP* line 40) were used to analyze the effect of Grx expression on PMMoV-I infection. In order to analyze the expression level of the *Cch* GrxS12 constructs in these plants, total leaf proteins were extracted from upper leaves prior to viral inoculation (six weeks old plants) and analyzed by Western blot assay by using *Cch* GrxS12 specific immunoserum.

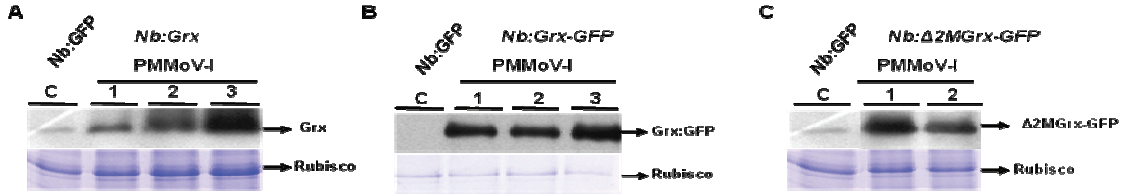

Fig.4.10. Western blot analysis of *Cch* GrxS12 constructs accumulation in the upper leaves of *N.benthamiana* transgenic plants indicated on the top of the figure. Grx specific immunoserum was used for detection. 1: samples from 1-4 plants; 2: samples from 5-8 plants; and 3: samples taken from 9-11 plants. Protein extracts in B were 1/10 diluted. Lower panels show Coomassie Blue staining of total proteins as loading control. The Grx constructs position is shown at the right of the figure.

The accumulation of the correspondant protein in either *Nb:Grx* plants (Fig. 4.10A) or *Nb:Δ2MGrx-GFP* plants (Fig.4.10C) was very similar, although some differences were observed among plants. *Nb:Grx-GFP* plants (Fig.4.10B) presented about 10x Grx-GFP protein accumulation than the observed for the above mentioned plants. Plants with similar accumulation levels within each line were selected for PMMoV-I inoculation.

4.5. PMMoV-I infection studies in *N. benthamiana* transgenic plants

4.5.1. Symptoms in PMMoV-I- infected plants

The first two expanded leaves from the selected *N. benthamiana* transgenic plants were inoculated with PMMoV-I at a concentration of 50 µg/ml and symptoms were recorded at different days post-inoculation (dpi). From the 4th day onwards the viral symptoms were visible in the upper non-inoculated plant leaves. The symptoms were first noticed in the apical two leaves. (Fig.4.11B)

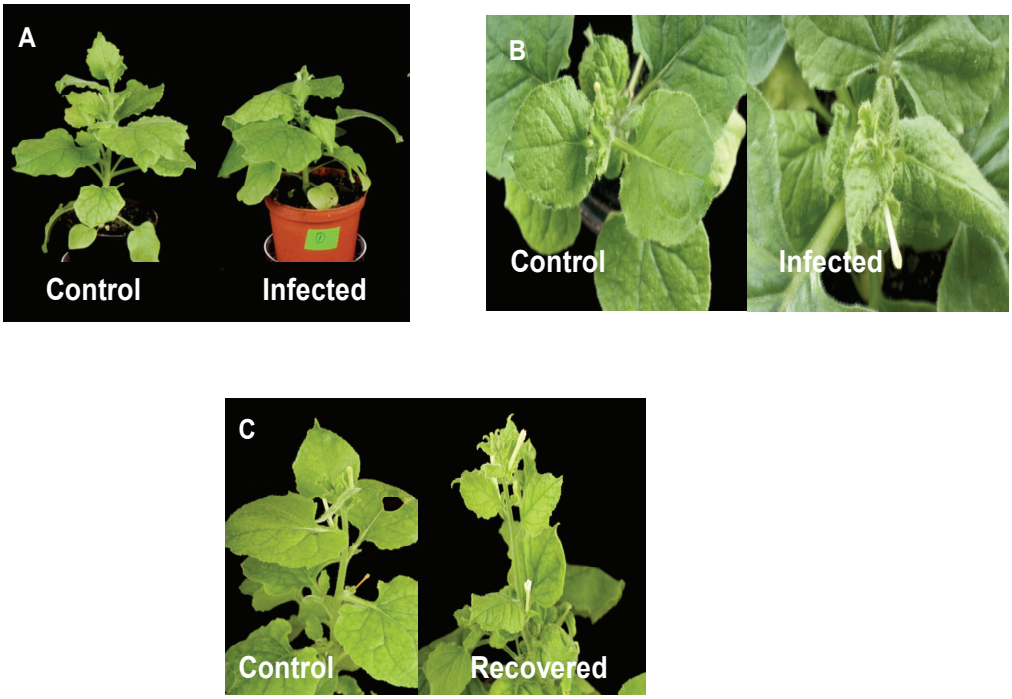

Fig.4.11.Representative images of PMMoV-I induced symptoms in *N. benthamiana* transgenic plants. A. Symptoms displayed at 14 dpi in *N. benthamiana* control and PMMoV-I-infected plants. B. Symptoms induced by PMMoV-I in *N .benthamiana* apical leaves of infected plants at 14 dpi. C. Symptoms displayed by *N.benthamiana* infected with PMMoV-I at 28 dpi.

The typical symptoms induced by PMMoV-I in the *N. benthamiana* infected plants were those of stunting due to the reduction in the number of leaves, a shorter intra nodal distance and reduced leaf size (Fig.4.11A). The leaves were curled at 14 dpi, (Fig.4.11B). These symptoms were found in the PMMoV-I-infected plants from 6 to 22 dpi. Later on, the plants started to recover from the viral infection. PMMoV-I infected plants began to elongate, new leaves looked asymptomatic and flowers began to appear (Fig.4.11C). The recovery of plants took place from 21 to 31 days, the latest day observed. Although the apical leaves of the plants got recovered, the infected plants are shorter than the control plants. On visualizing the different transgenic lines under the PMMoV-I infected condition, the Grx expressing lines were found to have better growth when compared with GFP expressing line.

4.5.2. Analysis of viral coat protein accumulation in plants

To analyze the PMMoV-I viral accumulation in the *N. benthamiana* transgenic plants indicated above, plant leaves were inoculated with PMMoV-I at 5 µg/ml. Samples were collected from inoculated leaves at 7 dpi, and from systemic leaves at 7, 14 and 28 dpi in both infected and mock inoculated control ones. For virus quantification, the accumulation of PMMoV-I CP was analyzed by SDS-PAGE from the different samples and was quantified by using a PMMoV-I standard curve as described under Materials and Methods section.

The results showed that PMMoV-I CP increased during the earlier periods of infection and reached a maximum at 14 dpi to be diminished at the later stage of infection (28 dpi). This pattern of viral accumulation depicts the same for all the transgenic lines. At 7 dpi, the viral accumulation in the inoculated leaves was almost similar for all of the plants while in the systemic leaves viral accumulation was lower for transgenic plants expressing the native *Cch* Grx (*Nb:Grx*) than for GFP plants. However, the transgenic plants transformed with GFP-fused Grx constructs showed higher level of viral accumulation than the control plants. At 14 dpi the level of viral accumulation was lower in all of the transgenic plants expressing the Grx constructs than in the GFP-expressing plants. The largest differences were found in *Nb:Grx-GFP* plants where the PMMoV-I CP only reached a 56% of the observed in GFP plants, while a decrease of 18 and 20% was observed in both *Nb:Grx* and *Nb:*Δ*2MGrx-GFP* plants, respectively (Fig. 4.12).

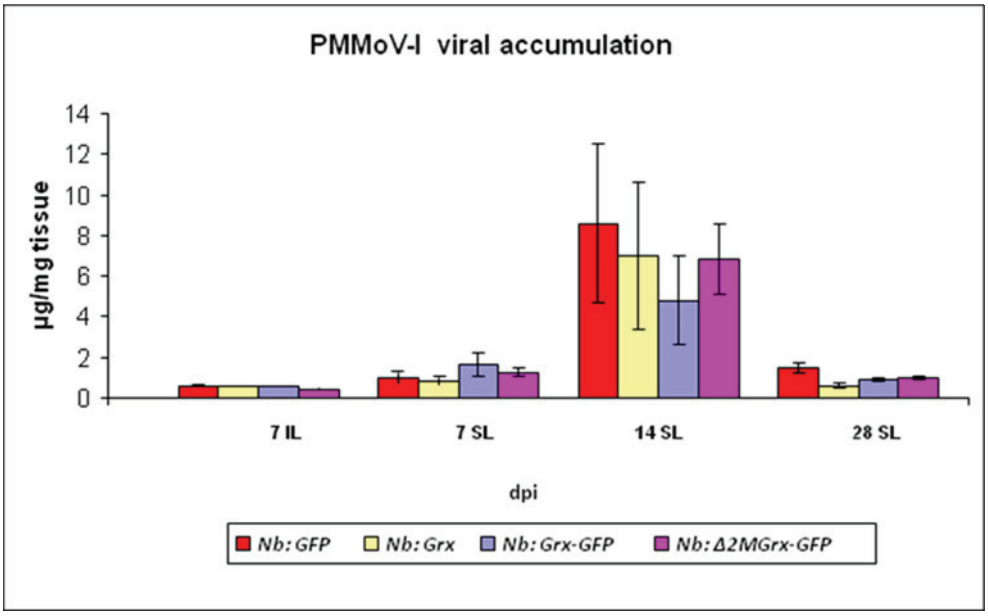

Fig.4.12. Analysis of viral CP accumulation in *N. benthamiana* transgenic plants inoculated with 5 µg/ml of PMMoV-I at the dpi showed in the figure. IL-Inoculated leaves, SL-Systemic leaves. Results are the media from three experiments and are expressed as µg of virus per mg of fresh tissue. Standard deviations are shown.

At 28 dpi, the samples were taken from the recovered leaves of the PMMoV-I infected plants. PMMoV-I accumulation in *Nb:Grx, Nb:Grx-GFP* and *Nb:Δ2MGrx-GFP* infected plants was reduced up to 60%, 37% and 32%, respectively, when compared with the GFP-expressing line (*Nb:GFP*) (Fig. 4.12).

4.5.3. Analysis of viral RNA accumulation

To analyze viral RNA accumulation, 20 plants from each transgenic line, expressing the Grx constructs, and control transgenic plants were inoculated with 50 µg/ml of PMMoV-I. The accumulation of viral RNA was analyzed by Northern blot assay at early (7dpi) and late (28 dpi) stages of the infection, as described under Materials and Methods, by using the viral RNA-specific probe.

At 7 dpi, no differences in genomic viral RNA accumulation was observed, in either inoculated or systemic leaves from the four transgenic plant lines analysed (Fig.4.13A). Thus the results further expand previous data in our working lab, and those showed in the above paragraph

(Fig.4.12), indicating that over-expression of *Cch* GrxS12 does not have any inhibitory effect over viral infection at early periods of infection.

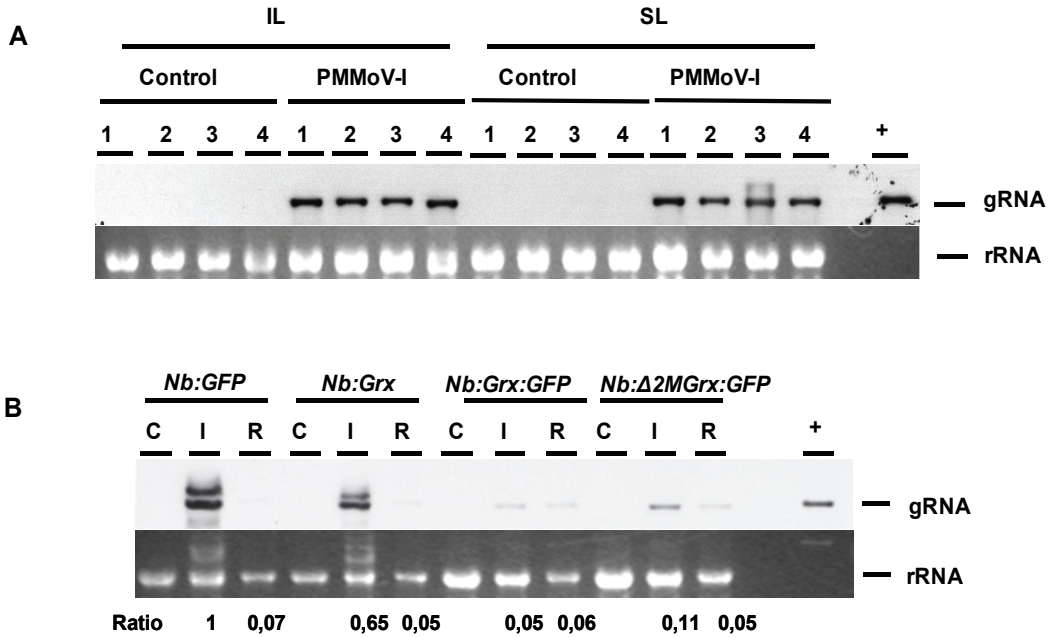

Fig.4.13. Northern blot analysis of viral RNA accumulation at 7 dpi (A) and 28 dpi (B). A.10 µg of total RNA extracted at 7 dpi from control mock and PMMoV-I infected plants of 1. *Nb:GFP*, 2. *Nb:Grx* ,3. *Nb:Grx-GFP* and 4. *Nb:Δ2MGrx-GFP* plants were assayed by Northern blot analysis and hybridized to digoxigenin-labelled specific riboprobe for viral RNA of plus polarity. IL-Inoculated leaves; SL-Systemic leaves. B. total RNA (10 µg) extracted at 28 dpi from PMMoV-I-infected and mock inoculated plants were assayed as above. The transgenic plants analyzed are indicated on the top of the figure. (C): control mock inoculated plants; (I): infected leaves; (R): recovered leaves. gRNA: viral genomic RNA. +: 50 ng of RNA extracted from PMMoV-I virus was used as positive control. The lower panels of both A and B show the ribosomic RNA (rRNA) stained with ethidium bromide and used as loading control.

To analyse viral RNA accumulation at late period of infection, samples were taken from symptomatic (infected), and asymptomatic leaves (recovered) from PMMoV-I- infected plants as well as from mock inoculated control plants. The level of viral RNA accumulation was higher in *Nb:GFP* infected leaves than in the infected leaves of *Cch* GrxS12-expressing constructs (native GrxS12, GrxS12-GFP and Δ2MGrxS12-GFP) plants (relative accumulation: 1 vs 0.65, 0.05, 0.11), thus indicating an inhibitory effect of the constitutive expression of Grx on PMMoV-I accumulation at that time of infection. However, the low accumulation of PMMoV-I gRNA in

the recovered leaves, was not altered in the *Cch* Grx expressing lines (relative accumulation: 0.05, 0.06, 0.05 vs 0.07) (Fig 12B).

4.5.4. Analysis of PMMoV-I viral accumulation in protoplasts of *N. benthamiana* transgenic plants

In order to analyse the effect of the constitutive expression of *Cch* GrxS12 and its derivatives on viral replication at the cellular level, plant protoplasts from the transgenic *N. benthamiana* plants used in this study were prepared and infected with PMMoV-I RNA by following the protocol described under Material and Methods. The protoplasts obtained from the different plant lines showed the same size and aspect as it is shown in Figure 4.14.

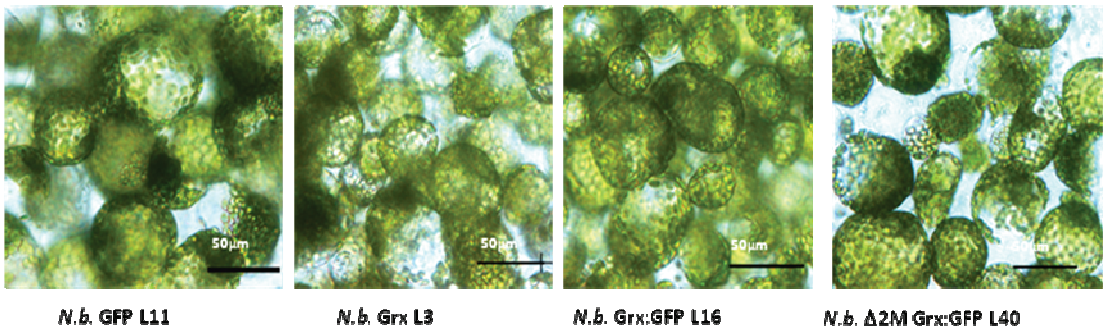

Fig.4.14.Protoplasts isolated from different transgenic lines used in this study and observed with a Leica DM2500 microscope. Protoplasts were obtained from the transgenic lines indicated at the bottom of the figure. Scale bars = 50 µm.

To determine the percentage of infected protoplast, detection of PMMoV-I CP was performed by either immunofluorescence or alkaline phosphatase staining, as described under Materials and Methods. There was no difference in the percentage of infected protoplasts in the different lines, which was about 30-34%. Figure 4.15 displays immunofluorescent staining of control and PMMoV-I-infected *Nb:Grx* protoplast.

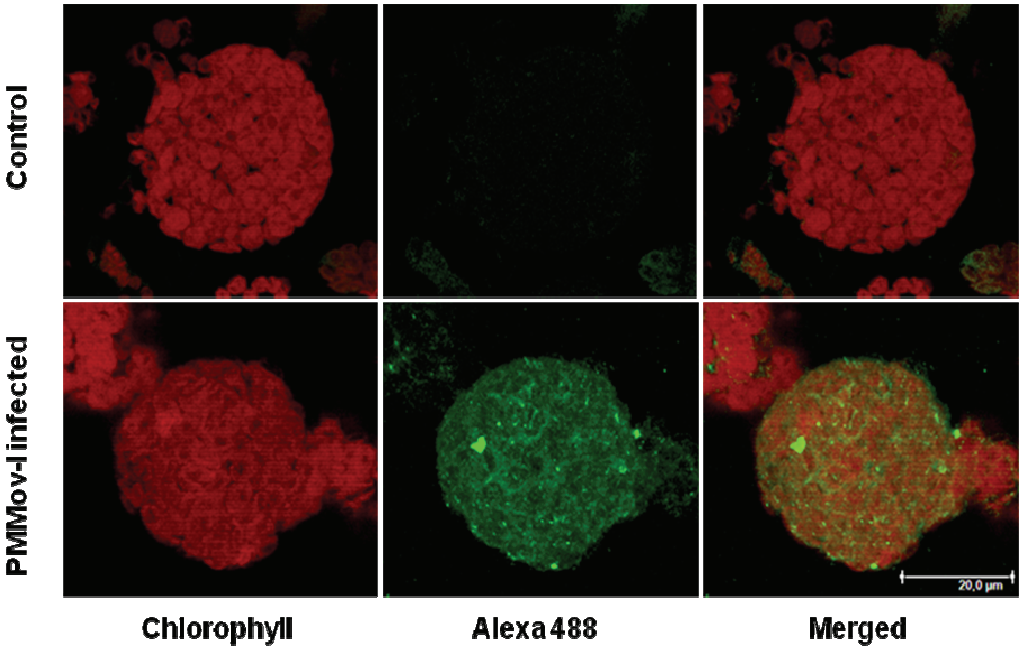

Fig.4.15.Immunofluorescence detection of PMMoV-I viral infection in protoplasts of *Nb:Grx*. From left to right: autofluorescence of chlorophyll (red), fluorescence of Alexa 488 (green) and merged. Scale bar =20µm

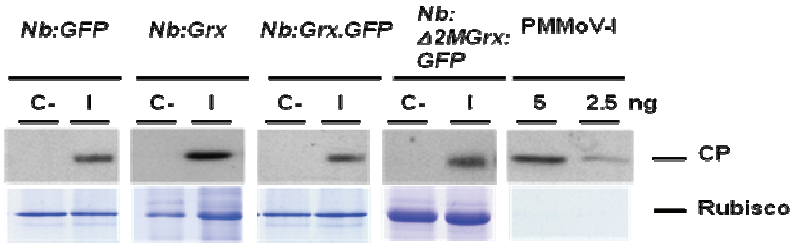

Fig.4.16.Detection of PMMoV-I CP by Western blot analysis in plant protoplast from transgenic lines indicated on the top of the figure. As positive control purified PMMoV-I (5 and 2.5 ng) was used. As negative control (C-) uninfected protoplasts were used. Lower panels show Coomassie Blue-stained Rubisco protein as a loading control.

The viral accumulation was analyzed by detecting the viral CP accumulation at 24 h after infection. As shown in figure 4.16 and taking into account the amount of total protein loaded onto the gel, accumulation level of viral CP was similar for all of the transgenic plants.

4.5.5. Kinetics of PMMoV-I viral CP accumulation in protoplasts of *N.benthamiana*

In order to study the effect of *Cch* GrxS12 expression in the transgenic lines on the kinetics of PMMoV-I viral replication, the infected protoplasts were grown along with the non-infected ones at 25°C for 10, 16, 24 and 48 hpi. The viral CP accumulation in the infected protoplasts was analysed by Western blot as indicative of viral replication.

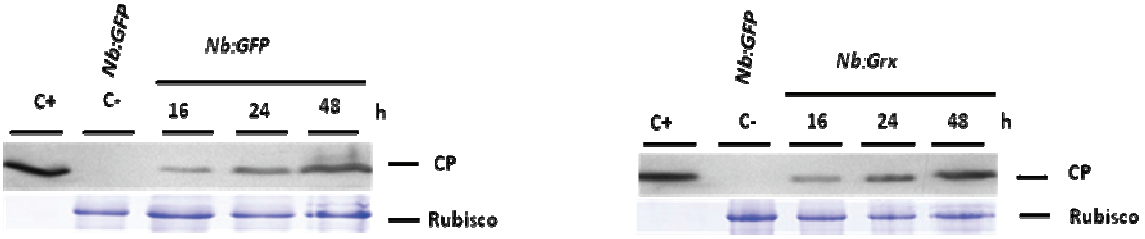

Fig.4.17. Accumulation kinetics of PMMoV-I viral CP as indicative of virus replication in protoplasts of the transgenic lines shown on top of the figure. Total protein extracts from protoplasts harvested at the post inoculation shown on the top of the figure were assayed by Western blot using PMMoV CP antiserum as before. As positive control purified PMMoV-I (5 ng) was loaded and for negative control (C-) uninfected protoplasts were used. Lower panels show Coomassie Blue-stained Rubisco protein as loading control.

As far as the kinetics of viral replication is concerned, the level of viral CP accumulation started to increase gradually from 16 hpi and it reached its maximum at 48 hpi, the latest point-time analysed, being both the kinetics and accumulation levels of viral coat protein in both plant protoplasts very similar (Fig.4.17), corroborating and further expanding the data obtained at 24 hrs. These data indicate that viral replication is not affected by the constitutive expression of *Cch* GrxS12 in plants.

4.6. Transcript analysis of defence related genes

4.6.1. Transcript accumulation of PR genes

In order to reveal whether the-over expression of *Cch* GrxS12 and its derivatives in *N. benthamiana* plants induced a defence mechanism against PMMoV-I infection, expression of SA or ET-mediated defence transcripts, such as those from acidic PR proteins (PR-1, PR-2a and PR-5), or basic PR (PR-2b) respectively (van Loon *et al*., 2006), were analyzed in mock- and

PMMoV-I-infected plants along the infection period (7, 21 and 28 dpi). Northern blot analysis was performed at 7, 21 and 28 dpi by using PR-specific riboprobes.

PMMoV-I-inoculated leaves from *N. tabacum* cv Xanthi nc plants, a well documented PR protein expressing host (Stintzi *et al.* 1993 ; Van Loon *et al*., 2006), was taken as positive control for the analysis.

At 7 dpi (Fig.4.18A) it was found a high level of PR mRNA accumulation in the PMMoV-I- inoculated leaves with no detection in the mock-inoculated ones, and at the same extent in all of the different transgenic plants assayed (Fig. 4.18A). By contrast, the basic PR-2b gene was expressed at the same level in either mock- or PMMoV-I- inoculated leaves (Fig. 4.18A). The amount of PR-1, PR-5 and PR-2b transcripts was similar to the detected, at 5 dpi, in PMMoV-I inoculated leaves from *N. tabacum* Xanthi nc that developed an HR response (Fig. 4.18A lane 6).

In the systemic leaves of PMMoV-I infected plants low level expression was found for all analyzed PR mRNAs and no expression was detected in the mock-inoculated control plants. Again, differences between transgenic lines were negligible (Fig. 4.18A).

At 21 dpi, samples were taken from the systemic leaves of mock- and PMMoV-I-infected plants. On analysing the PR transcripts accumulation, it was detected (Fig. 4.18B) that at variance with the accumulation of PR found at 7 dpi, in which no PR mRNAs were detected in the mock-inoculated transgenic control plants, all PRs were detected in the mock-inoculated *Nb:Grx-GFP* transgenic plants being the levels of PR-1 and PR-2a very high. A faint band of PR-2a was also detected in the other analyzed transgenic plants, as well as PR-5 in the *Cch* Grx-GFP and *Cch* Δ2MGrx-GFP-expressing plants. In addition, it was detected that in all of the PMMoV-I-infected systemic leaves, the different PR mRNAs were detected to a higher extent in the Grx-expressing plants than in the control GFP-expressing plant.

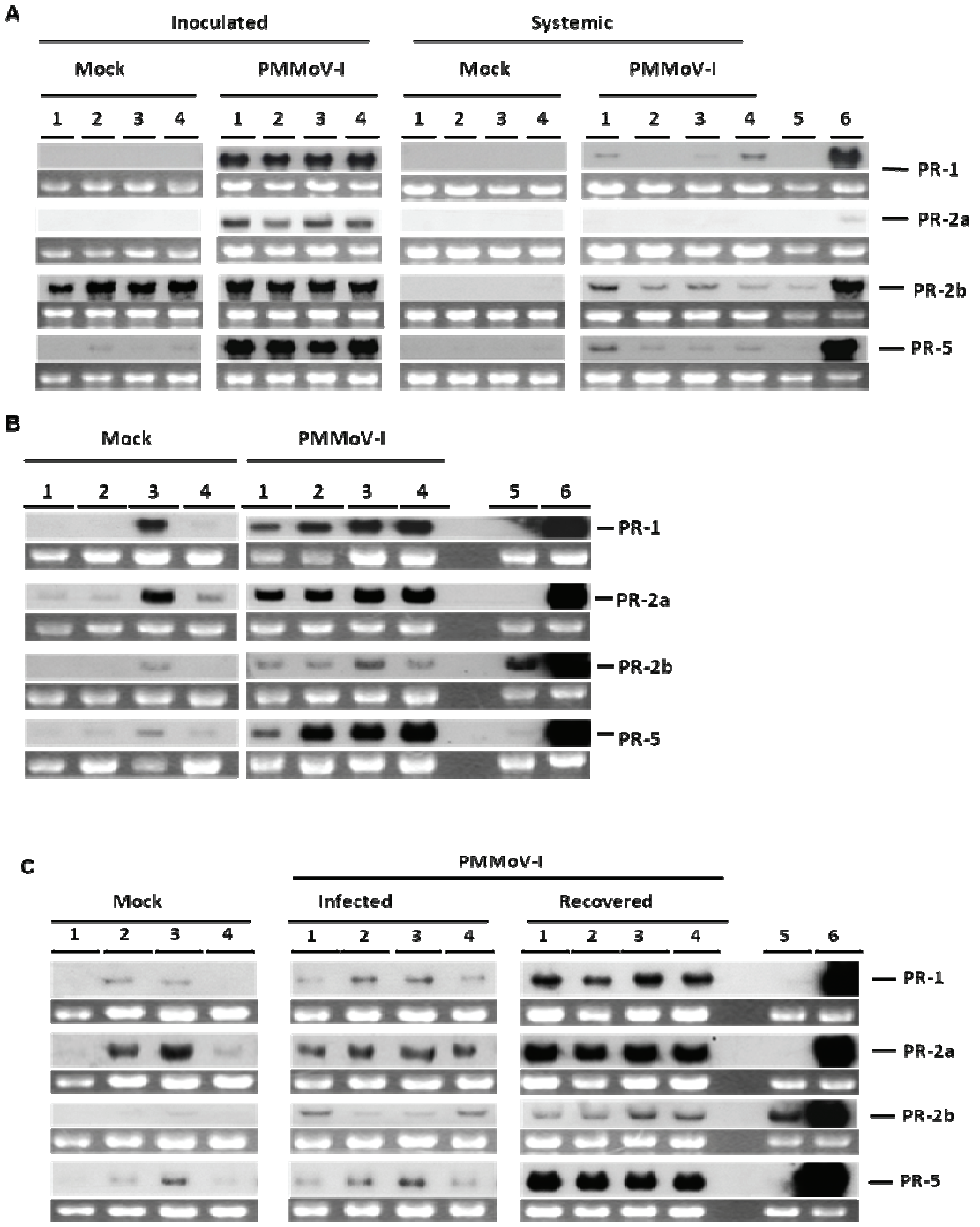

Fig.4.18. Northern blot analysis of PR gene expression from mock and PMMoV-I infected plants at 7 (A), 21(B) and 28 (C) dpi 1. *Nb:GFP;* 2. *Nb:Grx;* 3. *Nb:Grx-GFP;* 4. *Nb:Δ2MGrx-GFP*. 5 and 6. mock and PMMoV-I inoculated leaves from *N. tabacum* Xanthi nc. respectively. Mock: control mock inoculated plants. PMMoV-I: PMMoV-I infected plants. The lower panel of each probe shows the ribosomic RNA stained with ethidium bromide and used as loading control.

At 28 dpi, the plants recovered from the PMMoV-I infection, thus it was our interest to determine the PR mRNA expression in the recovered leaves. In the mock inoculated plants, as at 21 dpi (Fig.4.18C) PR-1, PR-2a and PR-5 mRNAs were detected in the Grx expressing plants. Among the PR mRNA, the PR-2a accumulation was found to be higher. It was also detected in the Δ2MGrx-GFP-expressing plants, although the accumulation level was much lower. The accumulation level of PR-1 mRNA was lower than the one at 21 dpi in the Grx-GFP-expressing line.

In the case of PMMoV-I infected leaves displaying disease symptoms the level of PR transcripts such as PR-1, PR-2a and PR-5 were found to be higher in the transgenic lines of *Nb:Grx*, and *Nb:Grx-GFP* than in the lines of *Nb:GFP* and *Nb:Δ2MGrx-GFP* where little mRNA accumulation was found. But the opposite was observed in the case of PR-2b transcript, in which little mRNA accumulation was found in the transgenic lines of *Nb:Grx*, and *Nb:Grx-GFP*.

In the recovered leaves, the accumulation of PR transcripts was found to be very high (2-3 fold) when compared with the mock- and PMMoV-I infected leaves. Similar levels of accumulation were detected in the different transgenic plants analyzed, except for the PR-2b transcripts that were higher in the Grx-expressing plants than in the control ones.

4.6.2. Analysis of 9-LOX, GR and GST transcript accumulation

For the expression study, leaf samples were taken from mock and PMMoV-I-inoculated plants at 7, 21 and 28 dpi, as in the above paragraph, and as indicated under Materials and Methods.

At 7 dpi, the analysis revealed that the accumulation level of 9-LOX mRNA was higher in the PMMoV-I-inoculated leaves than in the mock-inoculated ones. The amount of 9-LOX transcript was higher in the PMMoV-I-inoculated leaves from *Nb:Grx* and *Nb:Grx-GFP* plants than in either *Nb:GFP* or *Nb:Δ2MGrx-GFP* plants (Fig.4.19A). However, in the systemic leaves, 9-LOX mRNA was detected in both mock and PMMoV-I-infected plants, although expression was higher in the mock inoculated leaves, than in the PMMoV-I infected plants, being higher in the Grx-expressing plants than in the non-expressing ones. At 21 dpi, the expression level was found to be uniform both in the mock- and PMMoV-I-infected plants (Fig.4.19B).

At 28 dpi, the accumulation level of 9-LOX mRNA in the systemic leaves from mock inoculated plants was found to be higher in the *Nb:Grx-GFP* transgenic line than in control GFP expressing line, *Nb:Grx* and *Nb:Δ2MGrx-GFP* lines (Fig.4.19C). In PMMoV-I-infected plants the accumulation of 9-LOX mRNA was higher in the recovered leaves,with not much variance between the control line and *Cch* Grx protein-expressing lines (Fig.4.19C). Only a slight higher amount of signal was detected in plants expressing *Cch* Grx-GFP protein.

Next the level of GR mRNA was analyzed. At 7 dpi, the expression level of GR transcript got reduced in the PMMoV-I inoculated leaves when compared with the mock inoculated control leaves. In the systemic leaves, and at variance with 9-LOX, the expression level was found to be uniform for the transgenic plants analyzed, both in mock- and PMMoV-I-inoculated plants (Fig.4.19A), being the accumulation levels higher in the virus-infected leaves.

At 21 dpi, the level of GR expression was found to be uniform for both mock and PMMoV-I-inoculated plant leaves (Fig.4.19B).

At 28 dpi, an increase in GR mRNA accumulation was observed in mock-inoculated plants from *Nb:Grx-GFP* line. In the PMMoV-I-infected leaves, a reduction of GR mRNA was detected in the plants expressing all the *Cch* Grx constructs, whereas the accumulation level was found to be uniform in the systemic recovered leaves (Fig.4.19C).

Regarding the level of GST mRNA, at 7 dpi, higher level of GST mRNA accumulation was found in the PMMoV-I-inoculated leaves than in the mock-inoculated ones. No changes were detected in the systemic leaves of either PMMoV-I-infected or control plants (Fig.4.19A).

At 21 dpi, GST mRNA accumulation was found to be higher in the PMMoV-I-infected systemic leaves than in the mock ones, and no differences were observed between the *Cch* Grx-expressing plants and GFP expressing ones (Fig.4.19B).

At 28 dpi GST mRNA was detected in all the samples analyzed, being the accumulation level in the GFP-infected plants higher than in the *Cch* Grx-expressing plants, both in infected and recovered leaves (Fig.4.19C). In contrast, a higher accumulation of GST mRNA was detected in the mock-inoculated control plants expressing the *Cch* Grx-GFP protein.

In the positive control, PMMoV-I inoculated leaves from *N. tabacum* Xanthi nc plants, the expression of 9-LOX and GST genes was induced associated to the HR resistance mechanism, while GR gene was expressed at the same level in both mock and PMMoV-I inoculated leaves (Fig.4.19, lane 5 and 6).

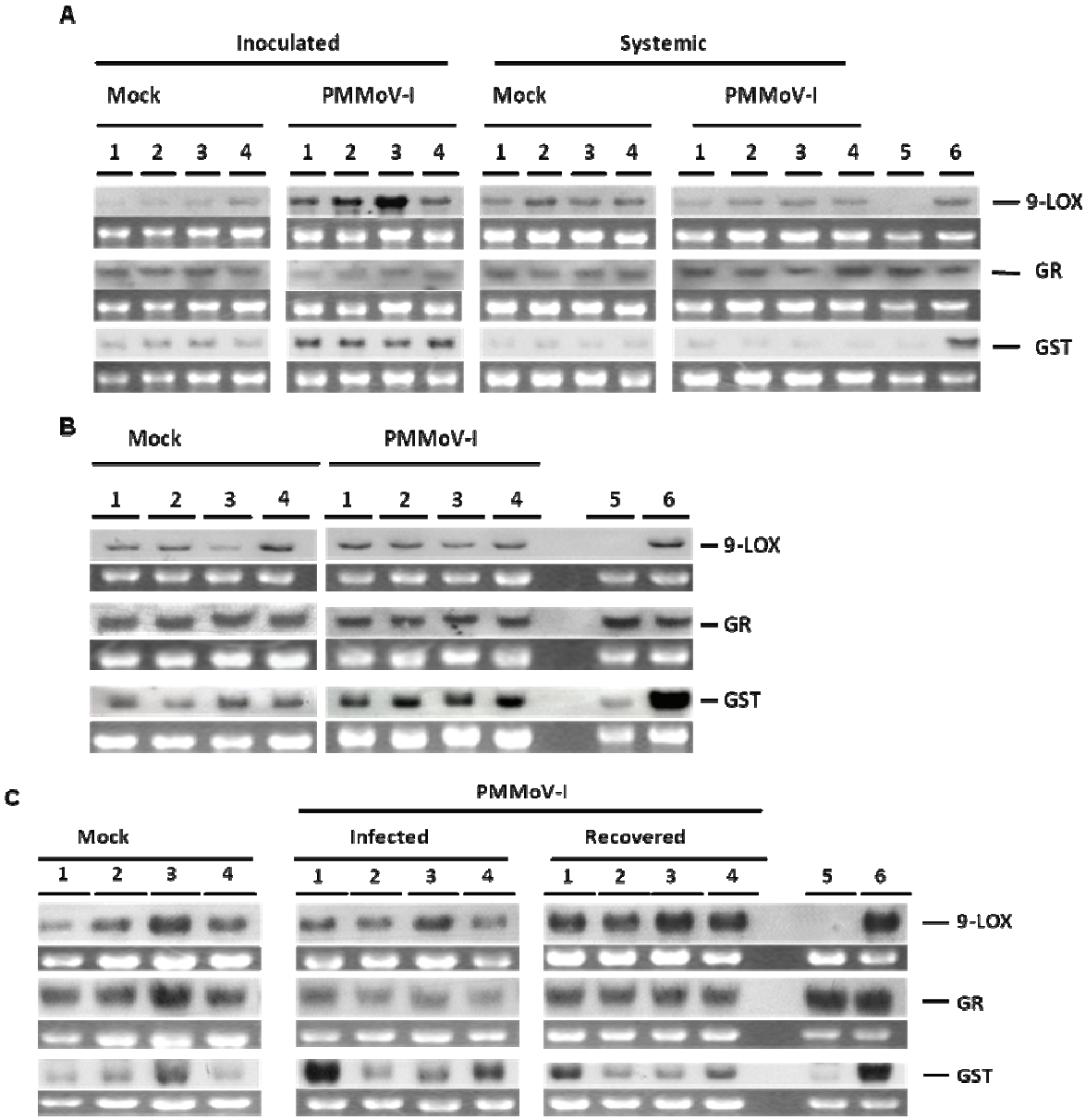

Fig.4.19. Northern blot analysis of 9-LOX, GR and GST mRNA from mock and PMMoV-I-infected plants at 7 (A), 21 (B) and 28 (C) dpi.1. *Nb:GFP;* 2. *Nb:Grx;* 3. *Nb:Grx-GFP;* 4. *Nb:Δ2MGrx-GFP;* 5 and 6. mock and PMMoV-I inoculated leaves from *N. tabacum* Xanthi nc. plants respectively. Mock: control mock inoculated plants. PMMoV-I: PMMoV-I infected plants. The lower panel of each probe shows the ribosomic RNA stained with ethidium bromide and used as loading control.

4.7. Analysis of PN contents in plants

In order to evaluate the influence of *Cch* GrxS12 expression in *N. benthamiana* plants over PNs accumulation, we determine the content of NAD^+, NADH, $NADP^+$ and NADPH in the transgenic lines at 21 and 28 dpi, in both PMMoV-I- and mock-inoculated plants, as described under Materials and Methods.

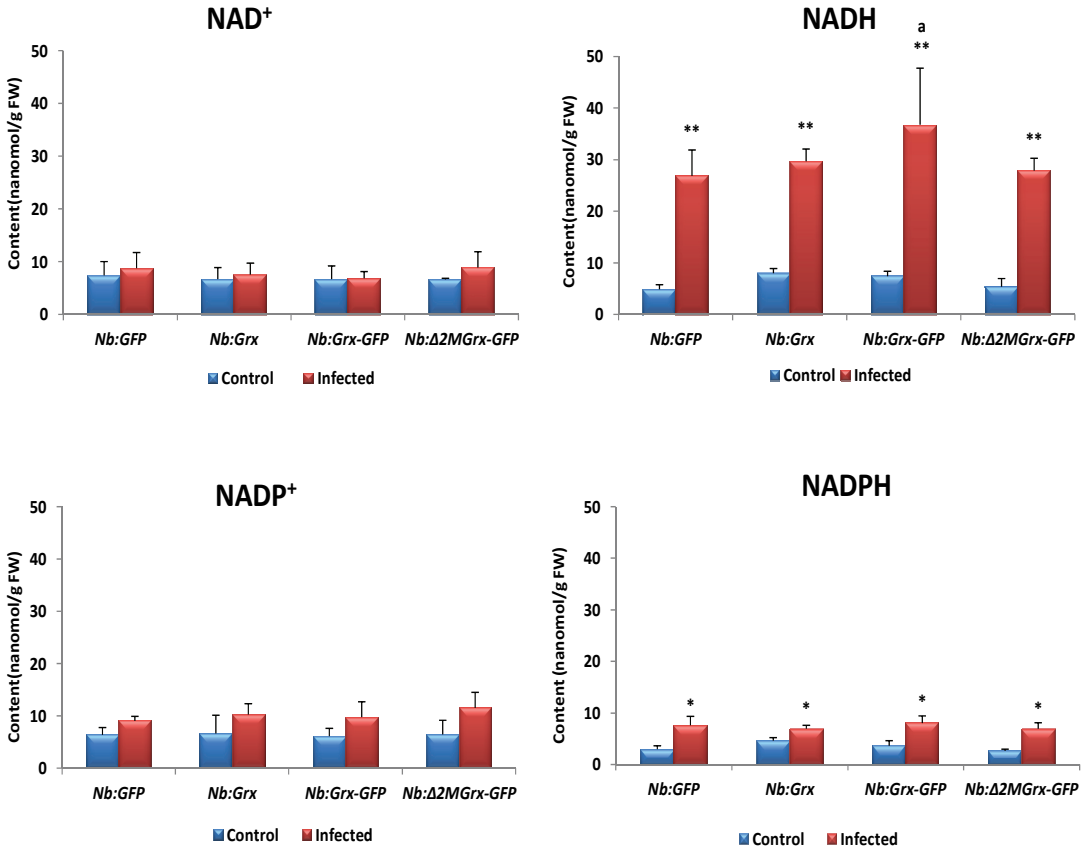

Fig.4.20. Analysis of the PN contents at 21 dpi in control and PMMoV-I-infected leaves from transgenic *N. benthamiana* plants. The levels of NAD^+, $NADP^+$, NADH and NADPH were expressed as nanomols per gram of fresh tissue (nmol/g FW).The significant difference between mock inoculated control plants and PMMoV-I infected plants is indicated by astericks in which single * is the significant difference when ($p<0.05$) and double ** is the significant difference when ($p<0.001$). Significant difference among the different lines in PMMoV-I infected plants is noted by the alphabetical letter a in which the value is ($p<0.05$). FW-Fresh Weight.

At 21 dpi, the data showed (Fig.4.20) that the concentration of NAD^+ in mock inoculated control plants was around 4-7 nmoles/g of fresh tissue and it was found to be uniform for all of the four transgenic plant lines. The level of NADH accumulation in those plans was in the range of 5-8 nmoles/g of fresh tissue and it was found to be slightly higher in *Nb:Grx* and *Nb:Grx-GFP* than in *Nb:GFP* plant leaves, but differences either in NAD^+ or NADH accumulation were not significant.

In the PMMoV-I infected plants the level of NAD^+ was similar to their corresponding control plants, with no differences among *Cch* Grx-expressing and GFP-expressing plants.

In contrast, the NADH levels increased from 4 to 5 times in the PMMoV-I infected systemic leaves with respect to the mock-inoculated control plants and significant differences were found ($P<0.001$). The values were in the range of 27-37 nmole/g fresh tissue. Among the different PMMoV-I-infected transgenic lines, *Nb:Grx-GFP* showed significant differences (about 37 nmole/g fresh tissue; $p<0.05$) to the rest of the transgenic infected plants.

The total content of NAD increased considerably in infected plants and most of that increase was due to the reduced form of NADH. So, the redox state of the NAD pool shifted considerably towards its reduced form in the PMMoV-I infected leaves. In addition, the highest NADH/NAD ratio (5.36) was found in this *Nb:Grx-GFP* line, followed by *Nb:Grx, Nb: GFP* and *Nb:Δ2MGrx-GFP* lines with values of 3.94, 3.12 and 3.05 respectively.

In the mock inoculated plants, the data showed no differences in either $NADP^+$ or NADPH accumulation between GFP- and *Cch* GrxS12 and its derivative-expressing lines, neither in the redox state of the NADP pool. The $NADP^+$ content was always higher than the NADPH one, in both mock-inoculated and PMMoV-I-infected leaves. An increase in both the $NADP^+$ and NADPH content was found in the PMMoV-I infected plants but the increase in the level of NADPH was found to be significantly higher when compared with the mock-inoculated control plants ($p<0,05$).

At 28 dpi, samples were taken from symptomatic (infected) and asymptomatic (recovered) leaves of PMMoV-I infected plants as well as from the mock inoculated control plants (Fig. 4.21).

In the mock inoculated systemic leaves, the levels of PNs such as NAD^+, NADH and $NADP^+$ were found to be higher than the ones observed at 21 dpi (Fig.4.21) and they were

similar in the different transgenic plant lines, irrespective of either GFP-expressing or *Cch* GrxS12 expressing plants, except for the accumulation level of NADPH that was found to be similar to the one observed at 21 dpi (Fig.4.20 and 4.21). No significant differences were observed in the PNs content between *Cch* GrxS12- and GFP-expressing plants at this time period.

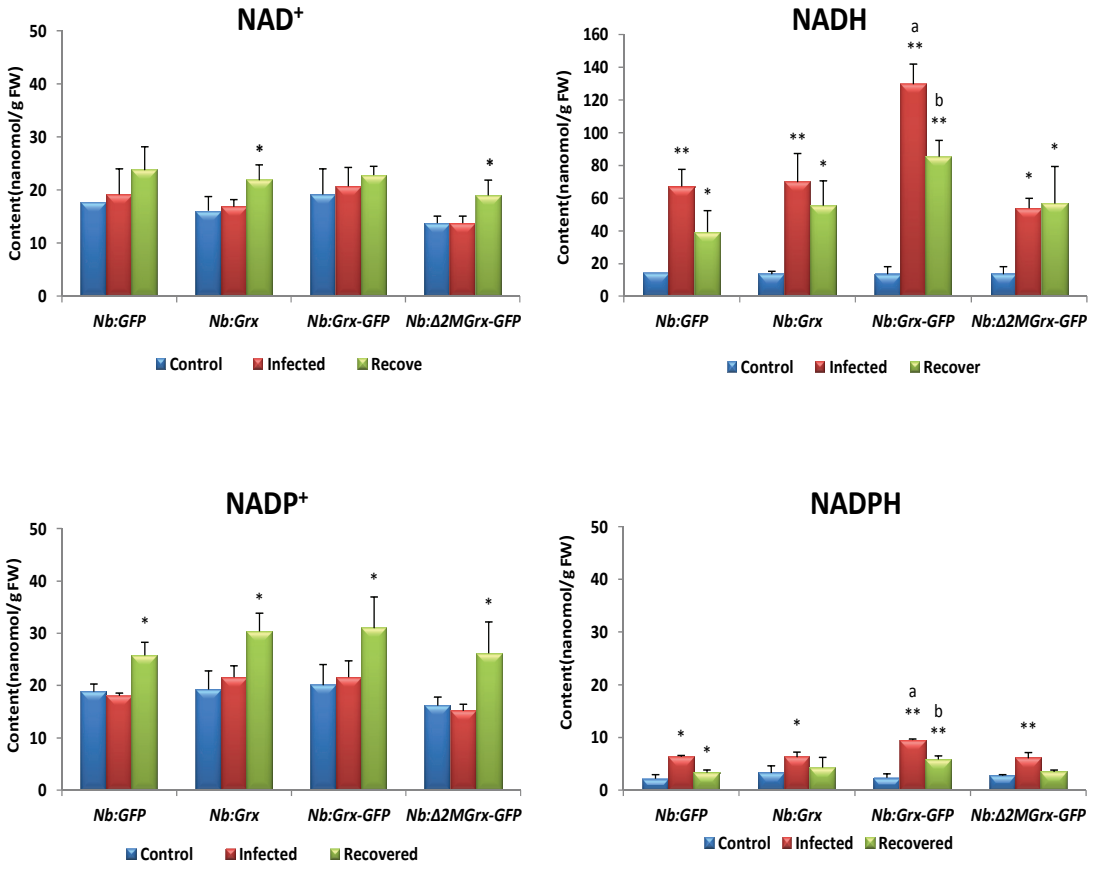

Fig.4.21. Analysis of PN contents at 28 dpi in control and PMMoV-I infected and recovered leaves in transgenic *N. benthamiana* plants. The levels of NAD^+, $NADP^+$, NADH and NADPH were expressed as nanomols per gram of fresh tissue (nmol/g FW). The significant difference between mock inoculated control plants and PMMoV-I infected plants is indicated by asterisks in which single * is the significant difference when ($p<0.05$) and double ** is the significant difference when ($p<0.001$). Significant difference among the different lines in PMMoV-I infected plants is noted by the alphabetical letter a in which the value is ($p<0.05$). FW-Fresh Weight.

In the PMMoV-I infected leaves, NAD^+ and $NADP^+$ content was similar to the one observed in mock inoculated plants, whereas in the recovered leaves a slight increase was observed mainly for $NADP^+$. Overall, the accumulation level of the reduced PNs (NADH and NADPH) was found to be significantly higher in the infected and recovered leaves when compared with the mock inoculated ones, although the levels reached in the infected leaves were higher than the ones observed in the recovered ones. Among the reduced nucleotides, NADH accumulation level got increased from 4 to 8 folds and from 2.7 to 6.5 folds, relative to control plants, in both infected and recovered leaves respectively. Maximum levels of NADH accumulation (108 nanomoles/g of tissue) were found in the infected leaves of *Nb:Grx-GFP* plants (Fig. 4.21). In addition, among the different PMMoV-I-infected transgenic plant lines (both in infected and recovered leaves), NADH and NADPH levels were found to be significantly higher in the Grx-GFP-expressing plants than in the corresponding leaves from the PMMoV-I-infected GFP-expressing plants ($p<0.05$).

As a result of the high NADH accumulation, the NAD pool was predominantly in its reduced form in both PMMoV-I infected and recovered leaves. However, even though the level of NADPH increased in the PMMoV-I infected plants, the NADP pool was maintained in the oxidized form.

4.8. Tolerance to oxidative stress in *N. benthamiana* plants over expressing *Cch* GrxS12

Contribution of *Cch* GrxS12 to oxidative stress tolerance of transgenic *N. benthamiana* plants was analysed by root growth assay as described under Materials and Methods.

The growth of primary roots of *Nb:GFP* plants was significantly inhibited in media containing either 3 mM H_2O_2 or 1 µM paraquat. The effect of 1 µM paraquat treatment was stronger than the one of 3 mM H_2O_2, but in both cases root growth was less inhibited in the transgenic plants expressing *Cch* GrxS12 and its derivatives than in the GFP-expressing plants with $P<0.05$ (Fig.4.22).

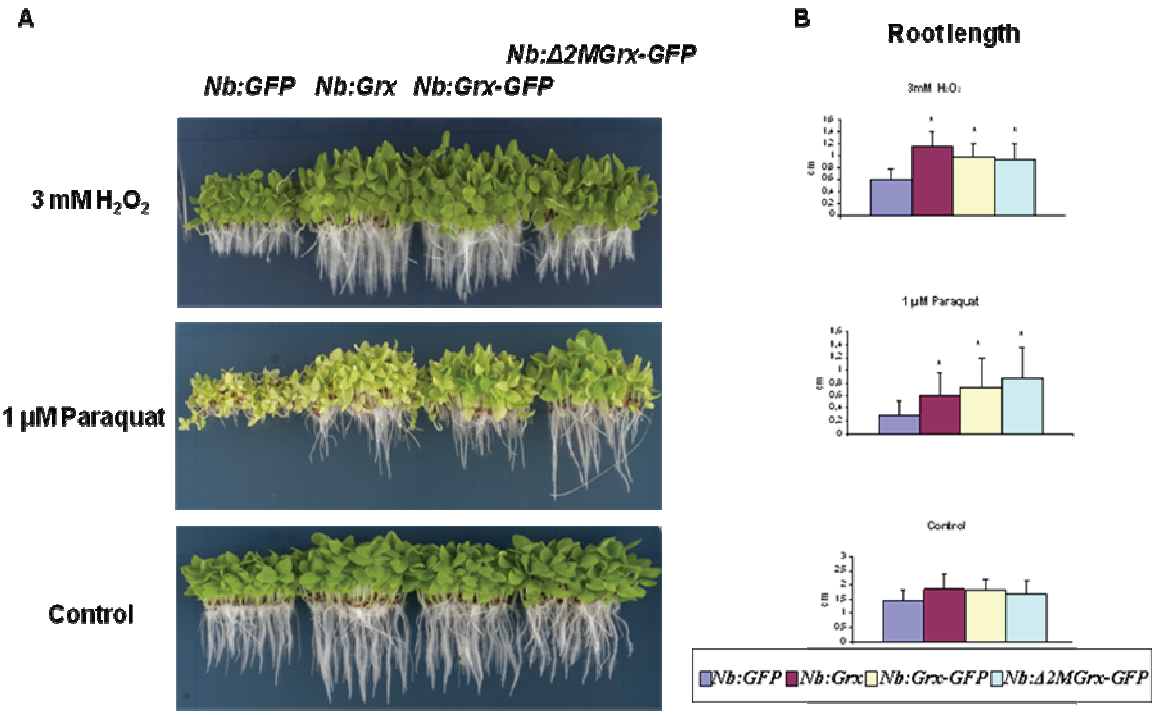

Fig.4.22. A.Visual phenotype of *N. benthamiana* transgenic lines indicated at the top of the figure grown under normal and oxidative stress conditions, as indicated on the left, for 12 days. B. Root growth measurement. The length of primary roots of seedlings was measured. Error bars, S.D. (n>30). Significant difference between *Nb:GFP* and *Cch* Grx over expressing lines (*Nb:Grx; Nb:Grx-GFP; Nb:Δ2MGrx-GFP*) are represented by asterisks (*P<0.05).

The plants grown on control media (without added H_2O_2 or paraquat) were also analysed for the root length (Fig.4.22B), and no significant difference were detected among the lines.

Thus, the over expression of *Cch* GrxS12 in plants increased their tolerance against oxidative stress conditions caused by either H_2O_2 or paraquat.

4.9. Heterologous expression of *Cch* GrxS12 in yeast *Δgrx5* mutant

By taking advantage of the availability of a *S. cerevisiae* mutant defective for the *grx5* gene (Rodríguez-Manzaneque *et al.*, 2002), we have used it as a model system to study the possible function of *Cch* GrxS12. With this purpose, *Cch grxS12* nucleotide sequence coding from aa positions 64-177 (mature protein) was cloned onto the yeast plasmid pMM221 which contains the *S. cerevisiae* sequence coding for the mitochondrial targeting sequence from GRX5 protein plus a 3' sequence coding a C-terminal 3HA/His_6 tag under the control of the *tetO*$_2$

promoter (Fig.4.23). The *Cch grx* sequence was cloned between the *Not*I and *Bgl*II site of the MCS region in the vector, thus obtaining the plasmid pMM1025. This plasmid was used to obtain transformed yeast T clones containing *Cch grx* sequence in the *Δgrx5* background as described under Materials and Methods. The resultant protein consisted of the Grx5 mitochondrial targeting sequence fused to the HA tagged *Cch* GrxS12 mature protein.

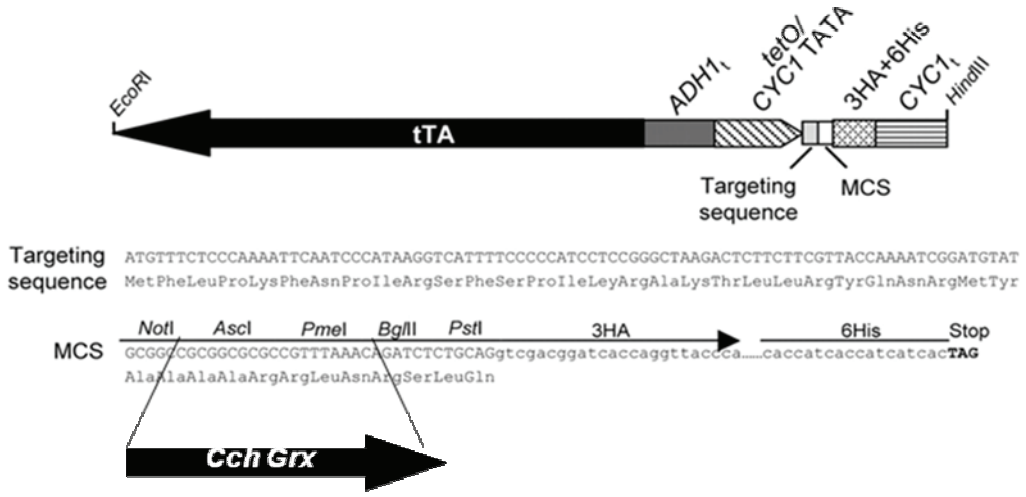

Fig.4.23. Cloning of *Cch* GrxS12 in Yeast plasmid pMM221. Schematic representation of PMM221 cloning vector (Molina *et al.,* 2004). *Cch* Grx sequence coding from amino acid 64-177 (mature protein) was cloned onto the yeast plasmid pMM221 which contains the *S. cerevisae* mitochondrial targeting sequence plus a C-terminal 3HA/His_6 tag under the control of $tetO_2$ promoter. The sequence was cloned between the *Not*I and *Bgl*II sites of the MCS region in the vector.

Many yeast clones transformed with the *Cch grx* sequence were selected and analyzed by Western blot assay by using HA tag specific monoclonal antibody to select clones with high *Cch* Grx protein expression for further studies (Fig.4.23).

The mobility of *Cch* GrxS12 protein corresponded to the expected size of the mature tagged protein (18 kDa), slightly smaller than yeast GRX5 tagged protein (19 kDa). In four of the clones, a lower mobility band was present in the total protein extract (Fig.4.23). This band could correspond to the non-processed precursor from the mitochondria located *Cch* GrxS12. The colony no. T11 was selected for further studies since its expression level was the highest.

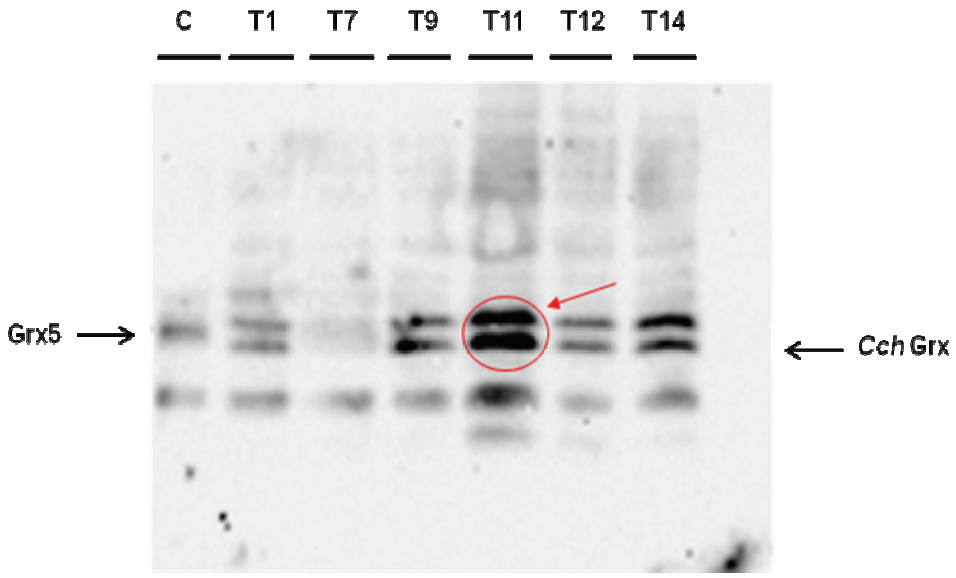

Fig.4.24.Western blot analysis of *Cch* GrxS12 expression in yeast. Yeast cells transformed with *Cch* GrxS12 were recognised by probing with specific antibody against HA tag. C: positive control (*Δgrx5* yeast strain expressing Grx5-3HA); T1, T7, T9, T11, T12 and T14 are yeast colonies transformed with *Cch* GrxS12.

4.9.1. *Cch* GrxS12 is not able to rescue the defects of *Δgrx5* mutant

In order to analyze whether *Cch* GrxS12 could be able to rescue the growth defects of yeast *Δgrx5* mutant, the wild type strain (W303-1B), MML100 (*Δgrx5* mutant), MML240 (*Δgrx5/GRX5)* and T11 (*Δgrx5/Cch Grx)* were plated on media containing glycerol (YPG) and also in the SD auxotrophic medium which lacks the amino acid Lys (Fig.4.25A). The strains were allowed to grow for 3 days at 30^{o}C. The *Δgrx5* mutant and *Cch Grx* transformed *Δgrx5* mutant failed to grow over the YPG and SD media whereas the wild type strain and 240 strain (*Δgrx5/GRX5)* were able to grow over the defective media (Fig.4.25A). The data clearly showed that *Cch* GrxS12 could not be able to rescue the growth defects of *Δgrx5* mutant.

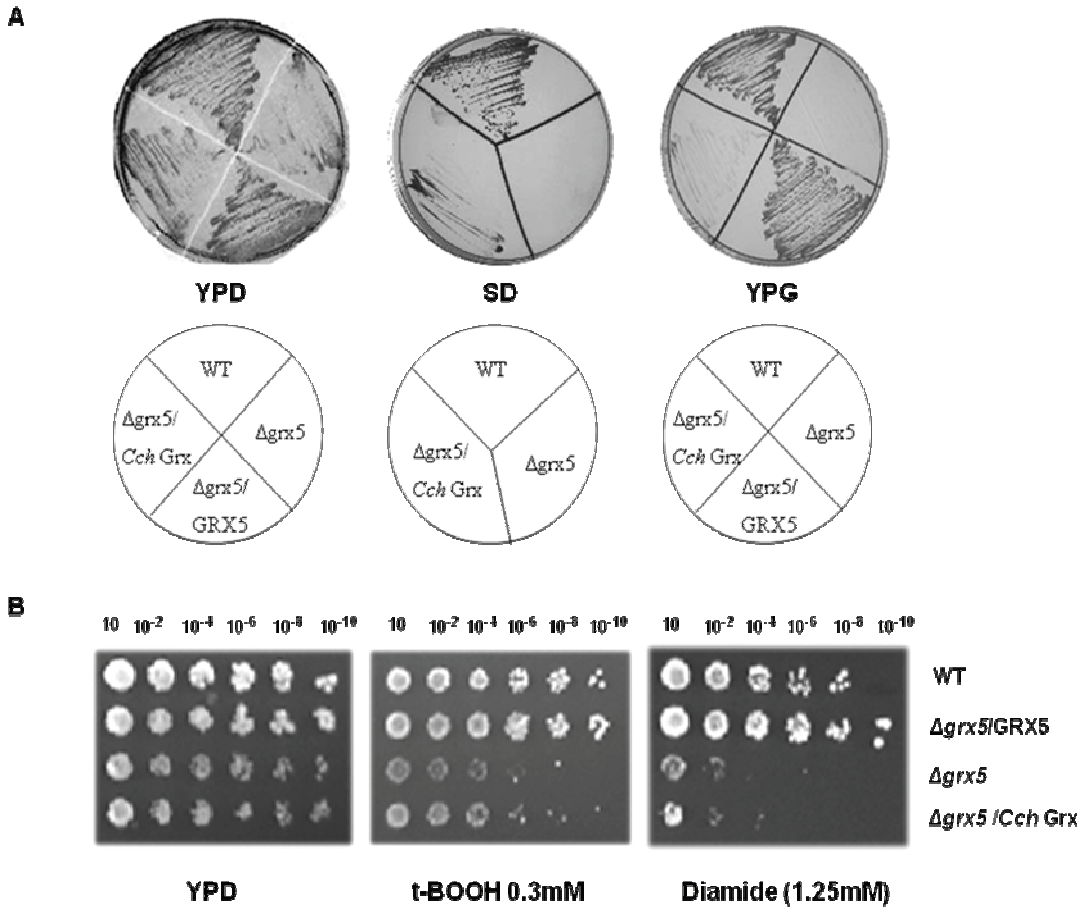

Fig.4.25. A. Analysis of the rescue effect of *Cch* GrxS12 over specific media in the *Δgrx5* mutant *S. cerevisae*. Wildtype (WT), *Δgrx5*, *Δgrx5*/Grx5 and *Δgrx5*/*Cch* Grx cells were grown over glucose (YPD), minimal (SD) and Glycerol (YPG) media for 3 days at 30°C. B. Sensitivity towards oxidants was analyzed by grown over YPD medium containing t-BOOH and diamide for 3 days at 30°C.

Earlier reports showed that Δ*grx5* mutants are sensitive to tert-butyl hydroperoxide (t-BOOH) and diamide (Luikenhuis *et al.,* 1998). Thus, in order to investigate whether *Cch* GrxS12 protein could rescue the hypersensitivity of Δ*grx5* mutant to those external oxidants, the four yeast strains mentioned above were grown over 0.3 mM t-BOOH and 1.5 mM diamide. The wild type and strain 240 could be able to grow over the oxidant containing media while the Δ*grx5* mutant and *Cch grx* transformed in *Δgrx5* mutant were unable to grow over the media containing either t-BOOH or diamide (Fig. 4.25B).

These results clearly showed that *Cch* GrxS12 failed to rescue the growth defects of Δ*grx5* mutant and also was not able to compensate the hypersensitivity of Δ*grx5* mutant against the external oxidants.

4.9.2. Determination of iron accumulation in the yeast strains

Further experiments were conducted in order to determine whether *Cch* GrxS12 could be able to suppress the iron accumulation in the Δ*grx5* yeast mutant. Therefore the accumulation of free iron was analyzed in yeast wild type strain, yeast *Δgrx5* mutant, yeast *Δgrx5* mutant transformed with GRX5 and *Δgrx5* mutant transformed with *Cch grx* (*Δgrx5*/*Cch grx*). The yeast strains were grown in YPD media at 30^{o}C and the accumulation of free iron was measured by the bathophenantroline method, as described under Materials and Methods. In the case of *Δgrx5* mutant, the relative ratio of free iron accumulation with respect to the wild type strain was found to be 2.5 fold higher (Fig.4.26A). In *GRX5* transformed *Δgrx5* mutant strain, the accumulation of free iron dropped as in wild type cells. But in *Cch grx* transformed yeast *Δgrx5* mutant the relative accumulation level of iron was found to remain the same as that from yeast *Δgrx5* mutant. Thus these experiments showed that *Cch* GrxS12 was not able to suppress the iron accumulation in the *Δgrx5* mutant.

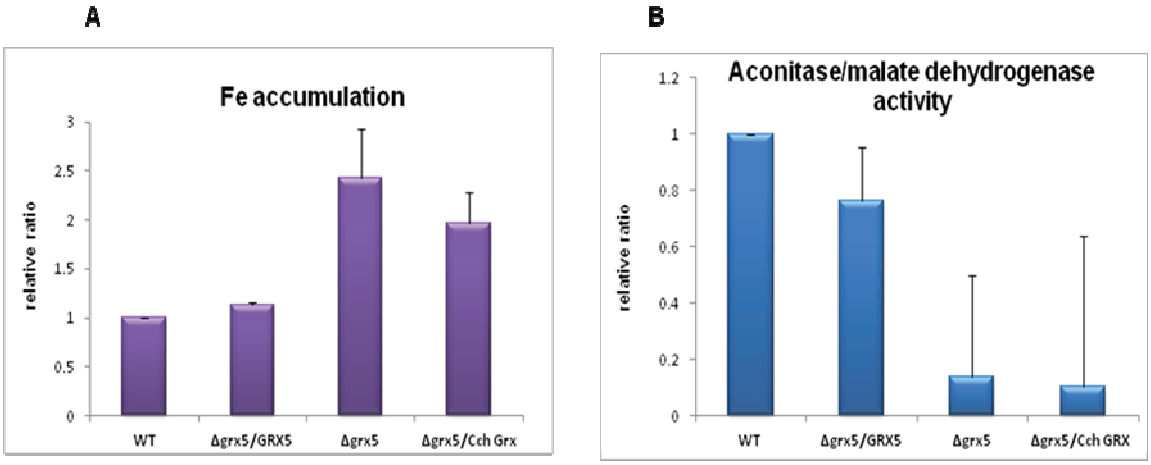

Fig.4.26.Deletion of GRX5 in yeast cell induces the accumulation of free iron and also defects in the activities of mitochondrial Fe/S proteins. A. Relative ratio of iron accumulation in wild type (WT), *Δgrx5*/GRX5, *Δgrx5* and *Δgrx5*/*Cch* Grx yeast strains. B. Relative ratio of aconitase to malate dehydrogenase activity in Wild type (WT), *Δgrx5*/GRX5, *Δgrx5* and *Δgrx5*/*Cch* Grx yeast strains. Error bars indicate the standard deviation of at least three independent experiments.

4.9.3. Determination of aconitase and malate dehydrogenase ratio

The ratio of aconitase to malate dehydrogenase activities was measured in all the four yeast strains, to determine whether *Cch* GrxS12 can restore the functions of yeast GRX5 in the Δ*grx5* defective mutant. In all the four strains tested, the activity of malate dehydrogenase did not show any significant variation. But a decrease in the level of aconitase activity was found in Δ*grx5* strain and *Cch grx* transformed Δ*grx5* mutant. The level of aconitase got reduced by 2-2.5 fold compared to the wild type and GRX5 expressed in Δ*grx5* strain (Fig.4.26B). All these results showed that the *Cch* GrxS12 protein was unable to restore the function of GRX5 in *S. cerevisiae* Δ*grx5* mutant.

5.DISCUSSION

In previous work of our group, it was identified a *C. chinense* L^3L^3 PI 159236 chloroplastic Grx gene whose expression was induced during both compatible and incompatible interactions between *C.chinense* plants and the Italian (I) and the Spanish (S) strains of PMMoV, respectively (Gilardi, 2000). It was also determined that the constitutive expression of the full length protein was directed to the chloroplast and a truncated form to the nucleus.

In higher plants Grx genes are encoded by multigene families with about 30 members, in contrast to Grx reported from *E. coli* and *S. cerevisiae* (Lillig *et al.,* 2008). Deduced amino acid sequence analysis showed that *Cch* Grx belongs to class I mono-thiol Grx with a CSYS active site (Couturier *et al.,* 2009a). BLAST search analysis carried out in this work have shown that CSYS active site Grxs and Grx-like proteins with this active site have been reported from plants, insect and fungi but not reported in prokaryotes. According to the classification proposed by Couturier *et al.,* (2009a), *Cch* Grx belongs to the C5/S12 subgroup having a WCSYC/S active site. This unusual active site is unique to plant Grxs. GrxS12 coding genes have been described in all studied land plants while GrxC5 coding ones were only found in Brassicaceae family (Couturier *et al.,* 2011). Because of gene duplication and divergence many Grx proteins were found to possess extra domains in addition to the Grx domain. Members of class I Grxs are generally characterized by having single domain Grxs with monothiol or dithiol active sites as the *Cch* GrxS12. Analysis of the *Cch* GrxS12 aa sequence with different Grxs searched through NCBI blast showed maximum identity to the Grx from *S. lycopersicum* (97%), followed by that from *V. vinifera* VviGrxC5 (85%), poplar PtrGrxS12 protein (81%), AthGrxS12 from *A. thaliana* (69%) and GrxS12 from monocots (*Zea mays*) (78%) whereas it shows the lowest identity to SceGrx6 reported from *S. cerevisae* (38%).

The phylogenetic tree shows that *Cch* GrxS12 is located in the same branch as that from tomato, and that all of them are grouped in one major branch whereas that from *S. cerevisae* is located in a different branch (Fig.4.2.)

The predicted *Cch* GrxS12 structure is very similar to the one described for other known Grxs. *Cch* GrxS12 structure displays the characteristics of Trx fold family proteins with a core of four β-strands surrounded by five α-helices on both sides as that for the known crystal structure of poplar PtrGrxS12 protein (Couturier *et al.,* 2009b), Fig. 4.3 and 4.4). The most important characteristics shared by these two proteins are that both of them have WCSYS sequence region as their active site located at the N-terminus of the α2 helix (Couturier *et al.,* 2009b) and that

other important amino acid motifs described to be involved in GSH binding in poplar PtrGrxS12, such as ^{75}TVP^{77}, ^{87}GG^{88} as well as the presence of a second Cys residue away from the active site (Couturier *et al.,* 2009b), were well conserved in *Cch* GrxS12 protein. Conservation of GSH binding site between the two proteins suggests that both of them share the same biochemical and physiological function.

To characterize *Cch* GrxS12 protein, it was expressed in different biological systems: bacteria, yeasts and plants. The expression of *Cch* GrxS12 mature protein in *E. coli* allowed us to obtain a soluble recombinant *Cch* GrxS12 protein with a His-tag at its N-terminus and with a calculated apparent Mr of 12.9 kDa well in accordance to the predicted one. The purified His-*Cch* GrxS12 was found to have GSH-disulphide oxidoreductase activity, being active in the classical Grx HED assay that tests deglutathionylation activity (Holmgren and Åslund 1995). The His-tag at the N terminus of the *Cch* GrxS12 protein did not abolish the protein activity, as well as it was reported for GRX1 from *Chlamidomonas reinherdtii*, a CPYC-type Grx (Zaffagnini *et al.,* 2008). On comparing the Grx activities from other monothiol Grxs, it was found that *Cch* GrxS12 (0.12 U/nM) possess less specific activity than those of yeast Grx6 (0.21 U/nM) and Grx7 (0.51 U/nM). The K_m and K_{cat} values also indicated that *Cch* GrxS12 was 10 times less active than PtrGrxS12 reported from *Populus* (Couturier *et al.,* 2009b). This *in vitro* HED assay clearly demonstrates that *Cch* GrxS12 may regulate many reactions inside the cell where the thiol status of the proteins are affected by glutathione level.

The catalytic action of individual Grx is found to be varied and thus make the individual Grx to have specific function at their compartments. Dithiol Grxs mainly confined to Class I Grx are found to be active in the HED assay eg. *C. reinhardtii* Grx1 and 2 (Gao *et al.,* 2010) and *A. thaliana* GrxC5 (Couturier *et al.,* 2011). But among the members of monothiol Grxs, different classes of Grxs have different enzymatic activity. Monothiol Grxs from Class I are found to participate in the deglutathionylation reaction eg. *S.cerevisae* Grxs such as *Sc*Grx6 and *Sc*Grx7 (Mesecke *et al.,* 2010) and poplar PtrGrxS12 (Couturier *et al.,* 2009b), whereas monothiol class II Grxs with CGFS active site were not found to be active in this deglutathionylation reaction eg. *S.cerevisae* Grx5 (Tamarit *et al.,* 2003), *E. coli* Grx4 (Fernandes *et al.,* 2005), *C. reinhardtii* GRX3 (Zaffagnini *et al.,* 2008), *A. thaliana* AtGRXcp (Cheng *et al.,* 2006) and AtGrx 4 (Cheng, 2008). In general it was concluded that Class I Grxs are found to possess this thiolreductase

activity (HED assay) irrespective of monothiol or dithiol active sites, whereas class II monothiol Grxs are not efficient in this reaction.

With regards to the active site amino acids required for deglutathionylation activity, mutation studies performed in other Grxs gave many clues about the sequences needed for this activity. *E. coli* Grx was found to be active in the HED assay when the second Cys of the active site (CPYC) was engineered to serine (Bushweller *et al.,* 1992). In the case of poplar PtrGrxS12, abolishment of protein activity was reported when the Cys residue of the CSYS active site was changed to Ser (Couturier *et al.,* 2009b), therefore the N-terminal Cys residue of the active site is required for this activity. But in *E.coli* Grx4, that does not have deglutathionylation activity, mutation of the CGFS active site to CGFC, and thus mimicking dithiol Grx, was not able to restore the activity in the HED assay (Fernandes *et al.,* 2005). Thus, these reports show that along with the N-terminal Cys of the active site region other regions of the protein are also essential for the Grx to be active in the HED assay.

Previous analysis in our lab using transient expression of GFP-tagged *Cch* GrxS12 constructions in *N. benthamiana* plant leaves revealed that *Cch* GrxS12-GFP protein and *Cch* Δ2M-Grx-GFP protein, where the 63 aa signal sequence for the plastid signal peptide was truncated, localized to the chloroplast and to the nuclei respectively (Montes-Casado *et al*., 2010), but at that moment it was not possible to rule out the possibility that the apparent nuclear localization of *Cch* Δ2M-Grx S12-GFP was due to the presence of free GFP in the transfected plant tissues. To further expand these data, and to confirm the nuclear localization of the truncated protein, protoplasts from *N. benthamiana* transgenic plant lines that constitutively expressed these two constructs as well as those expressing free GFP were assayed under confocal microscope. The results confirmed our previous data and expanded them in the sense that the full length *Cch* GrxS12-GFP was targeted to the chloroplast whereas Δ2M-GrxS12-GFP protein was found throughout the cytoplasm and nuclei, with a similar pattern as free GFP. This is in agreement with the sequence analysis by chloroP programm which shows that the first 63 aa region codes for the chloroplast targeting region. Similar to *Cch* GrxS12 many Grxs reported in other works also show a signal peptide of different length at their N-terminus as has been shown to in AtGRXcp-first 63aa, CarGRX3-first 68aa, AtGrx4 and poplar PtrGrxS12-first 74aa, all of them targeted to chloroplasts (Cheng *et al.,* 2006; Cheng, 2008; Couturier *et al.,* 2009b; Yadav *et al.,* 2012). Our results confirmed the nuclear localization of Δ2M-GrxS12-GFP protein and ruled

out the possibility that the apparent nuclear localization observed in our previous work was due to the presence of free GFP or to the over-expression of the protein (Montes-Casado *et al*., 2010).

Localization of plant Grxs were predicted for *A. thaliana* (Rouhier, 2010) and *Populus* (Bandyopadhyay *et al.,* 2008; Couturier *et al.,* 2009b) and it was shown that among the class I Grxs, Grxs belonging to GrxC5/S12 group are found to be localized to chloroplasts while others are localized at different compartments. It was also shown that Class I Grxs are co-existing with other class Grxs at their compartments (Rouhier *et al.,* 2004). In poplar chloroplasts, Grxs S14 and S16 (class II Grxs) were found to be co-localized along with GrxS12 (Class I) (Bandyopadhyay *et al.,* 2008; Couturier *et al.,* 2009b).

Monothiol Grxs have been described to participate in a diversity of cellular functions as protein redox regulators and in cell protection against protein oxidative damage (Cheng *et al.,* 2006; Herrero and de la Torre-Ruiz, 2007). Over-expression of a particular gene in transgenic plants is the best way to study the function of redundant genes (Ito and Meyerowitz, 2000; Nakazawa *et al.,* 2001). In this way, *N. benthamiana* plants constitutively expressing native *Cch* GrxS12 (*Nb:Grx*), a *Cch* GrxS12:GFP fusion protein (*Nb:Grx-GFP*) and a 63 aa truncated *Cch* GrxS12 fused to GFP (*Nb:Δ2MGrx-GFP*) were used to analyze the effect of *Cch* GrxS12 expression on PMMoV-I infection.

The accumulation of *Cch* GrxS12 and Δ2MGrxS12-GFP proteins in the different transgenic plants used was very similar while *Cch* GrxS12-GFP protein accumulated at a higher level. It is at present unknown if the observed differences come from a high expression of the *Cch* GrxS12-GFP transgene or from a slow turnover of the GFP tagged *Cch* GrxS12.

When the transgenic plants were infected with PMMoV-I, no difference in viral disease symptoms were observed at early stage of infection among the GFP and Grx constructs expressing *N. benthamiana* plants. However, at later stages of infection, i.e. at 28 dpi, recovery of the plants was more visible in the Grx expressing transgenic lines than in control *Nb:GFP* transgenic line. The results obtained after PMMoV-I viral accumulation analysis in *N. benthamiana* plants transformed with the three different *Cch* GrxS12 constructs and GFP transformed plants (*Nb:GFP*) showed that at 7 dpi the viral accumulation was similar in the inoculated leaves of all transgenic lines, thus suggesting that early events in plant virus infection such as replication and cell-to-cell viral movement were not affected by the expression of the

Cch GrxS12 constructs. These results were similar to the ones obtained when the transgenic plants were infected with the PMMoV-S strain tagged with the yellow fluorescent protein (PMMoV-S-YFP) (Montes-Casado *et al*., 2010). These preliminary data were further corroborated by protoplast infection studies among the different transgenic lines.

Protoplast infection was found to be similar in all the lines expressing the three *Cch* GrxS12 constructs as well as in the GFP expressing (*Nb:GFP*) plants **(**Fig.4.16.). As the kinetics and accumulation level of the viral CP in infected protoplasts is correlated to replication and translation kinetics (Hull 2002), we studied the kinetics of PMMoV-I CP accumulation in the protoplasts of the transgenic plants. PMMoV-I CP accumulation kinetic was found to be similar in the four lines assayed. Therefore the results from these studies collectively suggest that *Cch* GrxS12 does not inhibit PMMoV-I viral replication at the cellular level. Thus, our data are at variance with those previously reported by Auwerx *et al*., (2009) where they showed that the replication of human immunodeficiency virus (HIV) was inhibited by the expression of Grx-1 in the mammalian cell system.

Similarly, at 7 dpi no major difference in either viral coat protein or genomic PMMoV-I RNA accumulation was detected in the systemic leaves, thus indicating that over expression of *Cch* GrxS12 was not affecting PMMoV-I accumulation in the systemic leaves during early stages of infection.

Lately, the coat protein accumulation level got increased in the systemic leaves and reached its maximum at 14 dpi and again fall down at 28 dpi as plants recover from infection (Pérez-Bueno, 2003; Molina-Galdeano 2006). A negative effect on PMMoV-I accumulation was observed at 14 dpi, in the different *Cch* GrxS12 constructs-transformed plant lines. This effect was also observed at 28 dpi in the infected and recovered leaves of PMMoV-I infected plants.

The high reduction in viral RNA accumulation at 28 dpi in *Nb:Grx-GFP* plants was correlated to the high level of *Cch* GrxS12:GFP protein content in these plants (about 10 times more than in either *Nb:Grx* or *Nb:Δ2MGrx:GFP*). Thus suggesting a possible dose-response effect in the inhibition of viral RNA accumulation. As described in a previous work from the laboratory (Montes-Casado *et al*., 2010) the reduction on PMMoV-I virus accumulation was due to a lower number of infected cells in the systemic leaves of the *Cch* GrxS12 transgenic plants.

Overall, the *Cch* GrxS12-transformed *N. benthamiana* plants showed a diminished PMMoV-I accumulation at late stages of infection. Although monothiol Grxs have been

described conferring tolerance against different abiotic stresses (Sundaram *et al.,* 2009; Sundaram and Rathinasabapathi, 2010), this work and the previous work from our laboratory (Montes-Casado *et al*., 2010) is the first time to describe a plant Grx conferring resistance against plant virus infection. From the results obtained, the fusion protein *Cch* GrxS12:GFP was fully active in PMMoV-I infection. The preservation of Grx enzymatic activity has been also described in other Grx hybrid proteins (Rouhier *et al.,* 2006). It is interesting to note that chloroplast localization of the *Cch* GrxS12 protein was not required for its putative function in viral inhibition, as the truncated Grx protein that located in the cytoplasm and the nuclei was also active.

Similarly, the over expression of another member of Trx protein family, NtTRXh3, in *N. tabaccum* plants was found to reduce multiplication and pathogenicity of *Tobacco mosaic virus* and *Cucumber mosaic virus* which was accompanied with the activation of SAR defence related gene PR-1a (Sun *et al.,* 2010).

These data are in contrast with previous work (Wang *et al*., 2009) that showed that the over-expression of ROXY1/2, a CC-type Grx, in *Arabidopsis thaliana* leads to hyper-susceptibility of the transgenic plants to the infection by *Botrytis cinerea.* Furthermore, La Camera *et al.,* (2011) showed that another CC-type Grx, ATGRXS13, was required to facilitate *B. cinerea* infection in *A. thaliana.* These different results could be ascribed to the type of pathogen used in those studies, since *B. cinerea* is a necrotrophic pathogen while PMMoV-I is a biotrophic one and the type of plant defence response in each type of interaction is mediated by two different signaling pathways, either the JA or SA pathways, respectively (Glazebrook, 2005; van Loon *et al*., 2006). In this sense, it has been shown that an *Arabidopsis* CC-type Grx, GRX480, is SA inducible and when ectopically expressed in transgenic *Arabidopsis* plants strongly impaired the expression of the JA-dependent gene PDF1.2 (Ndamukong *et al.,* 2007).

In order to further know the underlying resistance mechanism mediated by *Cch* GrxS12 over expression, the accumulation level of PR-1, PR-2a and PR-5 mRNAs which are the usual markers of SA signaling pathway (Ryals *et al.,* 1996) and PR-2b, a marker for Ethylene pathway (van Loon *et al*., 2006), were analyzed in all the transgenic lines at 7, 21 and 28 dpi. At early stage (7dpi) of plant growth, SA- regulated PR gene expression was not detected in the mock inoculated control plants, but ET-regulated defence mRNA for protein PR-2b was detected in the mock inoculated control plants. This shows that ET-regulated genes got activated at the time of

mechanical injury caused during mock inoculation. It is worth emphasizing that at the late stage (21 and 28 dpi) of plant growth, SA-regulated PR mRNA expression was increased in the systemic leaves of mock inoculated *Cch* GrxS12 transformed *N. benthamiana* plant lines, whereas ET-regulated PR expression was found to be negligible. The expression level of SA-regulated PR protein was particularly high in the *Nb:Grx:GFP* line which may be due to the high level of GrxS12-GFP protein accumulation in this line. Thus at late stage of plant growth, *Cch* GrxS12 over expression mediates the accumulation of SA-regulated PR genes under non-infection conditions. Although the increase in the accumulation of PR proteins at the time of flowering (Lotan *et al.,* 1989), and at senescent plants (Obregon *et al.,* 2001) has been described in tobacco, the increase observed in the accumulation of SA-regulated PR mRNAs in the *Cch* GrxS12 transgenic plants seems to be related to the expression of *Cch* GrxS12 and its derivatives, because in *N. benthamiana* plants expressing free GFP, PR mRNA accumulation was not detected at that stage of development.

SA-regulated PR gene expression was induced in the PMMoV-I inoculated leaves at 7 dpi, but at this time post-inoculation no differences were observed between *Cch* GrxS12 *N. benthamiana* transgenic plants and the GFP transgenic ones. In the systemic leaves there was no or little expression of either the acidic or the basic PR genes as it was expected since the interaction PMMoV-I-*N. benthamiana* is a compatible interaction where a resistance response was not established and virus accumulation was high in those leaves. At late stages of infection (i.e. at 21 and 28 dpi) an increase of SA-regulated PR mRNA accumulation was observed in the systemic leaves of PMMoV-I infected plants whereas negligible level of ET-mediated PR gene accumulation was detected. The accumulation of the SA-regulated PR mRNAs was already described in the same plant-pathogen system by Tena (2012), who also described that a defence mechanism was established in the PMMoV-I- infected *N. benthamiana* recovered leaves at 28 dpi. But what it was remarkable is that our results showed that the over expression of *Cch* GrxS12 in *N. benthamiana* plants promotes a stronger induction of the expression of the SA-regulated PR genes at late stage of plant growth under both pathogenic and non-pathogenic conditions, which seems to indicate that the constitutive expression of either *Cch* GrxS12 or its derivatives promotes priming the *N. benthamiana* systemic defence mechanism of the recovered part of the plant, that it has been ruled out that is due to PTGS (Tena, 2012).

Our results are well in accordance with those described for *Arabidopsis* GRX480, that, when ectopically expressed in *Arabidopsis,* allowed the expression of marker genes for SA-inducible response while inhibited the expression of the JA-regulated genes (Nadmukong *et al.,* 2007).

In addition to the increase of the expression of the SA-regulated PR genes at late stage of PMMoV-I infection, the constitutive expression of *Cch* GrxS12 in *N. benthamiana* plants, also up regulated the expression of 9-LOX gene involved in a plant defence response through a JA-independent signaling pathway (Vellosillo *et al.,* 2007). Although at 7 dpi a weak accumulation of 9-LOX RNA was detected in the mock inoculated plant leaves from *Cch* GrxS12 transgenic plants, an increase with respect to the GFP expressing plants was observed. That increase was higher in the PMMoV-I inoculated leaves from *Nb:Grx* and *Nb:Grx-GFP* plants. But the highest increase was observed at 28 dpi in the PMMoV-I-infected and mock-inoculated *Nb:Grx-GFP* plants. It has been described that in compatible plant pathogen interaction, 9-LOX gene expression is delayed and accumulated at low levels (Hwang and Hwang, 2010), contrary to what happens in HR defence response where an increase in expression and activity of 9-LOX enzyme has been reported (Rancé *et al.,* 1998; Montillet *et al.,* 2002; Göbel *et al.,* 2002; Hwang and Hwang, 2010). These results suggest that *Cch* GrxS12 and its derivatives, constitutively expressed in *N. benthamiana* plants, activate more than one plant defence response pathway at late stage of plant development and during PMMoV-I infection.

GR is a key enzyme in the Grx-GSH and ascorbate-GSH pathways and it plays a key role in maintaining the antioxidant machinery of the cells, and the cellular redox state by utilizing the reducing power of GSH (Ansel *et al.,* 2006; Lillig *et al.,* 2008). The comparative analysis of the GR mRNA accumulation between the *Cch* GrxS12 expressing plant lines and the control GFP expressing plants showed little differences in the GR mRNA accumulation in both inoculated and systemic leaves of mock inoculated plants at the three time points assayed, indicating that the constitutive expression of *Cch* GrxS12 and its derivatives in *N. benthamiana* plants does not affect *GR* gene expression at those times post inoculation, at variance to what it was reported in *Rhodobacter capsulatus*, where the mutation in grx system affects the expression of GR under oxidative stress conditions (Li *et al.,* 2004). In PMMoV-I infected plants, GR mRNA analysis showed that GR mRNA accumulation was reduced only in the PMMoV-I inoculated leaves at 7 dpi and in the infected plant leaves at 28 dpi. However, the levels of GR mRNA got restored in

the recovered leaves at 28 dpi (Fig.4.19). These data are well in accordance to those previously reported by Hakmaoui *et al.,* (2012) about the increase in GR activity in PMMoV-I-infected *N. benthamiana* plants at that time post-inoculation.

Previous reports have shown variable results in the GR activity of pathogen- infected plants. A decrease was reported in tomato plants when infected with *Botrytis cinerea* (Kuzniak and Sklodowska, 2005), in apricot seeds when infected with *Prunus necrotic ringspot virus* (PNRSV) (Amari *et al.,* 2007) or in *N. benthamiana* plants infected with PMMoV-I at early steps of infection, up to 21 dpi, (Hakmaoui *et al.,* 2012), while GR level was found to increase in *Hibiscus cannabinus* plants when infected with *Mesta yellow vein mosaic disease* (Sarkar *et al.,* 2011). Thus, it seems that GR expression or activity could change depending either in the plant pathogen system or the post-inoculation time point analyzed.

GST gene expression is a good marker of plant response against oxidative cell damage (Fodor *et al.,* 1997; Sun *et al.,* 2010) and a rapid induction has been described in systemic leaves in response to infection with an avirulent pathogen preceding the induction of PR-1 gene expression (Lieberherr *et al.,* 2003; Wagner *et al.,* 2002).

Analysis of the GST mRNA accumulation in the different transgenic plant lines showed an increase in GST expression in PMMoV-I infected plant leaves at 7 and 21 dpi irrespective of the transgenic lines analyzed which shows that *Cch* GrxS12 constitutive expression did not change the plant response against oxidative stress due to PMMoV-I infection at this period of infection. This increase correlated well with the described up regulation of many antioxidant genes in PMMoV-I-infected *N. benthamiana* plants at that period of time, which was a response to the oxidative stress caused by PMMoV-I in the infected leaves up to 21 dpi (Hakmaoui *et al.,* 2012). However, at 28 dpi, expression level of GST in the infected and recovered leaves of *Cch* GrxS12 and its derivatives expressing lines was reduced to values similar to the mock inoculated control plants, whereas high levels of GST mRNA accumulation was detected in the PMMoV-I-infected and recovered leaves from GFP expressing line. Taking into account that in PMMoV-I-infected *N. benthamiana* plants a symptom recovering mechanism is induced at that time period and that it was associated to a reduction of H_2O_2 levels in the recovered plants (Hakmaoui *et al.,* 2012), it seems plausible to ascribed the low levels of GST mRNA accumulation in the *Cch* GrxS12 expressing lines to an enhanced ROS-scavenging effect in those plants, thus limiting the virus induced oxidative stress (Hakmaoui *et al.,* 2012).

Analysis of the NAD and NADP pools in the mock inoculated *N. benthamiana* transgenic plants at 21 and 28 dpi showed that constitutive expression of *Cch* GrxS12 and its derivatives does not affect the accumulation levels of those PNs. Thus showing that either their accumulation or their oxidized state is quite stable, as reported for barley leaf chloroplats (Wigge *et al.,* 1993) and it seems to depend more on the plant growth stage (Yamamoto, 1963; Bonzon *et al.,* 1983; Queval and Noctor, 2007) than in the accumulation of the *Cch* GrxS12 either in the chloroplasts or the cytoplasm and nuclei. The levels found at 28 dpi were higher than the ones observed at 21 dpi, except for NADPH, that was between 2 and 10 times lower than the $NADP^+$ levels found at either 21 or 28 dpi, respectively. This may be due to the metabolic stage of the plants, as it has been described a change from anabolic towards catabolic processes at late growth stages, which in turn is reflected by a drop of the NADPH/ NADPH+$NADP^+$ ratio, a marker of anabolic processes (Bonzon *et al.,* 1983).

PMMoV-I infection in the *N. benthamiana* transgenic plants alters the PNs towards a reduced condition as the levels of NADH and NADPH accumulation were found to be significantly higher in the PMMoV-I infected plants than in the mock-inoculated control plants either at 21 or 28 dpi (Fig. 4.20 and 4.21). Similarly, increase in NADH and NADPH was observed in *Arabidopsis* plants when infected with the bacteria *Pst-AvrRpm1* (Pétriacq *et al.,* 2012). In addition, it has been reported that the increase in PNs levels in *N. sylvestris CMSII* mutants was accompanied by enhanced tolerance to oxidative stresses induced by ozone and TMV (Dutilleul *et al.,* 2005).

Among the PN levels, NADH level was found to increase 4-8 folds in the PMMoV-I infected plants which shows that NADH is a good marker for PMMoV-I infection. Within the infected transgenic lines, only *Nb:Grx-GFP* line showed significantly higher NADH and NADPH accumulation at 28 dpi which was accompanied with enhanced virus resistance (Fig. 4.12 and 4.13). It is worthy to note that these transgenic plants showed high level of *Cch* GrxS12-GFP accumulation. The increase in NADH content in PMMoV-I infected and recovered plant leaves produces an imbalance in the NADH/NAD^+ ratio that might trigger the production of ROS (Millar *et al.,* 2001) or the regulation of cellular antioxidant systems (Dutilleul *et al.,* 2003). Although the function of NADH in these transgenic plants remains to be elucidated, in previous work a correlation between an increase in NADH content and resistance against virulent bacteria have been reported in *Arabidopsis* gfg1-1 mutant plants (Jambunathan and

Mahalingan, 2006) and in *Arabidopsis* plants expressing *nadC* gene from *E. coli,* that accumulated high levels of NADH and NADPH (Pétriacq *et al.,* 2012).

The precise mechanism by which these reduced nucleotides enhance the disease resistance needs to be determined, but it may be related to the activity of many antioxidant enzymatic reactions which required either NADH or NADPH as coenzymes (Berger *et al.,* 2004; Noctor, 2006), such as GR-mediated regeneration of GSH, and reduction of ascorbate and thioredoxin by NADPH-dependent reductases (Meister and Anderson, 1983; Holmgren, 1985).

In addition, the high levels of NADH and NADPH in PMMoV-I infected and recovered leaves might bring about changes in the expression of defence genes. In *Arabidopsis* plants a correlation between PN accumulation and the induction of plant defence gene expression as well as bacterial resistance has been reported (Ge *et al.,* 2007; Zhang and Mou, 2009; Pétriacq *et al.,* 2012). Furthermore, the expression of the human NAD(P)-methabolizing ectoenzyme CD38 in *Arabidopsis,* that alters the NAD(P) concentration, compromises biological induction of SAR (Zhang and Mou, 2012). However, the pattern of PR mRNA accumulation found in *Cch* GrxS12 *N. benthamiana* transgenic plants seems to indicate that a direct correlation between the levels of PNs and the induction of PR gene expression in the *Cch* GrxS12 transgenic plants does not exist, as deduced by the observed increase in PR mRNA accumulation in the mock-inoculated plants of *Cch* GrxS12 and its derivatives expressing lines either at 21 or 28 dpi without significant changes in the accumulation levels of the different pyridine nucleotides with respect to the ones observed in the mock-inoculated plants of the GFP expressing line. This shows that Grx-mediated PR gene expression must be independent of PN levels under non-pathogenic condition.

It has been demonstrated that many of the plant Grx proteins are involved in the regulation of plant tolerance against oxidative stress condition (Cheng *et al.,* 2006; Cheng, 2008). In this work it was shown that over expression of *Cch* GrxS12 enhances the plants tolerance against oxidative stress condition as revealed by the better growth of *Cch* GrxS12 expressing seedlings over either paraquat or H_2O_2 exogenously applied media. Treatment of plants with Paraquat generates ROS in chloroplasts due to auto oxidation of paraquat radicals generated by electrons from the reaction center of PSI (Taiz and Zeiger, 2010; Krieger-Liszkay *et al.,* 2011), thereby inducing oxidative damage. The results obtained showed, that constitutive expression of *Cch* GrxS12 can protect the plants from cellular oxidative stress including photooxidative stress. Taking into account that *Cch* GrxS12 is a chloroplastic protein, those

results suggest that *Cch* GrxS12 has a role in protection against photooxidative stress conditions as it was described for the cytosolic GRXS13 from *A. thaliana* (Laporte *et al.,* 2012). That effect was independent on the subcellular localization of the *Cch* GrxS12 protein, either the chloroplasts or the cytoplasm and nuclei, in a similar way to the results obtained for the protection against PMMoV-I infection. The mechanisms underlying this tolerance are not known, but according to the results described for other Grxs, such as tomato Grx (SIGRX1) (Guo *et al.,* 2010), it seems plausible to consider that the over-expression of *Cch* GrxS12 activates the expression of genes involved in the antioxidant mechanisms either in the cytoplasm or the chloroplast.

Many Fe-S cluster containing proteins were found to be abundant in the chloroplast and mitochondria and also found throughout the cell (Balk and Lobreaux, 2005). Involvement of Grx proteins in Fe-S cluster assembly was first studied in yeast Grx5 protein where the deletion of Grx5 caused deficient in the synthesis of Fe-S cluster containing proteins and further leads to the accumulation of iron which increases the sensitivity of yeast cells towards oxidative stress conditions (Rodríguez-Manzaneque *et al.*, 1999, 2002). Expression of *Cch* GrxS12 in yeast *Δgrx5* mutant could neither restore the Fe-S cluster containing enzyme activities nor suppress iron accumulation (Fig. 4.26). This shows that *Cch* GrxS12 could not be able to participate in Fe-S cluster assembly in yeast but in plants it is still uncertain.

Among the plant Grxs, the structure of *Populus* GrxS12 (Couturier *et al.,* 2009b) and *A.thaliana* Grxs such as AtGrxC5 (Courtier *et al.,* 2011) and AtGrxS14 (previously referred as AtGRXcp) (Li *et al.,* 2010) are available which give further insight with the structural determinants necessary for the Fe-S cluster assembly function. All Grx structures showed that the presence of the Cys residue at the N terminus of the active site is indispensable for the Fe-S cluster assembly. In the case of *Populus* GrxS12, with the same active site than *Cch* GrxS12 (WCSYS), it was shown that the presence of a Trp residue at -1 region of the CSYS active site prevents the Fe-S cluster assembly and it was confirmed by the substitution of the Trp with Tyr residue which then allows the Fe-S cluster assembly (Couturier *et al.,* 2009b). However, later studies on AtGrxC5 structure showed that Trp at the -1 region of the active site (WCSYC) did not inhibit the Fe-S cluster assembly, thus showing that Try is not the only important amino acid for Fe-S cluster assembly function of Grx, but it depends on the presence in the active site of amino acids that counterbalance the negative effect of Trp at -1 position (Couturier *et al.,* 2011).

Although further structural studies would be needed, it seems that Trp at -1 position of the active site in *Cch* GrxS12 has a negative effect on Fe-S cluster incorporation.

Thus yeast transformation studies show that the protein may not participate in the biogenesis of Fe-S cluster assembly or in the regulation of iron homeostasis in the chloroplasts.

6.CONCLUSION

1. **Nucleotide and amino acid sequence analysis revealed that *Cch* Grx is a monothiol glutaredoxin that belongs to group I subgroup C5/S12 with a WCSYS active site and the structural prediction showed that it belongs to the Trx-fold family proteins. It was termed *Cch* GrxS12.**

2. **Confocal microscopy observation of protoplast from *N. benthamiana* transgenic plants confirmed that *Cch* GrxS12 fused to the GFP is targeted to the chloroplast, whereas the N-63 aa truncated *Cch* GrxS12-GFP fused protein was found to be localized at the cytoplasm and nuclei.**

3. **Purified *Cch* GrxS12 protein possesses *in vitro* thiol oxidoreductase activity as it reduces the disulfide bond between glutathione and substrate in the HED assay.**

4. **At early stages of infection, *Cch* GrxS12 expression in *N. benthamiana* plants did not inhibit the viral accumulation and thus it shows that *Cch* Grx is not affecting the viral replication, as confirmed by the analysis of the kinetic of accumulation of viral CP in protoplasts, or cell-to-cell movement.**

5. **Constitutive expression of the different forms of *Cch* GrxS12 in *N. benthamiana* plants results in a diminished viral accumulation at later stages of infection. The expression of the GFP-fusion proteins also produces a decrease in PMMoV-I viral accumulation thus indicating that both forms of the protein fused to the GFP conserved their activity.**

6. **At late stage of plant growth, *Cch* GrxS12 expression enhances the mRNA accumulation of SA-regulated PR proteins but not the ethylene-mediated PR proteins both in mock-inoculated control and PMMoV-I infected plants.**

7. ***Cch* GrxS12 expression in *N.benthamiana* plants enhances the plants tolerance against oxidative stress caused by H_2O_2 and the herbicide paraquat under *in vitro* condition**

and it shows that the protein could be able to protect the plants against the abiotic stress.

8. **The truncated *Cch* Δ2MGrxS12-GFP protein targeted to the cytoplasm and to the nuclei could also be able to reduce the PMMoV-I viral accumulation and could be able to rescue the abiotic stress, thus indicating that chloroplast localization is not required for viral inhibition and protection against biotic or abiotic stress.**

9. **Expression of *Cch* GrxS12 did not alter the pyridine nucleotide contents in the mock-inoculated control plants and thus it shows that *Cch* GrxS12-mediated PR gene expression in the mock-inoculated control plants at late stage of plant growth is independent of the pyridine nucleotide accumulation.**

10. **PMMoV-I infection accumulates high level of NADH and NADPH in all the transgenic lines and the increase in the level of NADH is a good marker for PMMoV-I infection.**

11. **Increased PMMoV-I resistance, high PR accumulation and increased level of NADH and NADPH in *Nb:Grx-GFP* line was associated with high level of *Cch* GrxS12-GFP accumulation in this line.**

12. **Expression of *Cch* GrxS12 did not alter the antioxidant enzymes mRNA accumulation of GR but it reduces the accumulation of GST mRNA at the late stage of viral infection.**

13. ***Cch* GrxS12 is not able to participate in the Fe-S cluster assembly mechanism as it could not be able to suppress the iron accumulation or restore the Fe-S containing enzyme activities in the yeast Δ*grx5* mutants.**

7.BIBLIOGRAPHY

Abbink, T.E., Peart, J.R., Mos, T.N., Baulcombe, D.C., Bol, J.F., and Linthorst, H.J. (2002). Silencing of a gene encoding a protein component of the oxygen-evolving complex of photosystem II enhances virus replication in plants. *Virology*. **295:** 307-319.

Achebach, S., Tran, Q.H., Vlamis-Gardikas, A., Mullner, M., Holmgren, A., and Unden, G. (2004). Stimulation of Fe–S cluster insertion into apoFNR by *E. coli* glutaredoxins 1, 2 and 3 *in vitro*. *FEBS Lett.* **565:** 203–206.

Ahlquist, P., Noueiry, A.O., Lee, W.M., Kushner, D.B., and Dye, B.T. (2003). Host factors in positive-Strand RNA virus genome replication. *J Virol.* **77:** 8181-8186.

.

Alonso, E., Garcia-Luque, I., de la Cruz, A., Wicke, B., Avila-Rincon, M.J., Serra, M.T., Castresana, C., and Diaz-Ruiz, J.R. (1991). Nucleotide sequence of the genomic RNA of pepper mild mottle virus, a resistance-breaking tobamovirus in pepper. *J Gen Virol.* **72:** 2875-2884.

Altschul, S.F., Madden, T.L., Schäffer, A.A., Zhang, J., Zhang, Z., Miller, W., and Lipman D.J. (1997). Gapped BLAST and PSI-BLAST: a new generation of protein database search programs. *Nucleic Acids Res.* **25:** 3389-3402.

Alvares, M.E., Pennell, R.I., Meijer, P.J., Ishikawa, A., Dixon, R.A., and Lamb, C. (1998). Reactive oxygen intermediates mediate a systemic signal network in the establishment of plant immunity. *Cell.* **92:** 773–784.

Amari, K., Díaz-Vivancos, P., Pallás, V., Sánchez-Pina, M.A., and Hernández, J.A. (2007). Oxidative stress induction by *Prunus necrotic ringspot virus* infection in apricot seeds. *Physiol Plant*. **131:** 302-310.

Ansel, D.C., Franklin, M.L.T., De Carvalho, M.H.C., Lameta, A.D.A., and Fodil, Y.Z. (2006). Glutathione reductase in leaves of cowpea: cloning of two cDNAs, expression and enzymatic activity under progressive drought stress desiccation and abscisic acid treatment. *Ann Bot.* **98:** 1279-1287.

Antignus, Y., Lachman, O., Pearlsman, M., Maslenin, L., and Rosner, A. (2008). A new pathotype of *pepper mild mottle virus* (PMMoV) overcomes the *L*4 resistance genotype of pepper cultivars. *Plant Dis*. **92:** 1033-1037.

Aslund, F., Ehn, B., Miranda-Vizuete, A., Pueyo, C., and Holmgren, A. (1994). Two additional glutaredoxins exist in *Escherichia coli*: glutaredoxin 3 is a hydrogen donor for ribonucleotide reductase in a thioredoxin/glutaredoxin 1 double mutant. *Proc Natl Acad Sci USA.* **91:** 9813–9817.

Asurmendi, S., Berg, R.H., Koo, J.C., and Beachy, R.N. (2004). Coat protein regulates formation of replication complexes during tobacco mosaic virus infection. *Proc Natl Acad Sci USA*. **101:** 1415-1420.

Auwerx, J., Isacsson, O., Söderlund, J., Balzarini, J., Johansson, M., and Lundberg M. (2009). Human glutaredoxin-1 catalyzes the reduction of HIV-1 gp120 and CD4 disulfides and its inhibition reduces HIV-1 replication. *Int J Biochem Cell Biol.* **41:** 1269-1275.

Ávila-Rincón, M.J., Ferrero, M.L., Alonso, E., Garcia-Luque, I., and Diaz-Ruiz, J.R. (1989). Nucleotide sequences of 5' and 3' non-coding regions of pepper mild mottle virus strain S RNA. *J Gen Virol.* **70:** 3025-3031.

Balk, J., and Lobreaux, S. (2005). Biogenesis of iron-sulfur proteins in plants. *Trends Plant Sci.* **10:** 324–331.

Bandyopadhyay, S., Gama, F., Molina-Navarro, M.M., Gualberto, J.M., Claxton, R., Naik, S.G., Huynh, B.H., Herrero, E., Jacquot, J.P., and Rouhier, N. (2008). Chloroplast monothiol glutaredoxins as scaffold proteins for the assembly and delivery of [2Fe–2S] clusters. *EMBO J.* **27:** 1122–1133

Bedhomme, M., Adamo, M., Marchand, C.H., Couturier, J., Rouhier, N., Lemaire, S.D., Zaffagnini, M., and Trost, P. (2012). Glutathionylation of cytosolic glyceraldehyde-3-phosphate dehydrogenase from the model plant *Arabidopsis thaliana* is reversed by both glutaredoxins and thioredoxins *in vitro*. *Biochem J.* **445:** 337–347.

Bedhomme, M., Zaffagnini, M., Marchand, C.H., Gao, X.H., Moslonka-Lefebvre, M., Michelet, L., Decottignies, P., and Lemaire, S.D. (2009). Regulation by glutathionylation of isocitrate lyase from *Chlamydomonas reinhardtii*. *J Biol Chem.* **284:** 36282–36291.

Berger, F., Ramirez–Hernandez, M.H., and Ziegler, M. (2004). The new life of a centenarian: signalling functions of NAD(P). *Trends Biochem Sci.* **29:** 111-118.

Berzal-Herranz, A., de la Cruz, A., Tenllado, F., Diaz-Ruiz, J.R., Lopez, L., Sanz, A.I., Vaquero, C., Serra, M.T., and Garcia-Luque, I. (1995). The *Capsicum* L^3 gene-mediated resistance against the tobamoviruses is elicited by the coat protein. *Virology.* **209:** 498-505.

Billeter, M.A., Weissman, C., and Warner, R.C. (1966). Replication of double stranded RNA from *Escherichia coli* infected with bacteriophage MS2. *J Mol Biol.* **17:**145-173.

Bonas, U., and Lahaye, T. (2002). Plant disease resistance triggered by pathogen-derived molecules: refined models of specific recognition. *Curr Opin Microbiol*. **4:** 44-50.

Bonzon, M., Simon, P., Greppin, H., and Wagner, E. (1983). Pyridine-nucleotides and redox charge evolution during the induction of flowering in spinach leaves. *Planta.* **159:** 254-260.

Boot, K.J.M., van der Zaal, B.J., Velterop, J., Quint, A., Mennes, A.M., Hooykaas, P.J.J., and Libbenga, K.R. (1993). Further characterization of expression of auxin-induced genes in tobacco *(Nicotiana tabacum)* cell-suspension cultures. *Plant Physiol.* **102:** 513-520.

Boukema, I.W., Janse, K., and Hofman, K. (1980). Presented in the *Eucarpia Capsicum Working Group,* Synopses of the 4th meeting, Wageningen.

Boukema, I.W. (1982). Resistance to TMV in *Capsicum chacoense* Hunz is governed by an allele of the *L*-locus. *Capsicum Newsl.* **3:** 47-48.

Buck, K.W. (1996). Comparison of the replication of positive-stranded RNA viruses of plants and animals. *Adv Virus Res.* **47:** 159–251.

Bushweller, J.H., Aslund, F., Wuthrich, K., and Holmgren, A. (1992*).* Structural and functional characterization of the mutant *Escherichia coli* glutaredoxin (C14-S) and its mixed disulfide with glutathione. *Biochemistry.* **31:** 9288–9293.

Cacas, J.L., Vailleau, F., Davoine, C., Ennar, N., Agnel, J.P., Tronchet, M., Ponchet, M., Blein, J.P., Roby, D., Triantaphylides, C., and Montillet, J.L. (2005). The combined action of 9 lipoxygenase and galactolipase is sufficient to bring about programmed cell death during tobacco hypersensitive response. *Plant Cell Environ.* **28:** 1367-1378.

Carrington, J.C., Kasschau, K.D., Mahajan, S.K., and Schaad, M.C. (1996). Cell-to-cell and long-distance transport of viruses in plants. *Plant Cell.* **8:** 1669-1681.

Chaerle, L., Pineda, M., Romero-Aranda, R., Van Der Straeten, D., and Barón, M. (2006). Robotized thermal and chlorophyll-fluorescence imaging of pepper mild mottle virus infection in *Nicotiana benthamiana. Plant Cell Physiol.* **47:** 1323-1336.

Chen, M.H., Sheng, J., Hind, G., Handa, A., and Citovsky, V. (2000). Interaction between the tobacco mosaic virus movement protein and host cell pectin methylesterases is required for viral cell-to-cell movement. *EMBO J.* **19:** 913–920.

Chen, M.H., Tian, G.W., Gafni, Y., and Citovsky, V. (2005). Effects of calreticulin on viral cell-to-cell movement. *Plant Physiol.* **138:** 1866-1876.

Chen, W., and Singh, K.B. (1999). The auxin, hydrogen peroxide and salicylic acid induced expression of the *Arabidopsis* GST6 promoter is mediated in part by an ocs element. *Plant J.* **19:** 667–677.

Chen, Y.P., Xing, L.P., Wu, G.J., Wang, H.Z., Wang, X.E., Cao, A.Z., and Chen, P.D. (2007). Plastidial glutathione reductase from *Haynaldia villosa* is an enhancer of powdery mildew resistance in wheat (*Triticum aestivum*). *Plant Cell Physiol.* **48:** 1702–1712.

Chenchik, A., Zhu, Y.Y., Diatchenko, L., Li, R., Hill, J., and Siebert, P.D. (1998). Gene cloning and analysis by RT-PCR. Siebert P., Larrick J., editors. Natick, MA*: BioTechniques Books,* 305-319.

Chen, M.H., and Citovsky, V. (2003). Systemic movement of a tobamovirus requires host cell pectin methylesterase. *Plant J***. 35:** 386-392.

Cheng, N.H. (2008). AtGRX4, an *Arabidopsis* chloroplastic monothiol glutaredoxin, is able to suppress yeast grx5 mutant phenotypes and respond to oxidative stress. *FEBS Lett.* **582:** 848–854.

Cheng, N.H., Liu, J.Z., Brock, A., Nelson, R.S., and Hirschi, K.D. (2006). AtGRXcp, an *Arabidopsis* chloroplastic glutaredoxin, is critical for protection against protein oxidative damage, *J Biol Chem.* **281:** 26280–26288.

Cheng, N.H., Liu, J.Z., Liu, X., Wu, Q., Thompson, S.M., Lin, J., Chang, J., Whitham, S.A., Park, S., Cohen, J.D., and Hirschi, K.D. (2011). *Arabidopsis* monothiol glutaredoxin, AtGRXS17, is critical for temperature-dependent postembryonic growth and development via modulating auxin response. *J Biol Chem*. **286:** 20398–20406.

Chomczynski. P., and Sacchi. N. (1987). Single-step method of RNA isolation by acid guanidinium thiocyanate-phenol-chloroform extraction. *Anal Biochem.* **162:** 156-159.

Chrisholm, S.T., Coaker, G., Day, B., and Staskawickz, B.J. (2006). Host-microbe interactions: shaping the evolution of the plant immune response. *Cell.* **124:** 803-814.

Citovsky, V., Knorr, D., Schuster, G., and Zambryski, P. (1990). The P30 movement protein of tobacco mosaic virus is a single-strand nucleic acid binding protein. *Cell.* **60:** 637-647.

Citovsky, V., Wong, M.L., Shaw, A.L., Prasad, B.V., and Zambryski, P. (1992). Visualization and characterization of tobacco mosaic virus movement protein binding to single-stranded nucleic acids. *Plant Cell.* **4:** 397-411.

Collinson, E.J., and Grant, C.M. (2003). Role of yeast glutaredoxins as glutathione S-transferases. *J Biol Chem.* **278:** 22492-22497.

Collinson, E.J., Wheeler, G.L., Garrido, E.O., Avery, A.M., Avery, S.V., and Grant, C.M. (2002). The yeast glutaredoxins are active as glutathione peroxidases. *J Biol Chem*. **277:** 16712–16717.

Colson, P., Richet, H., Desnues, C., Balique, F., Moal, V., Grob, J.J., Berbis, P., Lecoq, H., Harle, J.R., Berland, Y., and Raoult, D. (2010). Pepper mild mottle virus, a plant virus associated with specific immune responses, fever, abdominal pains, and pruritus in humans. *PLoS One.* **5:** e10041.

Couturier, J., Jacquot, J.P., and Rouhier, N. (2009a). Evolution and diversity of glutaredoxins in photosynthetic organisms. *Cell Mol Life Sci.* **66:** 2539–2557.

Couturier, J., Koh, C.S., Zaffagnini, M., Winger, A.M., Gualberto, J.M., Corbier, C., Decottignies, P., Jacquot, J.P., Lemaire, S.D., Didierjean, C., and Rouhier, N. (2009b). Structure–function relationship of the chloroplastic glutaredoxin S12 with an atypical WCSYS active site. *J Biol Chem.* **284:** 9299–9310.

Couturier, J., Stroher, E., Albetel, A.N., Roret, T., Muthuramalingam, M., Tarrago, L., Seidel, T., Tsan, P., Jacquot, J.P., Johnson, M.K., Dietz, K.J., Didierjean, C., and Rouhier, N. (2011). *Arabidopsis* chloroplastic glutaredoxin C5 as a model to explore the molecular determinants for iron-sulfur cluster binding into glutaredoxins. *J Biol Chem.* **286:** 27515–27527.

Creissen, G.P., Mullineaux, P.M. (1995). Cloning and characterisation of glutathione reductase cDNAs and identification of two genes encoding the tobacco enzyme. *Planta.* **197:** 422-425.

Culver, J. N., and Dawson, W.O. (1989). Tobacco mosaic virus coat protein: an elicitor of the hypersensitive reaction but not required for the development of mosaic symptoms in *Nicotiana sylvestris*. *Virology.* **173:** 755-758

Culver, J.N. (2002). Tobacco mosaic virus assembly and disassembly: determinants in pathogenicity and resistance. *Annu Rev Phytopathol*. **40:** 287-308.

Cummins, I., Dixon, D.P., Freitag-Pohl, S., Skipsey, M., and Edwards, R. (2011). Multiple roles for plant glutathione transferases in xenobiotic detoxification. *Drug Metab Rev*. **43:** 266–280.

Dalton, D.A., Boniface, C., Turner, Z., Lindashl, A., Kim, H.J., Jelinek, L., Govindarajulu, M., Finger, R.E., and Taylor, C.G. (2009). Physiological roles of glutathione S-transferases in soybean root nodules. *Plant Physiol.* **150:** 521-530.

Dangl, J.L., and Jones, J.D.G. (2001). Plant pathogens and integrated defence responses to infection. *Nature*. **411:** 826–833.

Dardick, C.D., Taraporewala, Z., Lu, B., and Culver, J.N. (1999). Comparison of tobamovirus coat protein structural features that affect elicitor activity in pepper, eggplant, and tobacco. *Mol Plant Microbe Interact.* **12:** 247-251.

Dawson, D.O., Bubrick, P., and Grantham, G.L. (1988). Modifications of the tobacco mosaic virus coat protein gene affect replication, movement and symptomatology. *Phytopathology.* **78:** 783-789.

Day, D.A., and Wiskich, J.T. (1981). Glycine metabolism and oxalacetate transport by pea leaf mitochondria. *Plant Physiol*. **68:** 425–429.

Deom, C.M., Oliver, M.J., and Beachy, R.N. (1987). The 30-kilodalton gene product of tobacco mosaic virus potentiates virus movement. *Science.* **237:** 389-394.

Desender, S., Andrivon, D., and Val, F. (2007). Activation of defence reactions in *Solanaceae* where is the specificity? *Cell Microbiol*. **9:** 21-30.

Ding, X.S., Liu, J., Cheng, N.H., Folimonov, A., Hou, Y.M., Bao, Y., Katagi, C., Carter, S.A., and Nelson, R.S. (2004). The Tobacco mosaic virus 126-kDa protein associated with virus replication and movement suppresses RNA silencing. *Mol Plant Microbe Interact.* **17:** 583-592.

Dixon, D.P., and Edwards, R. (2010). Glutathione *S*-transferases. *The Arabidopsis Book* **8**, e0131. doi/full/10.1199/tab.0131

Djebbar, R., Rzigui, T., Pétriacq, P., Mauve, C., Priault, P.O., Fresneau, C., De Paepe, M., Florez-Sarasa, I., Benhassaine-Kesri, G., Streb, P., Gakière, B., Cornic, G. and De Paepe, R. (2012). Respiratory complex I deficiency induces drought tolerance by impacting leaf stomatal and hydraulic conductances. *Planta.* **235:** 603–614.

Dorokhov, Y.L., Makinen, K., Frolova, O.Y., Merits, A., Saarinen, J, Kalkkinen, N., Atabekov, J.G., and Saarma, M. (1999). A novel function for a ubiquitous plant enzyme pectin methylesterase: the host-cell receptor for the tobacco mosaic virus movement protein. *FEBS Lett.* **461:** 223–228.

Douglas, K.T. (1987). "Mechanism of action of glutathione-dependent enzymes". *Adv Enzymol Relat Areas Mol Biol.* **59:** 103–167.

Dunigan, D.D., and Zaitlin, M. (1990). Capping of tobacco mosaic virus RNA. Analysis of viral-coded guanylyltransferase-like activity. *J Biol Chem*. **265:** 7779-7786.

Dutilleul, C., Garmier, C., Noctor, G., Mathieu, C., Chétrit, P., Foyer, C.H., and De Paepe, R. (2003). Leaf mitochondria modulate whole cell redox homeostasis, set antioxidant capacity, and determine stress resistance through altered signaling and diurnal regulation. *Plant Cell.* **15:** 1212–1226.

Dutilleul, C., Lelarge, C., Prioul, J.L., De Paepe, R., Foyer, C.H., and Noctor, G. (2005). Mitochondria-driven changes in leaf NAD status exert a crucial influence on the control of nitrate assimilation and the integration of carbon and nitrogen metabolism. *Plant Physiol.* **139:** 64- 78.

Elvira, M.I., Galdeano, M.M., Gilardi, P., Garcia-Luque, I., and Serra, M.T. (2008). Proteomic analysis of pathogenesis-related proteins (PRs) induced by compatible and incompatible interactions of pepper mild mottle virus (PMMoV) in *Capsicum chinense L*[3] plants. *J Exp Bot.* **59:** 1253-1265.

Emanuelsson, O., Nielsen, H., and von Heijne, G. (1999). ChloroP, a neural network-based method for predicting chloroplast transit peptides and their cleavage sites. *Protein Sci.* **8:** 978-984.

Eyidogan, F., and Oz, M.T. (2007). Effect of salinity on antioxidant responses of chickpea seedlings. *Acta Physiol Plant*. **29:** 485-493.

Fernandes, A.P., Fladvad, M., Berndt, C., Andresen, C., Lillig, C.H., Neubauer, P., Sunnerhagen, M., Holmgren, A., and Vlamis-Gardikas, A. (2005). A novel monothiol glutaredoxin (GRX4) from *Escherichia coli* can serve as a substrate for thioredoxin reductase. *J Biol Chem.* **280:** 24544–24552.

Finkemeier, I., Goodman, M., Lamkemeyer, P., Kandlbinder, A., Sweetlove, L.J., and Dietz, K.J. (2005). The mitochondrial type II peroxiredoxin F is essential for redox homeostasis and root growth of *Arabidopsis thaliana* under stress. *J Biol Chem.* **280:** 12168–12180.

Fish, W.W. (1988). Rapid colorimetric micromethod for the quantitation of complexed iron in biological samples. *Methods Enzymol.* **158:** 357–364.

Fodor, J., Gullner, G., Ádám, A.L., Barna, B., Kömives, T. and Király, Z. (1997). Local and systemic responses of antioxidants to tobacco mosaic virus infection and to salicylic acid in tobacco: Role in systemic acquired resistance. *Plant Physiol.* **114:** 1443–1451.

Foyer, C.H., and Noctor, G. (2003). Redox sensing and signaling associated with reactive oxygen in chloroplasts, peroxisomes and mitochondria. *Physiol Plant.* **119:** 355-364.

Fraile, A., Pagán, I. Anastasio, G., Sáez, E., and García-Arenal, F. (2011). Rapid genetic diversification and high fitness penalties associated with pathogenicity evolution in a plant virus. *Mol Biol Evol.* **28:** 1425-1437.

Fu, Z.Q., and Dong, X. (2013). Systemic acquired resistance: Turning local infection into global defense. *Annu Rev Plant Biol.* **64:** 839-863.

Gallie, D.R. (1996). Translational control of cellular and viral mRNAs. *Plant Mol Biol.* **32:** 145-158.

Gallie, D.R., and Walbot, V. (1992). Identification of the motifs within the tobacco mosaic virus 5'-leader responsible for enhancing translation. *Nucleic Acids Res.* **20:** 4631-4638.

Gao, X., Starr, J., Göbel, C., Engelberth, J., Feussner, I., Tumlinson, J., and Kolomiets, M. (2008). Maize 9-lipoxygenase ZmLOX3 controls development, root-specific expression of defense genes, and resistance to root-knot nematodes. *Mol Plant Microbe Interact*. **21:** 98–109.

Gao, X.H., Zaffagnini, M., Bedhomme, M., Michelet, L., Cassier-Chauvat, C., Decottignies, P., and Lemaire, S.D. (2010). Biochemical characterization of glutaredoxins from *Chlamydomonas reinhardtii*: kinetics and specificity in deglutathionylation reactions. *FEBS Lett.* **584:** 2242–2248.

Garcia-Luque, I., Serra, M.T., Alonso, E., Wicke, B., Ferrero, M.L., and Diaz-Ruiz, J.R. (1990). Characterization of a Spanish Strain of Pepper Mild Mottle Virus (PMMoV-S) and its relationship to other tobamoviruses. *J Phytophathol.* **129:** 1-8.

García-Marcos, A., Pacheco, R., Manzano, A., Aguilar, E., and Tenllado, F. (2013). Oxylipin biosynthesis genes positively regulate programmed cell death during compatible infections with the synergistic pair *Potato Virus X-Potato Virus Y* and *Tomato Spotted Wilt Virus*. *J Virol.* **87:** 5769-5783.

García-Marcos, A., Pacheco, R., Martiáñez, J., González-Jara, P., Díaz-Ruíz, J.R., and Tenllado, F. (2009). Transcriptional changes and oxidative stress associated with the synergistic interaction between *Potato virus X* and *Potato virus Y* and their relationship with symptom expression. *Mol Plant Microbe Interact.* **22:** 1431–1444.

Ge, X., Li, G.-J., Wang, S.-B., Zhu, H., Zhu, T., Wang, X. and Xia, Y. (**2007).** AtNUDT7, a negative regulator of basal immunity in *Arabidopsis*, modulates two distinct defense response pathways and is involved in maintaining redox homeostasis. *Plant Physiol.* **145:** 204–215.

Genda, Y., Kanda, A., Hamada, H., Sato, K., Ohnishi, J., and Tsuda, S. (2007). Two amino acid substitutions in the coat protein of pepper mild mottle virus are responsible for overcoming the L^4 gene-mediated resistance in *Capsicum* spp. *Phytopathology.* **97:** 787-793.

Gera, A., Deom, C.M., Donson, J., Shaw, J.J., Lewandowski, D., and Dawson, D.O. (1995). Tobacco mosaic tobamovirus does not require concomitant synthesis of movement protein during vascular transport. *Mol Plant Microbe Interact.* **8:** 784-787.

Gibon, Y., Blaesing, O.E., Hannemann, J., Carillo, P., Hohne, M., Hendriks, J.H.M., Palacios, N., Cross, J., Selbig, J., and Stitt, M. (2004). A robot-based platform to measure multiple enzyme activities in *Arabidopsis* using a set of cycling assays: comparison of changes in enzyme activities and transcript levels during diurnal cycles and in prolonged darkness. *Plant Cell*. **16:** 3304–3325.

Gilardi, P. (2000). Análisis de los inductores virales en la resistencia frente a tobamovirus en plantas del género *Capsicum*. phD Thesis, Universidad Complutense de Madrid (UCM).

Gilardi, P., García-Luque, I., and Serra, M.T. (1998). Pepper mild mottle virus coat protein alone can elicit the *Capsicum spp*. L^3 gene-mediated resistance. *Mol Plant Microbe Interact.* **11:** 1253-1257.

Gilardi, P., Garcia-Luque, I., and Serra, M.T. (2004). The coat protein of tobamovirus acts as elicitor of both L^2 and L^4 gene-mediated resistance in *Capsicum*. *J Gen Virol*. **85:** 2077-2085.

Gilardi, P., Wicke, B., Castillo, S., de la Cruz, A., Serra, M.T., and García-Luque, I. (1999). Resistance in *Capsicum spp*. against the tobamoviruses. In: Pandalai SG (ed) *Recent research developments in virology,* vol 1. Transworld Research Network, India, pp 547–558.

Gill, S.C., and von Hipple, P.H. (1989). Calculation of protein extinction coefficients from amino acid sequence data. *Anal Biochem.* **182:** 319-326.

Glazebrook, J. (2005). Contrasting mechanisms of defense against biotrophic and necrotrophic pathogens. *Ann Rev Phytopathol.* **43:** 205–227.

Göbel, C., Feussner, I., Hamberg, M., and Rosahl, S. **(2002).** Oxylipin profiling in pathogen-infected potato leaves. *Biochim Biophys Acta.* **1584:** 55–64.

Goldbach, R., Bucher, E., and Prins, M. (2003). Resistance mechanisms to plant viruses: an overview. *Virus Res.* **92:** 207-212.

Goodman, R.N., Király, Z., and Wood, K.R. (1986). The biochemistry and physiology of plant disease. University of Missouri Press. Columbia.

Goregaoker, S.P., and Culver, J.N. (2003). Oligomerization and activity of the helicase domain of the tobacco mosaic virus 126- and 183-kilodalton replicase proteins. *J Virol*. **77:** 3549-3556.

Goregaoker, S.P., Lewandowski, D.J., and Culver, J.N. (2001). Identification and functional analysis of an interaction between domains of the 126/183-kDa replicase-associated proteins of tobacco mosaic virus. *Virology.* **282:** 320-328.

Greenberg, J.T., and Yao, N. (2004). The role and regulation of programmed cell death in plant-pathogen interactions. *Cell Microbiol.* **6:** 201-211.

Gullner, G., Künstler, A., Király, L., Pogány, M., and Tobia, I. (2010). Up-regulated expression of lipoxygenase and divinyl ether synthase genes in pepper leaves inoculated with Tobamoviruses. *Physiol Mol Plant Pathol.* **74:** 387–393.

Guo, Y., Huang, C., Xie, Y., Song, F., and Zhou, X. (2010). A tomato glutaredoxin gene SlGRX1 regulates plant responses to oxidative, drought and salt stresses. *Planta*. **232:** 1499-1509.

Hakmaoui, A., Pérez-Bueno, M.L., García-Fontana, B., Camejo, D., Jiménez, A., Sevilla, F., and Barón, M. (2012). Analysis of the antioxidant response of *Nicotiana benthamiana* to infection with two strains of *Pepper mild mottle virus*. *J Exp Bot*. **63:** 5487-5496.

Hajirezaei, M-R., Peisker, M., Tschiersch, H., Palatnik, J.F., Valle, E.M., Carrillo, N. and Sonnewald. U. (2002). Small changes in the activity of choroplastic $NADP^+$-dependent ferredoxin oxidoreductase lead to impaired plant growth and restrict photosynthetic activity of transgenic tobacco plants. *Plant J.* **29:** 281-293.

Hammerschmidt, R. (2009). Systemic acquired resistance. *Adv Bot Res*. **51:** 173–222.

Hamza, I.A., Jurzik, L., Uberla, K., and Wilhelm, M. (2011). Evaluation of pepper mild mottle virus, human picobirnavirus and Torque teno virus as indicators of fecal contamination in river water. *Water Res*. **45:** 1358-1368.

Hanahan, D. (1983). Studies on transformation of *Escherichia coli* with plasmids. *J Mol Biol.* **166:** 557-580.

Harries, P.A., Schoelz, J.E., and Nelson, R.S. (2010). Intracellular transport of viruses and their components: utilizing the cytoskeleton and membrane highways. *Mol Plant Microbe Interact.* **23:** 1381-1393.

Heineke, D., Riens, B., Grosse, H., Hoferichter, P., Peter, U., Flügge ,U.I., and Heldt, H.W. (1991). Redox transfer across the inner chloroplast envelope membrane. *Plant Physiol*. **95:** 1131-1137.

Heinlein, M., Padgett, H.S., Gens, J.S., Pickard, B.G., Casper, S.J., Epel, B.L., and Beachy, R.N. (1998). Changing patterns of localization of the tobacco mosaic virus movement protein and replicase to the endoplasmic reticulum and microtubules during infection. *Plant Cell.* **10:** 1107-1120.

Herrero, E., and de la Torre-Ruiz, M.A. (2007). Monothiol glutaredoxins: a common domain for multiple functions. *Cell Mol Life Sci.* **64:** 1518–1530.

Hirashima, K., and Watanabe, Y. (2001). Tobamovirus replicase coding region is involved in cell-to-cell movement. *J Virol.* **75:** 8831-8836.

Hirashima, K., and Watanabe, Y. (2003). RNA helicase domain of tobamovirus replicase executes cell-to-cell movement possibly through collaboration with its nonconserved region. *J Virol.* **77:** 12357-12362.

Holmgren, A. (1976). Hydrogen donor system for *E. coli* ribonucleotide diphosphate reductase dependent upon glutathione. *Proc Natl Acad Sci USA*. **73:** 2275-2279.

Holmgren, A. (1985). Thioredoxin. *Annu Rev Biochem.* **54:** 237-271.

Holmgren, A. (1995). Thioredoxin structure and mechanism: conformational change on oxidation of the active-site sulfhydryls to a disulfide. *Structure.* **15:** 15.

Holmgren, A., and Åslund, F. (1995). Glutaredoxin. *Methods Enzymol*. **252**: 283-292.

Holmgren, A. (2000). Antioxidant function of thioredoxin and glutaredoxin systems. *Antioxid Redox Signal***. 2:** 811-820.

Holt, C.A., and Beachy, R.N. (1991). In vivo complementation of infectious transcripts from mutant tobacco mosaic virus cDNAs in transgenic plants. *Virology*. **181:** 109-117.

Hon, W.C., Griffith, M., Mlynarz, A., Kwok, Y.C., and Yang, D.S.C. (1995). Antifreeze proteins in winter rye are similar to pathogenesis related proteins. *Plant Physiol.* **109:** 879–889.

Hull, R. (2002). Matthews' Plant Virology, 4th edition ed. Academic Press, New York.

Hunt, L., and Gray, J.E. (2009). The relationship between pyridine nucleotides and seed dormancy. *New Phytol.* **181:** 62-70.

Hunt, L., Lerner, F., and Ziegler, M. (2004). NAD-New roles in signaling and gene regulation in plants. *New Phytol.* **163:** 31–44.

Hwang I.S., and Hwang, B.K. (2010). The pepper 9-lipoxygenase gene *CaLOX1* functions in defense and cell death responses to microbial pathogens. *Plant Physiol.* **152:** 948–967.

Igamberdiev, A.U., and Gardestro, M.P. (2003). Regulation of NAD- and NADP-dependent isocitrate dehydrogenases by reduction of levels of pyridine nucleotides in mitochondria and cytosol of pea leaves. *Biochim Biophys Acta*. **1606:** 117–125.

Ikegashira, Y., Ohki, T., Ichiki, U., Higashi, T., Hagiwara, K., Omura, T., Honda, Y., and Tsuda, S. (2004). An immunological system for the detection of Pepper mild mottle virus in soil from green pepper fields. *Plant Dis*. **88:** 650-656.

Ishibashi, K., Nishikiori, M., and Ishikawa, M. (2010). Interactions between tobamovirus replication proteins and cellular factors: their impacts on virus multiplication. *Mol Plant Microbe Interact.* **23**: 1413-1419.

Ishikawa, M., Meshi, T., Motoyoshi, F., Takamatsu, N., and Okada, Y. (1986). *In vitro* mutagenesis of the putative replicase genes of tobacco mosaic virus. *Nucleic Acids Res.* **14:** 8291-8305.

Ito, T., and Meyerowitz, E.M. (2000). Overexpression of a gene encoding a cytochrome P450, CYP78A9, induces large and seedless fruit in *Arabidopsis. Plant Cell.* **12:** 1541-1550.

Jain, M., Ghanashyam, C., and Bhattacharjee, A. (2010). Comprehensive expression analysis suggests overlapping and specific roles of rice glutathione S-transferase genes during development and stress responses. *BMC Genomics.* **11:** 73.

Jambunathan, N., and Mahalingam, R. (2006). Analysis of *Arabidopsis* Growth Factor Gene 1 (GFG1) encoding a nudix hydrolase during oxidative signaling. *Planta.* **224:** 1-11.

Johnson, G.P., Goebel, S.J., Perkus, M.E., Davis, S.W., Winslow, J.P., and Paoletti, E. (1991). Vaccinia virus encodes a protein with similarity to glutaredoxins. *Virology.* **181:** 378–381.

Johnson, M.K., and Smith, A.D. (2005). Iron-sulfur proteins. Encyclopedia of Inorganic chemistry. 2589–2619.

Jones, J.D.G., and Dangl, J.L. (2006). The plant immune system. *Nature.* **444:** 323–329.

Journet, E.P., Neuburger, M., and Douce, R. (1981). Role of glutamate-oxaloacetate transaminase and malate dehydrogenase in the regeneration of NAD^+ for glycine oxidation by spinach leaf mitochondria. *Plant Physiol* .**67:** 467–469.

Juang, C.H., and Thomas, J.A. (1996). S-glutathiolated hepatocyte proteins and insulin disulfides as substrates for reduction by glutaredoxin, thioredoxin, protein disulfide isomerase, and glutathione. *Arch Biochem Biophys.* **335:** 61–72.

Kaiser, C., Michaelis, S., and Mitchell, A. (1994). Methods in Yeast Genetics, a Cold Spring Harbor Laboratory course manual, Cold Spring Harbor Laboratory Press, Cold Spring Harbor,N.Y..

Ketterer, B., Meyer, D., and Clark, A.G. (1988). Soluble glutathione transferase isozymes. In H Sies, B Ketterer, eds, Glutathione Conjugation.Academic Press, London, pp 73-135.

Kolomiets, M.V., Hannapel, D.J., Chen, H., Tymeson, M., and Gladon, R.J. (2001). Lipoxygenase is involved in the control of potato tuber development. *Plant Cell.* **13:** 613–626.

Koonin, E.V., and Dolja, V.V. (1993). Evolution and taxonomy of positive strand RNA viruses: implications of comparative analysis of amino acid sequences. *Crit Rev Biochem Mol Biol*. **28:** 375-430.

Kornyeyev, D., Logan, B.A., Payton, P.R., Allen R. D., and Holaday, A.S. (2003). Elevated chloroplastic glutathione reductase activities decrease chilling-induced photoinhibition by increasing rates of photochemistry, but not thermal energy dissipation, in transgenic cotton. *Funct Plant Biol.* **30:** 101-110.

Krieger-Liszkay, A., Kos, P.B., and Hideg, E. (2011). Superoxide anion radicals generated by methylviologen in photosystem I damage photosystem II. *Physiol Plant.* **142:** 17-25.

Kubota, K., Tsuda, S., Tamai, A., and Meshi, T. (2003). Tomato mosaic virus replication protein suppresses virus-targeted posttranscriptional gene silencing. *J Virol.* **77:** 11016-11026.

Kuzniak, E., and Sklodowska M. (2005). Compartment-specific role of the ascorbate–glutathione cycle in the response of tomato leaf cells to *Botrytis cinerea* infection. *J Exp Bot*. **56:** 921–933.

La Camera, S., L'haridon, F., Astier, J., Zander, M., Abou-Mansour, E., Page, G., Thurow, C., Wendehenne, D., Gatz, C., Métraux, J.P., and Lamotte, O. (2011). The glutaredoxin ATGRXS13 is required to facilitate *Botrytis cinerea* infection of *Arabidopsis thaliana* plants. *Plant J.* **68:** 507-519.

Laemmli, U.K. (1970). Cleavage of structural proteins during the assembly of the head of bacteriophage T4. *Nature.* **227:** 680-685.

Laporte, D., Olate, E., Salinas, P., Salazar, M., Jordana, X., and Holuigue, L. (2012). Glutaredoxin GRXS13 plays a key role in protection against photo-oxidative stress in *Arabidopsis*. *J Exp Bot*. **63:** 503–515.

Lartey, R.T., Ghoshroy, S. and Citovsky, V. (1998). Identification of an *Arabidopsis thaliana* mutation (vsm1) that restricts systemic movement of tobamoviruses. *Mol Plant Microbe Interact.* **11:** 706–709.

Leisner, S.M., and Turgeon, R. (1993). Movement of virus and photoassimilate in the phloem: a comparative analysis. *Bioessays.* **15:** 741-748.

Lemaire, S.D. (2004). The glutaredoxin family in oxygenic photosynthetic organisms. *Photosynth Res.* **79:** 305–318.

León, A.M., Palma, J.M., Corpas, F.J., Gomez, M., Romeropuertas, M.C., Chatterjee, D., Mateos, R.M., Del Rio, L.A., and Sandalio, L.M. (2002). Antioxidative enzymes in cultivars of pepper plants with different sensitivity to cadmium. *Plant Physiol Biochem*. **40:** 813-820.

Levine, A., Tenhaken, R., Dixon, R., and Lamb, C. (1994). H_2O_2 from the oxidative burst orchestrates the plant hypersensitive disease resistance response. *Cell.* **79:** 583–593.

Lewandowski, D.J., and Dawson, W.O. (2000). Functions of the 126- and 183-kDa proteins of tobacco mosaic virus. *Virology.* **271:** 90-98.

Li, K., Hein, S., Zou, W., and Klug, G. **(2004).** The glutathione-glutaredoxin system in *Rhodobacter capsulatus*: part of a complex regulatory network controlling defense against oxidative stress. *J Bacteriol*. **186:** 6800–6808.

Li, S., Lauri, A., Ziemann, M., Busch, A., Bhave, M., and Zachgo, S. (2009). Nuclear activity of ROXY1, a glutaredoxin interacting with TGA factors, is required for petal development in *Arabidopsis thaliana*. *Plant Cell.* **21:** 429–441.

Li, L., Cheng, N., Hirschi, K.D., and Wang, X. (2010). Structure of *Arabidopsis* monothiol glutaredoxin AtGRXcp. *Acta crystallogr D*. **66:** 725-732.

Liang, P., and Pardee, A.B. (1992). Differential display of eukaryotic messenger RNA by means of the polymerase chain reaction. *Science.* **257:** 967-971.

Lieberherr D., Wagner U., Dubuis P.H., Métraux J.P., and Mauch, F. (2003). The rapid induction of glutathione S-transferases *At*GSTF2 and *At*GSTF6 by avirulent *Pseudomonas syringae* is the result of combined salicylic acid and ethylene signaling. *Plant Cell Physiol.* **44:** 750–757.

Lillig, C.H., Berndt, C., and Holmgren, A. (2008). Glutaredoxin systems. *Biochim Biophys Acta.* **1780:** 1304–1317.

Liu, C., and Nelson, R. S. (2013). The cell biology of *Tobacco mosaic virus* replication and movement. *Front Plant Sci*. doi**:** 10.3389/fpls.2013.00012.

López, M.A., Vicente, J., Kulasekaran, S., Vellosillo, T., Martínez, M., Irigoyen, M.L., Cascón, T., Bannenberg, G., Hamberg, M., and Castresana, C. (2011). Antagonistic role of 9-lipoxygenase derived oxylipins and ethylene in the control of oxidative stress, lipid peroxidation and plant defence. *Plant J.* **67:** 447–458.

Lotan, T., Ori, N., and Fluhr, R. (1989). Pathogenesis-related proteins are developmentally regulated in tobacco flowers. *Plant Cell.* **1:** 881–887.

Lucas, W.J., and Gilbertson, R.L. (1994). Plasmodesmata in relation to viral movement within leaf tissues. *Annu Rev Phytopathol.* **32:** 387-411.

Matsumoto, K., Johnishi, K., Hamada, H., Sawada, H., Takeuchi, S., Kobayashi, K. Suzuki, K., and Hikichi, Y. (2009). Single amino acid substitution in the methyltransferase domain of *Paprika mild mottle virus* replicase proteins confers the ability to overcome the high temperature-dependent *Hk* gene-mediated resistance in *Capsicum* plants. *Virus Res.* **140:** 98-102.

Mahalingam, R., and Fedoroff, N. (2003). Stress response, cell death and signaling: the many faces of reactive oxygen species. *Physiol Plant*. **119:** 56–68.

Mannervik, B., and Danielson, U.H. (1988). Glutathione transferases structure and catalytic activity. *Crit Rev Biochem.* **23:** 283-337.

Marathe, R., Guan, Z., Anandalakshmi, R., Zhao, H., and Dinesh-Kumar, S.P. (2004). Study of *Arabidopsis thaliana* resistome in response to cucumber mosaic virus infection using whole genome microarray. *Plant Mol Biol.* **55:** 501-520.

Marrs, A.M. (1996). The functions and regulation of glutathione S-transferases in plants. *Annu Rev Plant Physiol Plant Mol Biol.* **47:**127–58.

Martin, J.L. (1995). Thioredoxin: A fold for all reasons. *Structure*. **3:** 245-250.

Mas, P., and Beachy, R.N. (1999). Replication of tobacco mosaic virus on endoplasmic reticulum and role of the cytoskeleton and virus movement protein in intracellular distribution of viral RNA. *J Cell Biol.* **147:** 945-958.

Mauch, F., and Dudler, R. (1993). Differential induction of distinct glutathione-S-transferases of wheat by xenobiotics and by pathogen attack. *Plant Physiol*. **102:** 1193–1201.

Maule, A., Leh. V., and Lederer, C. (2002). The dialogue between viruses and hosts in compatible interactions. *Curr Opin Plant Biol.* **5:** 279-284.

McLean B.G., Zupan J., and Zambryski, P.C. (1995). Tobacco mosiac virus movement protein associates with the cytoskeleton in tobacco cells. *Plant Cell.* **7:** 2101–2114.

Meister, A., and Anderson, M.E. (1983). Glutathione. *Annu Rev Biochem.* **52:** 711–760.

Mesecke, N., Spang, A., Deponte, M., and Herrmann, J.M. (2008). A novel group of glutaredoxins in the cis-Golgi critical for oxidative stress resistance. *Mol Biol Cell*. **19:** 2673–2680.

Mesecke, N., Mittler, S., Eckers, E., Herrmann, J.M., and Deponte, M. (2010). Two novel monothiol glutaredoxins from *Saccharomyces cerevisiae* provide further insight into iron–sulfur cluster binding, oligomerization, and enzymatic activity of glutaredoxins. *Biochemistry.* **47:** 1452–1463.

Meshi, T., Watanabe, Y., Saito, T., Sugimoto, A., Maeda, T., and Okada, Y. (1987). Function of the 30 kd protein of tobacco mosaic virus: involvement in cell-to-cell movement and dispensability for replication. *EMBO J*. **6:** 2557–2563.

Meyer, Y., Buchanan, B.B., Vignols, F., and Reichheld, J.P. (2009). Thioredoxins and glutaredoxins: unifying elements in redox biology. *Ann Rev Genet.* **43:** 335–367.

Millar, H., Considine, M.J., Day, A.A., and Whelan, J. (2001). Unraveling the role of mitochondria during oxidative stress in plants. *IUBMB Life.* **51:** 201–205.

Minakuchi, K., Yabushita, T., Masumara, T., Ichihara, K., and Kunisuke, T. (1994). Cloning and analysis of a cDNA encoding rice glutaredoxin. *FEBS Lett.* **337:** 157-160.

Molina-Galdeano, M. (2006). El virus del moteado suave del pimiento (PMMoV): Análisis del efecto de la temperatura sobre la acumulación viral y la respuesta vegetal. PhD thesis. Universidad Complutense de Madrid.

Molina, M.M., Bellí, G., de la Torre, M.A., Rodríguez-Manzaneque, M.T., and Herrero, E. (2004). Nuclear monothiol glutaredoxins of *S. cerevisiae* can function as mitochondrial glutaredoxins. *J Biol Chem*. **279:** 51923–51930.

Molina-Navarro, M.M., Casas, C., Piedrafita, L., Bellí, G., and Herrero, E. (2006). Prokaryotic and eukaryotic monothiol glutaredoxins are able to perform the functions of Grx5 in the biogenesis of Fe/S clusters in yeast mitochondria. *FEBS Lett.* **580:** 2273–2280.

Montillet, J, L., Agne, J,P., Ponchet, M., Vailleau, F., Roby, D., and Triantaphylidès, C. (2002). Lipoxygenase-mediated production of fatty acid hydroperoxides is a specific signature of the hypersensitive reaction in plants. *Plant Physiol Biochem.* **40:** 633–639.

Montillet, J.L., Chamnongpol, S., Rusterucci, C., Dat, J., van de Cotte, B., Agnel, J.P., Battesti, C., Inze, D., Van Breusegem, F., and Triantaphylidès, C. (2005). Fatty acid hydroperoxides and H_2O_2 in the execution of hypersensitive cell death in tobacco leaves. *Plant Physiol.* **138:** 1516–1526.

Montes-Casado, N., Tena F, Ramasamy, S., Bonilla-Martínez A, Cebolla, M., Pardo C, Montesinos C, García-Luque, I., and Serra, M. (2010). La expresión constitutiva de una glutaredoxina (GRX) de *C. chinense* en plantas de *Nicotiana benthamiana* conlleva una reducción en la acumulación viral de PMMoV-I. *Resúm. X Reunión de Biología Molecular de Plantas.* Valencia**.** pág 175.

Moons, A. (2005). Regulatory and functional interactions of plant growth regulators and plant glutathione S-transferases (GSTs). *Vitam Horm.* **72:** 155-202.

Morris, K.A.H., Mackerness, S., Page, T., John, C.F., Murphy, A.M., Carr, J.P., and Buchanan-Wollaston, V. **(2000).** Salicylic acid has a role in regulating gene expression during leaf senescence. *Plant J.* **23:** 677–685.

Mou, Z., Fan, W., and Dong, X. (2003). Inducers of plant systemic acquired resistance regulate NPR1 function through redox changes. *Cell.* **113:** 935–944.

Murashige, T., and Skoog, F. (1962). A revised medium for rapid growth and bio-assays with tobacco tissue cultures. *Physiol Plant*. **15:** 473-497.

Mühlenhoff, U., Gerber, J., Richhardt, N., and Lill, R. (2003). Components involved in assembly and dislocation of iron–sulfur clusters on the scaffold protein Isu1p. *EMBO J.* **22:** 4815–4825.

Nakazawa, M., Yabe, N., Ichikawa, T., Yamamoto, Y.Y., Yoshizumi, T., Hasunuma, K., and Matsui, M. (2001). *DFL1*, an auxin-responsive *GH3* gene homologue, negatively regulates shoot cell elongation and lateral root formation, and positively regulates the light response of hypocotyl length. *Plant J.* **25:** 213-221.

Ndamukong, I., Abdallat, A.A., Thurow, C., Fode, B., Zander, M., Weigel, R., and Gatz, C. (2007). SA-inducible *Arabidopsis* glutaredoxin interacts with TGA factors and suppresses JA-responsive PDF1.2 transcription, *Plant J.* **50:** 128–139.

Nelson, R.S., and van Bel, A.J.E. (1998). The mystery of virus trafficking into, through and out of vascular tissue. *Progr Bot.* **59:** 476-533.

Niehl, A. and Heinlein, M. (2011). Cellular pathways for viral transport through plasmodesmata. *Protoplasma*. **248:** 75-99.

Niehl, A., Peña, E.J., Amari, K., and Heinlein, M. (2013). Microtubules in viral replication and transport. *Plant J.* **75:** 290-308.

Noctor, G. (2006). Metabolic signalling in defence and stress: the central roles of soluble redox copules. *Plant Cell Environ*. **29:** 409–425.

Nulton-Persson, A.C., Starke, D.W., Mieyal, J.J., Szweda, L.I. (2003). Reversible inactivation of alpha-ketoglutarate dehydrogenase in response to alterations in the mitochondrial glutathione status. *Biochemistry.* **42:** 4235–4242.

Obregón, P., Martín, R., Sanz, A. and Castresana, C. (2001). Activation of defence-related genes during senescence: a correlation between gene expression and cellular damage. *Plant Mol Biol.* **46:** 67–77.

Oparka, K.J., Prior, D.A., Santa Cruz, S., Padgett, H.S., and Beachy, R.N. (1997). Gating of epidermal plasmodesmata is restricted to the leading edge of expanding infection sites of tobacco mosaic virus (TMV). *Plant J.* **12:** 781-789.

Padgett, H.S., Watanabe, Y. and Beachy, R.N. (1997). Identification of the TMV replicase sequence that activates the *N* gene-mediated hypersensitive response. *Mol Plant Microbe Interact.* **10:** 709-715.

Padilla, C.A., Martínez-Galisteo, E., Bárcena, J.A., Spyrou, G., and Holmgren, A. (1995). Purification from placenta, amino acid sequence, structure comparisons and cDNA cloning of human glutaredoxin. *Eur J Biochem.* **227:** 27–34.

Pallas, V., and García, J.A. (2011). How do plant viruses induce disease? Interactions and interference with host components. *J Gen Virol.* **92:** 2691–2705.

Pellny, T.K., Locato, V., Vivancos, P.D., Markovic, J., De Gara, L., Pallardo, F. V. and Foyer, C.H. (2009). Pyridine nucleotide cycling and control of intracellular redox state in relation to poly(ADP-ribose) polymerase activity and nuclear localisation of glutathione during exponential growth of *Arabidopsis* cells in culture. *Mol Plant*. **2:** 442–456.

Peltier, J.B., Friso, G., Kalume, D.E,, Roepstorff, P., Nilsson, F., Adamska, I., and van Wijk, K.J. (2000). Proteomics of the chloroplast: Systematic identification and targeting analysis of lumenal and peripheral thylakoid proteins. *Plant Cell.* **12:** 319-341.

Peña, J., and Heinlein, M. (2012). RNA transport during TMV cell-to-cell movement. *Front Plant Sci.* doi: 10.3389/fpls.2012.00193.

Pérez Bueno, M.L. (2003). Fotosistema II e infección viral. Análisis de fluorescencia de imagen y regulación de la biosíntesis de las proteínas OEC durante la patogénesis. PhD thesis. Universidad de Granada.

Pérez-Bueno, M.L., Rahoutei, J., Sajnani, C., García-Luque, I., and Barón, M. (2004). Proteomic analysis of the oxygen-evolving complex of photosystem II under biotec stress: Studies on *Nicotiana benthamiana* infected with tobamoviruses. *Proteomics.* **4:** 418-425.

Pérez-Bueno, M.L., Barón, M., and García-Luque, I. (2011). PsbO, PsbP, and PsbQ of photosystem II are encoded by gene families in *Nicotiana benthamiana*. Structure and functionality of their isoforms. *Photosynthetica.* **49:** 573-580.

Pérez-Bueno, M.L., Ciscato, M., vande Ven, M., García-Luque, I., Valcke, R., and Barón, M. (2006). Imaging viral infection. Studies on *Nicotiana benthamiana* plants infected with the Pepper mild mottle tobamovirus. *Photosynth Res.* **90:** 111–123.

Pétriacq, P., de Bont, L., Hager, J., Didierlaurent, L., Mauve, C., Guérard, F., Noctor,G., Pelletier,S., Renou,J., Tcherkez,G., and Gakiére,B.(2012). Inducible NAD overproduction in *Arabidopsis* alters metabolic pools and gene expression correlated with increased salicylate content and resistance to *Pst-AvrRpm1*. *Plant J.* **70:** 650-665.

Pétriacq, P., de Bont, L., Tcherkez, G., and Gakiére,B. (2013). NAD: Not just a pawn on the board of plant-pathogen interactions. *Plant Signal Behav*. **8**: e22477.

Pieterse, C.M.J., and Van Loon, L.C. (2004). NPR1: the spider in the web of induced resistance signaling pathways. *Curr Opin Plant Biol.* **7:** 456–464.

Pieterse, C.M.J., Van der Does, D., Zamioudis, C., Leon-Reyes, A., and Van Wees, S.C.M. (2012). Hormonal modulation of plant immunity. *Annu Rev Cell Dev Biol*. **28:** 489–521.

Pineda, M., Olejníčková, J., Cséfalvay, L., Barón, M. (2011). Tracking viral movement in plants by means of chlorophyll fluorescence imaging. *J Plant Physiol*. **9:** 2035–2040.

Pineda, M., Sajnani, C., and Baron, M. (2010). Changes induced by the Pepper mild mottle tobamovirus on the chloroplast proteome of *Nicotiana benthamiana*. *Photosynth Res.* **103:** 31-45.

Porta, H., and Rocha-Sosa, M. (2002). Plant lipoxygenases. Physiological and molecular features. *Plant Physiol*. **130:** 15–21.

Postnikova, O.A., and Nemchinov, L.G. (2012). Comparative analysis of microarray data in *Arabidopsis* transcriptome during compatible interactions with plant viruses. *Virology J.* **9:** 101.

Qiagen, Inc. (2003). The QIAexpressionist handbook, 5th ed. Qiagen, Inc., Valencia, CA.

Queval, G., and Noctor, G. (2007). A plate-reader method for the measurement of NAD, NADP, glutathione and ascorbate in tissue extracts. Application to redox profiling during *Arabidopsis* rosette development. *Anal Biochem*. **363:** 58–69.

Rahoutei, J., Barón, M., García-Luque, I., Droppa, M., Nemenyi, A., and Hórvath, G. (1999). Effect of tobamovirus infection on thermoluminescence characteristics of chloroplasts from infected plants. *Z. Naturfosch.* **54:** 634-639.

Rancé, I., Fournier, J., and Esquerré-Tugayé, M.T. (1998). The incompatible interaction between *Phytophtora parasitica var nicotianae* race 0 and tobacco is suppressed in transgenic plants expressing antisense lipoxygenase sequences. *Proc Natl Acad Sci USA*. **95:** 6554–6559.

Reumann, S., Heupel, R., and Heldt, H.W. (1994). Compartmentation studies on spinach leaf peroxisomes. II. Evidence for the transfer of reductant from the cytosol to the peroxisomal compartment via a malate shuttle. *Planta*. **193:** 167–173.

Roberts, A.G., Cruz, S.S., Roberts, I.M., Prior, D., Turgeon, R., and Oparka, K.J. (1997). Phloem unloading in sink leaves of *Nicotiana benthamiana*: Comparison of a fluorescent solute with a fluorescent virus. *Plant Cell.* **9:** 1381-1396.

Robert-Seilaniantz, A., Grant, M., y Jones, J.D. (2011). Hormone crosstalk in plant disease and defense: more than just jasmonate-salicylate antagonism. *Annu Rev Phytopathol*. **49:** 317-343.

Rodriguez-Manzaneque, M.T., Ros, J., Cabiscol, E., Sorribas, A., and Herrero, E. (1999). Grx5 glutaredoxin plays a central role in protection against protein oxidative damage in *Saccharomyces cerevisiae*. *Mol Cell Biol***. 19:** 8180–8190.

Rodríguez-Manzaneque, M.T., Tamarit, J., Bellí, G., Ros, J., and Herrero, E. (2002). Grx5 is a mitochondrial glutaredoxin required for the activity of iron/sulfur clusters. *Mol Biol Cell.* **13:** 1109–1121.

Rosario, K., Symonds, E.M., Sinigalliano, C., Stewart, J., and Breitbart, M. (2009). Pepper mild mottle virus as an indicator of fecal pollution. *Appl Environ Microbiol*. **75:** 7261-7267.

Ross, A.F. (1961). Systemic acquired resistance induced by localized virus infections in plants. *Virology*. **14:** 340–358.

Roossinck, M.J. (2005). Symbiosis versus competition in plant virus evolution. *Nat Rev Microbiol*. **3:** 917–924.

Rouhier, N., Couturier, J., Johnson, M.K., and Jacquot, J.P. (2009). Glutaredoxins: roles in iron homeostasis. *Trends Biochem Sci*. **35:** 43-52.

Rouhier, N., Gelhaye, E., and Jacquot, J.P. (2002). Glutaredoxin-dependent peroxiredoxin from poplar: protein-protein interaction and catalytic mechanism. *J Biol Chem.* **277:** 13609–13614.

Rouhier, N., Gelhaye, E., and Jacquot, J.P. (2004). Plant glutaredoxins: still mysterious reducing systems. *Cell Mol Life Sci.* **61:** 1266–1277.

Rouhier, N., Gelhaye, E., Sautiere, P.E., Brun, A., Laurent, P., Tagu, D., Gerard, J., de Fay, E., Meyer, Y. and Jacquot, J.P. (2001). Isolation and characterization of a new peroxiredoxin from poplar sieve tubes that uses either glutaredoxin or thioredoxin as a proton donor. *Plant Physiol.* **127:** 1299–1309.

Rouhier, N., Couturier, J., and Jacquot, J.P. (2006). Genome-wide analysis of plant glutaredoxin systems. *J Exp Bot***. 57:**1685–1696.

Rouhier, N., Lemaire, S.D., and Jacquot, J.P. (2008). The role of glutathione in photosynthetic organisms: emerging functions for glutaredoxins and glutathionylation. *Ann Rev Plant Biol.* **59:**143–166.

Rouhier, N., Unno, H., Bandyopadhyay, S., Masip, L., Kim, S.K., Hirasawa, M., Gualberto, J.M., Lattard, V., Kusunoki, M., Knaff, D.B., Georgiou, G., Hase, T., Johnson, M.K., and

Jacquot, J.P. (2007). Functional, structural, and spectroscopic characterization of a glutathione-ligated [2Fe-2S] cluster in poplar glutaredoxin C1. *Proc Natl Acad Sci USA.* **104:** 7379–7384.

Rouhier, N. (2010). Plant glutaredoxins: pivotal players in redox biology and iron-sulphur centre assembly. *New Phytol.* **186:** 365–372.

Ruíz del Pino, M., Moreno, A., García de Lacoba, M., Castillo-Lluva, S., Gilardi, P., Serra, M.T., and García-Luque, **I. (2003).** Biological and molecular characterization of P101 isolate, a tobamoviral pepper strain from Bulgaria. *Arch Virol.* **148:** 2115-2135.

Ryals, J.A., Neuenschwander, U.H., Willits, M.G., Molina, A., Steiner, H.Y., and Hunt, M.D. (1996). Systemic acquired resistance. *Plant Cell.* **8:** 1809-1819.

Sambrook, J., Fritsch, E.F., and Maniatis, F. (1989). Molecular cloning. A laboratory manual. Cold Spring Harbor Laboratory Press. New York.

Santino, A., Iannacone, R., Hughes, R., Casey, R., and Mita, G. (2005). Cloning and characterization of an almond 9-lipoxygenase expressed early during seed development. *Plant Sci*. **168:** 699–705.

Sappl, P.G., Carroll, A.J., Clifton, R., Lister, R., Whelan, J., Millar, A.H., and Singh, K.B. (2009). The *Arabidopsis* glutathione transferase gene family displays complex stress regulation and co-silencing of multiple genes results in altered metabolic sensitivity to oxidative stress. *Plant J* **.58:** 53–68.

Sareila, O., Hohkuri, M., Wahlroos, T., and Susi, P. (2004). Role of viral movement and coat proteins and RNA in phloem-dependent movement and phloem unloading of tobamoviruses. *J Phytopathol.* **152:** 622-629.

Sarkar, T. S., Bhattacharjee, A., Majumdar, U., Roy A., Maiti, D., Goswamy, A.M., Ghosh, S.K., and Ghosh, S. (2011). Biochemical characterization of compatible plant-viral interaction: A case study with a begomovirus-kenaf host- pathosystem. *Plant Signal Behav*. **6 :** 501–509.

SAS Institute Inc. (2004). What's New in SAS®9.0, 9.1, 9.1.2, and 9.1.3.Cary, NC: SAS Institute Inc.

Sayegh-Alhamdia, M., Marmey, P., Jalloul, A., Champion, A., Petitot, S., Clerivet, A., and Nicole, M. (2008). Association of lipoxygenase response with resistance of various cotton genotypes to the bacterial blight disease. *J Phytopathol.* **156:** 542–549.

Shimabukuro, R.H., Frear, D.S., Swanson, H.R., and Walsh, W.C. (1971). Glutathione conjugation: an enzymatic basis for atrazine resistance in corn. *Plant Physiol.* **47:** 10–14.

Siedow, J.N. (1991). Plant lipoxygenase: structure and function. *Annu Rev Plant Physiol Plant Mol Biol.* **42:**145–188.

Simon-Buela, L., and Garcia-Arenal, F. (1999). Virus particles of cucumber green mottle mosaic tobamovirus move systemically in the phloem of infected cucumber plants. *Mol Plant Microbe Interact.* **12:** 112-118.

SPSS Inc. (1999). SPSS Base 10.0 for Windows User's Guide. SPSS Inc., Chicago IL.

Su, S., Liu, Z., Chen, C., Zhang, Y., Wang, X., Zhu, L., Miao, L., Wang, X.C. and Yuan, M. (2010). *Cucumber mosaic virus* movement protein severs actin filaments to increase the plasmodesmal size exclusion limit in tobacco. *Plant Cell.* **22:**1373-1387.

Sun, L., Ren, H., Liu, R., Li, B., Wu, T., Sun, F., Liu, H., Wang, X., and Dong, H. (2010). An h-type thioredoxin functions in tobacco defense responses to two species of viruses and an abiotic oxidative stress. *Mol Plant Microbe Interact.* **23:** 1470-1485.

Sundaram, S., and Rathinasabapathi, B. (2010). Transgenic expression of fern *Pteris vittata* glutaredoxin PvGrx5 in *Arabidopsis thaliana* increases plant tolerance to high temperature stress and reduces oxidative damage to proteins. *Planta.* **231:** 361–369.

Sundaram, S., Wu, S., Ma, L.Q., and Rathinasabapathi, B. (2009). Expression of a *Pteris vittata* glutaredoxin PvGRX5 in transgenic *Arabidopsis thaliana* increases plant arsenic tolerance and decreases arsenic accumulation in the leaves. *Plant Cell Environ*. **32:** 851-858.

Szederkenyi, J., Komor, E., and Schobert, C. (1997). Cloning of the cDNA for glutaredoxin, an abundant sieve-tube exudate protein from *Ricinus communis L*. and characterisation of the glutathione-dependent thiol-reduction system in sieve tubes. *Planta.* **202:** 349–356.

Takahama, U., Shimizu-Takahama, M., and Heber, U. (1981). The redox state of the NADP system in illuminated chloroplasts. *Biochim Biophys Acta.* **637:** 530–539.

Tamarit, J., Bellí, G., Cabiscol, E., Herrero, E., and Ros, J. (2003). Biochemical characterization of yeast mitochondrial Grx5 monothiol glutaredoxin. *J Biol Chem.* **278:** 25745–25751.

Tamura, K., Peterson, D., Peterson, N., Stecher, G., Nei, M., and Kumar, S. (2011). MEGA5: Molecular Evolutionary Genetics Analysis using Maximum Likelihood, Evolutionary Distance, and Maximum Parsimony Methods. *Mol Biol Evol*. **28:** 2731-2739.

Tarrago, L., Laugier, E., Zaffagnini, M., Marchand, C., Le Marechal, P., Rouhier, N., Lemaire, S.D., and Rey, P. (2009). Regeneration mechanisms of *Arabidopsis thaliana* methionine sulfoxide reductases B by glutaredoxins and thioredoxins. *J Biol Chem.* **284:** 18963–18971.

Tena, F. (2012). Patogénesis del virus del moteado suave del pimiento en solanáceas. Ph. D. Thesis. Faculty of Biological Sciences. University Autónoma of Madrid.

Tena, F., Molina-Galdeano, M., Serra, M.T., García-Luque, I. (2012). A single amino acid in the helicase domain of PMMoV-S is responsible for its enhanced accumulation in *C. chinense* (*L* ^{3} *L* ^{3}) plants at 32°C. *Virology.* **427:** 34-43.

Tenllado, F., García-Luque, I., Serra, M.T., and Díaz-Ruíz, J.R. (1994). Rapid detection and differentiation of tobamoviruses infecting L-resistant genotypes of pepper by RT-PCR and restriction analysis. *J Virol Methods*. **47:** 165-174.

Tenllado, F., García-Luque, I., Serra, M.T., and. Díaz-Ruíz, J.R. (1997). Pepper resistance-breaking tobamoviruses: Can they co-exist in single pepper plants?. *Eur J Plant Pathol.* **103:** 235–243.

Thivierge, K., Nicaise, V., Dufresne, P.J., Cotton, S., Laliberte, J.F., Le Gall, O., and Fortin, M.G. (2005). Plant virus RNAs. Coordinated recruitment of conserved host functions by (+) ssRNA viruses during early infection events. *Plant Physiol***. 138:** 1822-1827.

Torres, M.A. **(2010).** ROS in biotic interactions. *Physiol Plant.* **138:** 414–429.

Ueki, S., Spektor, R., Natale, D.M., and Citovsky, V. (2010). ANK, a host cytoplasmic receptor for the tobacco mosaic virus cell-to-cell movement protein, facilitates intercellular transport through plasmodesmata. *PLoS Pathog.* **6:** e1001201.

Van Loon, L.C., and Van Kammen, A. (1970). Polyacrylamide disc electrophoresis of the soluble leaf proteins from *Nicotiana tabacum* var. "Samsun" and "Samsun NN" II. Changes in protein constitution after infection with tobacco mosaic virus. *Virology.* **40:** 199-211.

Van Loon, L.C., Rep, M., and Pieterse, C.M.J. (2006). Significance of inducible defense related proteins in infected plants. *Ann Rev Phytopathol*. **44:** 135-162.

Vellosillo, T., Martínez, M., López, M.A., Vicente, J., Cascón, T., Dolan, L., Hamberg, M., and Castresana, C. (2007). Oxylipins produced by the 9-lipoxygenase pathway in *Arabidopsis* regulate lateral root development and defense responses through a specific signaling cascade. *Plant Cell.* **19:** 831–846.

Vicente, J., Cascón, T., Vicedo, B., García-Agustín, P., Hamberg, M., and Castresana, C. (2012). Role of 9-lipoxygenase and α-dioxygenase oxylipin pathways as modulators of local and systemic defense. *Mol Plant.* **5:** 914–928.

Vlamis-Gardikas, A., and Holmgren, A. (2002). Thioredoxin and glutaredoxin isoforms. *Methods Enzymol.* **347:** 286–296.

Vollenweider, S., Weber, H., Stolz, S., Chetelat, A. and Farmer, E.E. (2000). Fatty acid ketodienes and fatty acid ketotrienes: Michael addition acceptors that accumulate in wounded and diseased *Arabidopsis* leaves. *Plant J.* **24:** 467–476.

Wagner U., Edwards R., Dixon D.P., and Mauch F. (2002). Probing the diversity of the *Arabidopsis* glutathione S-transferase gene family. *Plant Mol Biol*. **49:** 515–532.

Wang, X., Kelman, Z., and Culver, J.N. (2010). Helicase ATPase activity of the tobacco mosaic virus 126-kDa protein modulates replicase complex assembly. *Virology*. **402:** 292-302.

Wang, Z., Xing, S., Birkenbihl, R.P., and Zachgo, S. (2009). Conserved functions of *Arabidopsis* and rice CC-type glutaredoxins in flower development and pathogen response. *Mol Plant.* **2:** 323–335.

Wetter, C., Conti, M., Altschuh, D., Tabillion, R., and van Regenmortel, M.H.V. (1984). Pepper mild mottle virus, a tobamovirus infecting pepper cultivars in Sicily. *Phytopathology*. **74:** 405-410.

Whitham, S.A., Yang, C.L., and Goodin, M.M. (2006). Global impact: Elucidating plant responses to viral infection. *Mol Plant Microbe Interact*. **19:** 1207-1215.

Whitham, S.A., Sheng, Q., Chang, H.S., Cooper, B., Estes, B., Zhu, T., Wang, X., and Hou Y.M. (2003). Diverse RNA viruses elicit the expression of common sets of genes in susceptible *Arabidopsis thaliana* plants. *Plant J.* **33:** 271–283.

Wigge, B., Kromer, S., and Gardestrom, P. (1993). The redox levels and subcellular distribution of pyridine nucleotides in illuminated barley leaf protoplasts studied by rapid fractionation. *Physiol Plant*. **88:** 10-18.

Wilson, T. M.A. (1985). Nucleocapsid disassembly and early gene expression by positive-strand RNA viruses. *J Gen Virol.* **66:** 1201-1207.

Wolf, S., Deom, C.M., Beachy, R.N., and Lucas, W.J. (1989). Movement protein of tobacco mosaic virus modifies plasmodesmatal size exclusion limit. *Science.* **246:** 377-379.

Wu, Q., Lin, J., Liu, J.Z., Wang, X., Lim, W., Oh, M., Park, J., Rajashekar, C.B., Whitham, S.A., Cheng, N.H., Hirschi, K.D., and Park, S. (2012). Ectopic expression of *Arabidopsis* glutaredoxin AtGRXS17 enhances thermotolerance in tomato. *Plant Biotechnol J.* **10:** 945–955.

Wu, X., and Shaw, J. (1996). Bidirectional uncoating of the genomic RNA of a helical virus. *Proc Natl Acad Sci USA.* **93:** 2981-2984.

Xing, S., and Zachgo, S. (2008). ROXY1 and ROXY2, two *Arabidopsis* glutaredoxin genes, are required for anther development. *Plant J.* **53:** 790–801.

Xing, S., Rosso, M.G., and Zachgo, S. (2005). *ROXY1*, a member of the plant glutaredoxin family, is required for petal development in *Arabidopsis thaliana. Development.* **132:** 1555–1565.

Yadav, S., Kushwaha, H.R., Kumar, K., and Verma, P.K. (2012). Comparative structural modeling of a monothiol GRX from chickpea: Insight in iron-sulfur cluster assembly. *Int J Biol Macromol.* **51:** 266-273.

Yamamoto, Y. (1963). Pyridine nucleotide content in higher plant: Effect of age of tissue. *Plant Physiol.* **38:** 45-54.

Zaffagnini, M., Bedhomme, M., Marchand, C.H., Morisse, S., Trost, P., and Lemaire. S.D. (2012). Redox regulation in photosynthetic organisms: Focus on glutathionylation. *Antioxid Redox Signal.* **16:** 567-586.

Zaffagnini, M., Michelet, L., Massot, V., Trost, P., and Lemaire, S.D. (2008). Biochemical characterization of glutaredoxins from *Chlamydomonas reinhardtii* reveals the unique properties of a chloroplastic CGFS-type glutaredoxin. *J Biol Chem.* **283:** 8868–8876.

Zeenko, V.V., Ryabova, L.A., Spirin, A.S., Rothnie, H.M., Hess, D., Browning, K.S., and Hohn, T. (2002). Eukaryotic elongation factor 1A interacts with the upstream pseudoknot domain in the 3' untranslated region of tobacco mosaic virus RNA. *J Virol*. **76:** 5678-5691.

Zeier, J., Pink, B., Mueller, M.J. and Berger, S. (2004). Light conditions influence specific defense responses in incompatible plant–pathogen interactions: uncoupling systemic resistance from salicylic acid and PR-1 accumulation. *Planta*. **219:** 673–683.

Zhang, T., Breitbart, M., Lee, W.H., Run, J.Q., Wei, C.L., Soh, S.W., Hibberd, M.L., Liu, E.T., Rohwer, F., and Ruan, Y. (2006). RNA viral community in human feces: prevalence of plant pathogenic viruses. *PLoS Biol.* **4:** e3.

Zhang, X., and Mou, Z. (2009). Expression of the human NAD (P)-metabolizing ectoenzyme CD38 compromises systemic acquired resistance in *Arabidopsis*. *Mol Plant Microbe Interact*. **25:** 1209-1218.

Zhu, Q., Maher, E.A., Masoud, S., Dixon, R.A., and Lamb, C. (1994). Enhanced protection against fungal attack by constitutive co–expression of chitinase and glucanase genes in transgenic tobacco. *Nat Biotechnol.* **12:** 807–812.